Process Optimization on Raith-150 TWO E-Beam Lithography Tool for sub-100nm CMOS device fabrication

Submitted in partial fulfillment of the requirements

of the degree of

Master of Technology

by

Kunal Promode Ghosh
07307R07

under the guidance of

Prof. R. Pinto
and
Prof. Anil Kottantharayil

Department of Electrical Engineering
Indian Institute of Technology, Bombay
Oct 2009

Abstract

Lithography using beam of electrons to expose resist was one of the earliest processes for IC circuit fabrication. Essentially, all high volume production, even down to <200nm feature sizes, is done using optical techniques. Electron beam systems, like Raith 150 TWO, plays a vital role in generating the mask plate for optical lithography. The intent of this project is to optimize the tool as well as the process conditions to attain minimum resolution, use the mix-and-match capabilities of the tool for sub-100nm MOSFET fabrication and generate mask plates for feature sizes above 500nm.

Acknowledgements

I would like to express my profound gratitude to my guides, Prof. R. Pinto and Prof. Anil Kottantharayil, for their kind help during the initial stages of my work. I am deeply indebted to them for their valuable guidance, suggestions and constant encouragement throughout my project work. Furthermore, I would thank Prof. Dipankar Saha and Prof. Swaroop Ganguly with whom I discussed and solved the mask plate issues. This work would not have taken present form without the creative inputs from my colleagues Ms. Gayatri Vaidya and Ms. Rajashree Rajagopal. I would like to thank Ms. Neha Raorane for her help and support in the optimization phase. I would also like to thank IISc, Bangalore, for giving me an opportunity to work with them. The work reported in this thesis was carried out at the Center of Excellence in Nanoelectronics (CEN) Department of Electrical Engineering at IIT Bombay. I was also financially supported by the CEN during the course of this work. I would like to thank Suresh G., PhD student, Electrical Engg. for providing images from process simulations. I would also like to thank all people directly or indirectly involved in my project.

Contents

List of Figures

List of Tables

Nomenclature

α and β	Empirical constants
δ	Resist density
λ	Electron wavelength
ε	Absorbed energy density
A_0	Avogadro's number
d_g	Diameter of filament tip
d_p	Probe diameter
D_{CL}	Clearing Dose
E_0	Incident electron energy
M_0	Initial molecular weight
m_0	Mass of electron
BSE	Back scattered electron
c	Speed of light
CMTF	Critical Modulation Transfer Function
e	Elementary Charge
g	Chain Scission Efficiency
h	Plank's constant
HSQ	Hydrogen SilsesQuioxane
IC	Integrated Circuit

LE	Line scan Error
LS	Line scan Successful
MOSFET	Metal Oxide Semiconductor Field Effect Transistor
MTF	Modulation Transfer Function
p	Momentum
PMMA	PolyMetyhl MethaAcrylate
R	Development Rate
SE	Secondary Electron
SEM	Scanning Electron Microscope
TEM	Transmission Electron Microscope
TFE	Thermal Field Emission
U	Electric potential
WD	Working Distance
z	Resist depth

Chapter 1

Introduction

This chapter focuses on the physics underlying the e-beam lithography process and our e-beam lithography tool - Raith 150 Two. It begins with the fundamental reasons for moving towards e-beam lithography and moves onto how an e-beam lithography tool essentially works. It details some of the important concepts of tool working such as beam spot size and astigmatism. Further, performance specifications and test results obtained using the Raith 150 Two tool have been outlined. Steps involved in a typical e-beam lithography process using PMMA are listed as a guideline. The chapter ends with a section outlining the contents in rest of this report.

1.1 Why E-Beam Lithography?

In optical lithography, the resolution is limited by wavelength & numerical aperture. To increase the numerical aperture in optical lithography, various techniques like lens immersion technique can be used. However, the resolution is still limited as we can't go below a particular wavelength. Hence, a new technique has to be adapted to beat the diffraction limit of light.[9]
The wavelength of an electron is given by de Broglie equation[9]

$$\lambda = \frac{h}{p} \tag{1.1}$$

h is Planck's constant and p is the momentum of the electron. The electrons are accelerated to the desired velocity in an electric potential U.

$$\nu = \sqrt{\frac{2eU}{m_0}} \tag{1.2}$$

The mass of the electron is m_0, and e is the elementary charge. The electron wavelength is then given by[9]

$$\lambda = \frac{h}{p} = \frac{h}{m_0 \nu} = \frac{h}{\sqrt{2 m_0 e U}} \tag{1.3}$$

In an electron microscope, the accelerating potential is usually several thousand volts causing the electron to travel at an appreciable fraction of the speed of light. A SEM operating at accelerating potential of 10 kV gives an electron velocity which is approximately 20% of the speed of light, while a typical TEM operating at 200 kV raises the electron velocity to 70% of speed of light. We therefore need to take relativistic effects into account and hence the electron wavelength is modified to

$$\lambda = \frac{h}{\sqrt{2 m_0 e U}} \frac{1}{\sqrt{1 + \frac{eU}{2 m_0 c^2}}} \tag{1.4}$$

c is the speed of light. The first term in this final expression is recognized as the non-relativistic expression derived above, while the last term is a relativistic correction factor. The wavelength of the electrons in a 10 kV SEM is then 12.3 X 10^{-12}m (12.3 pm), while in a 200 kV TEM, the wavelength in 2.5 pm.

Electron Beam Lithography is better than optical lithography as it is capable of very high resolution and can work with variety of substrates. However, it is much slower than optical lithography, more expensive and highly complicated in operation when compared to optical lithography.

1.2 How E-Beam Lithography Works

Fig. 1.1 shows the microscope column which generates the electron beam and focuses it on to the specimen. It consists of the following:[4]

- A source of electron beam - the electron gun
- A series of condenser and objective lenses which control the diameter of the beam as well as focus the beam on to the specimen
- A magnetic or electrostatic deflector is used to move the focused beam over the surface of the specimen
- A beam blanker that consists of a combination of an aperture and a deflector, to turn off the beam

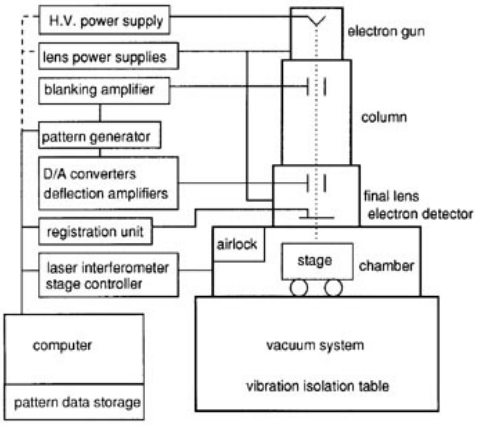

Figure 1.1: Microscope Column which generates the electron beam and focuses it on to the specimen and specimen Chamber[3]

- A series of apertures which affects the physical properties of the beam
- A laser interferometer stage for loading, unloading and moving the sample around in the chamber
- A vacuum system associated with the chamber to maintain high vacuum levels (up-to 2 X 10^{-9}mbar) throughout the column

The focused electron beam generated from the column can interact with the coulomb field of both the specimen nucleus and electrons. These interactions are responsible for a multitude of events : inelastic events and elastic events. Refer Fig. 1.2 and Fig. 1.3

When an electron beam hits a specimen, it interacts with the electric field of a specimen atom electron. Hence, there is a potential expulsion of an electron from specimen atom due to transfer of energy to that atom. These electron are known as secondary electrons and have energy, typically, less than 50eV. This is referred to as inelastic event.

Elastic events occurs when an electron beam, hitting the specimen, interacts with the electric field of the nucleus of a specimen atom, that results in a change in direction of the electron beam without a significant change ($<$ 1 eV) in the electron beam energy. The elastically scattered electron which is deflected back out of the specimen is termed as back scattered electron (BSE). BSEs can have an energy range from 50 eV to nearly the incident

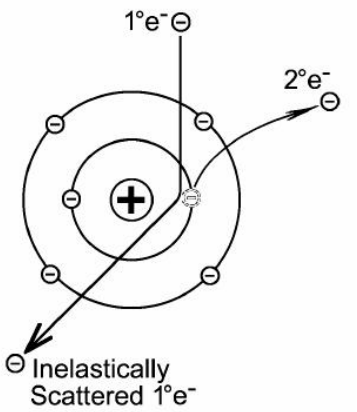

Figure 1.2: Inelastic Events due to electron beam interaction with the electric field of specimen atom electron, resulting in emission of secondary electrons[4]

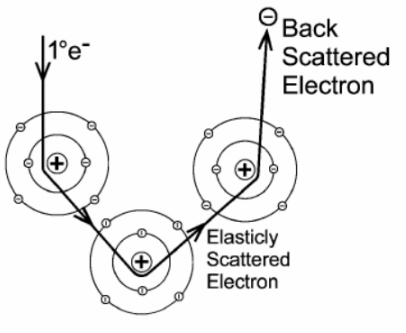

Figure 1.3: Elastic Events due to electron beam interaction with the electric field of the nucleus of specimen atom resulting in emission of back-scattered electrons[4]

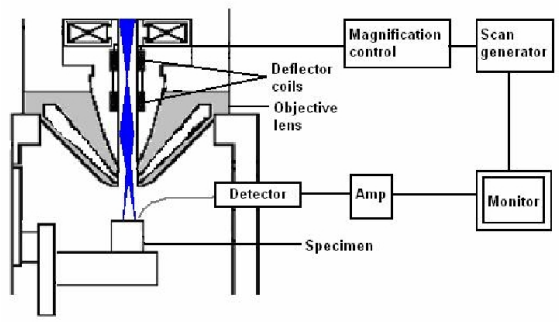

Figure 1.4: Column Electronics with secondary electron detector[4]

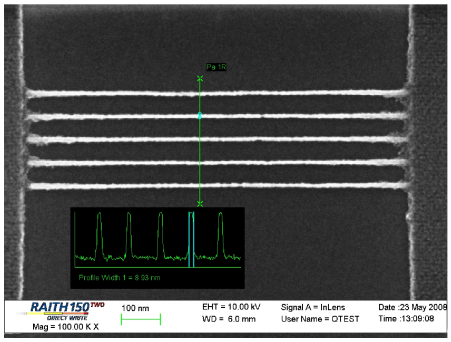

Figure 1.5: High Resolution SEM Image using secondary electron detector of Raith 150 TWO E-Beam Lithography tool

beam energy. However, most back scattered electrons retain at least 50% of the incident beam energy.

These secondary electrons from specimen generates a signal which is acquired by the detector (Fig. 1.4), and processed to produce an image or spectrum on the monitor display. Fig. 1.5 shows SEM image taken on Raith 150 TWO. The tool has a secondary electron detector which collects the secondary electrons from the specimen, and hence Raith 150 TWO could be used SEM imaging.

1.3 Column Controller - Heart of Lithography

The electron column shown in Fig. 1.1, is the heart of any E-Beam Lithography system. A simplified ray diagram of round-beam electron lithography instrument is shown in Fig. 1.6. There are various Shaped-Beam instruments available viz. fixed square-spot instruments and shaped rectangular-spot instruments.
The current density within the spot, produced by a round-beam machine, is non-uniform, conforming to bell-shaped distribution. Hence, Pfeiffer and Loeffler[10] pointed out that electron optical systems that produced square, uniformly illuminated spots, could be built.

1.3.1 Filament and Electron Emission

The column consists of a filament which emits the electrons. Our Raith 150 TWO system contains Schottky field emitter which is a thermal field emission (TFE) cathode made up of ZrO/W. Electrons are emitted from a heated tungsten tip due to an electrical field applied as extractor voltage (refer Fig. 1.7). The emitter consists of a sharply pointed single crystal tungsten filament, oriented along <100> axis. The shank of the filament tip is covered by a zirconium oxide (ZrO) reservoir. The single crystal tungsten filament is mounted onto a polycrystalline tungsten heating filament. Tip radius is 0.5 μm (+/- 0.1 μm)

1.3.2 Beam spot size variation

Fig. 1.8 shows a simplified column with one condenser lens, an objective lens, and an aperture for each lens.[4]

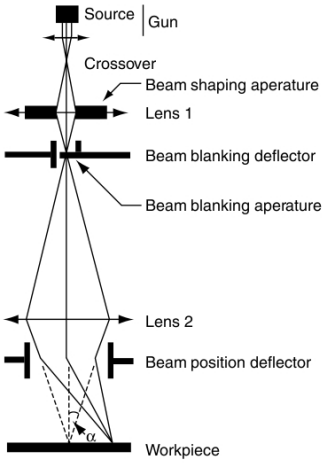

Figure 1.6: Electron Optical System for round-beam E-Beam Lithography system[5]

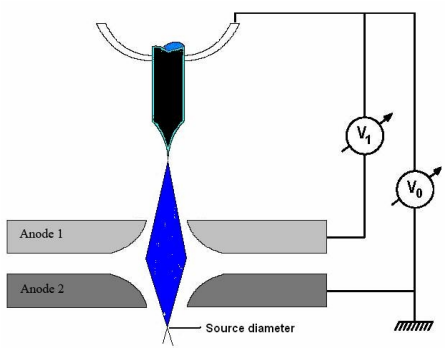

Figure 1.7: Thermionic Field Emission mechanism[4]

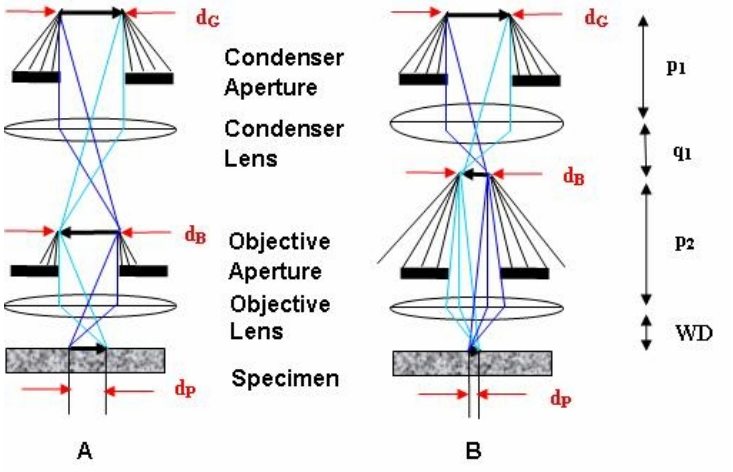

Figure 1.8: Spot size variation with varying excitation current of condenser lens[4]

A and B represent the source diameter of electron beam exiting the gun. d_g is the diameter of filament tip, d_p is the probe diameter. The amount of de-magnification of the source diameter to the beam d_b is[4]

$$d_b = \frac{d_g}{p_1/q_1} \tag{1.5}$$

And likewise, the amount of de-magnification of the beam at d_b to the electron probe (d_p) is

$$\frac{p_2}{WD} \tag{1.6}$$

So, the diameter of the electron probe at the specimen is

$$d_p = \frac{d_b}{p_2/WD} \tag{1.7}$$

The magnitude of excitation current of condenser lens in B is high as compared to that of A which causes more of the beam to be stopped by the objective aperture and thus a reduction in probe current occurs. Thus, the probe diameter or the spot size can be varied by altering current to a condenser lens.

1.3.3 Astigmatism Correction

The electromagnetic lenses used in a SEM are not always perfectly symmetrical. A converged beam would appear circular on the specimen provided the fields produced by the lenses were perfectly symmetrical. If not, then this results in streaking of image on both sides of focus. Even if streaking is not evident, astigmatism still needs to be fine-tuned to obtain high quality images.

Objective lens astigmatism can be compensated by applying current differentially to a ring of stigmator coils around the objective lens (refer Fig. 1.9)

1.4 Raith150-TWO System Specifications

RAITH150-TWO is Raith's highly automated E-beam writer for long-lasting and large area exposures. It ideally suits nanotechnology research centers and industry labs.[11]

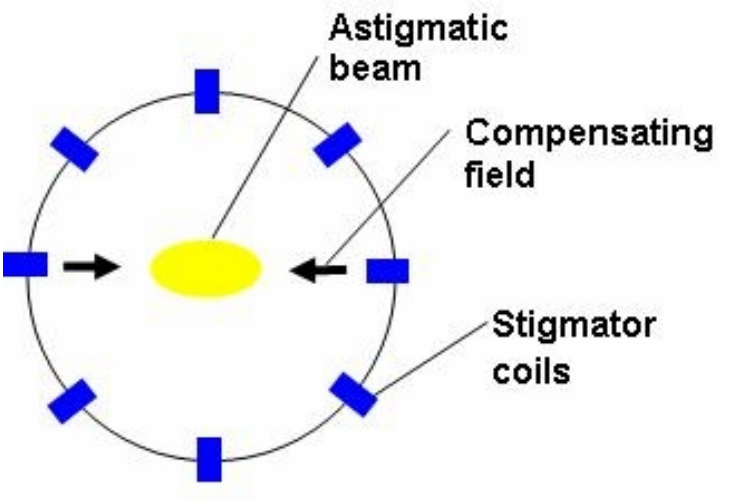

Figure 1.9: Objective lens astigmatism compensation technique by applying current differentially to a ring of stigmator coils around the objective lens[4]

1.4.1 List's of Tests Performed

Beam Size Test

Fig. 1.10 and Fig. 1.11 shows beam size test performed at 20kV and 1kV, respectively.

- At 20 kV, beam size is 1.78 nm with horizontal line scan, and 1.56 nm with vertical line scan
- At 1 kV, beam size is 3.63 nm with horizontal line scan, and 3.13 nm with vertical line scan

Beam Stability Test

Beam position drift measurement was done with resting stage and registering 1 mark every 15 min, at 10 kV (refer Fig. 1.12). Beam current drift measurement was also done with resting stage and reading the current value in Faraday cup, at 10 kV (refer Fig. 1.13).

- Beam position drift is maximum 80 nm for 14 hours
- Beam current drift is below 0.5% in 11 hours

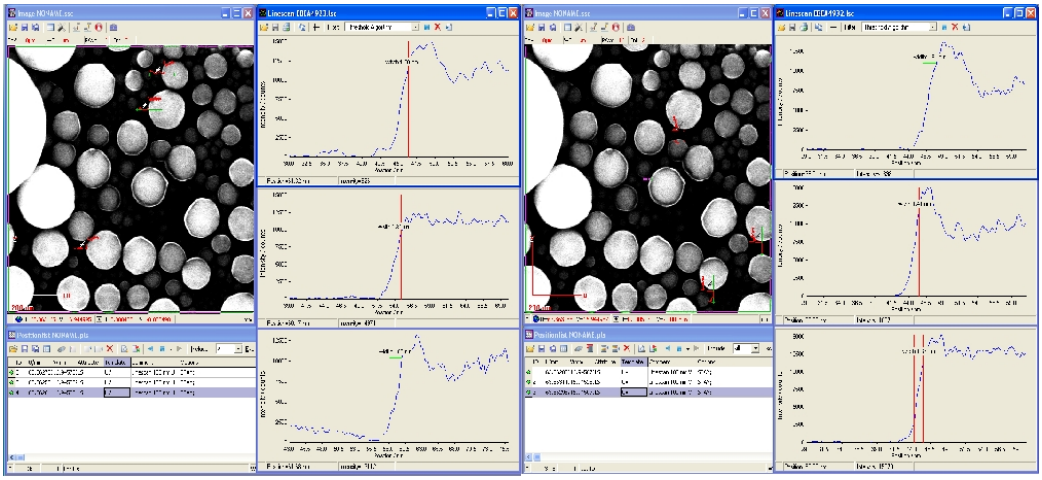

Figure 1.10: Beam size test using horizontal and vertical scan at 20 kV

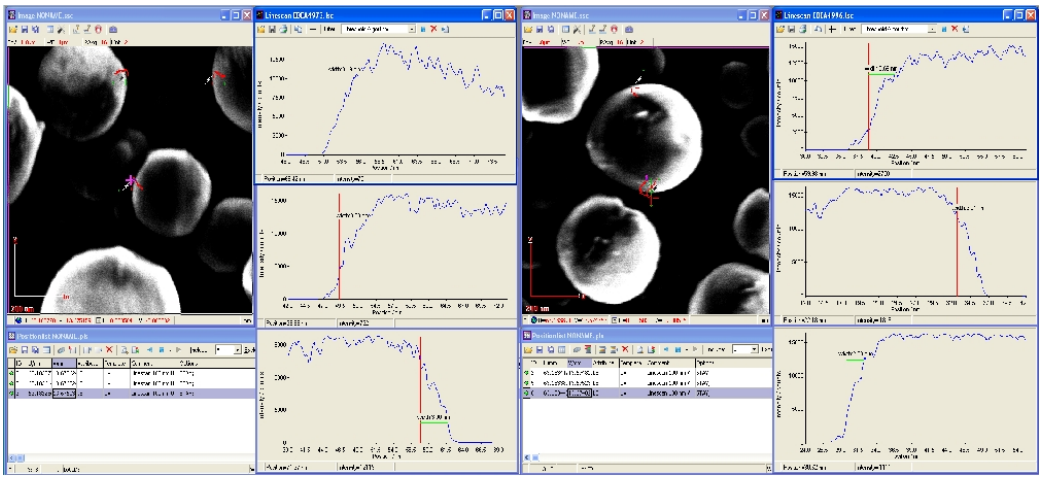

Figure 1.11: Beam size test using horizontal and vertical scan at 1 kV

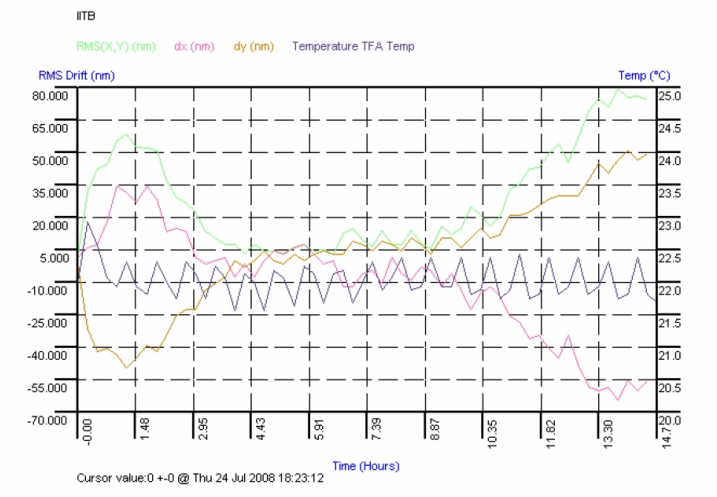

Figure 1.12: Beam position drift done with resting stage and registering 1 mark every 15 min, at 10 kV

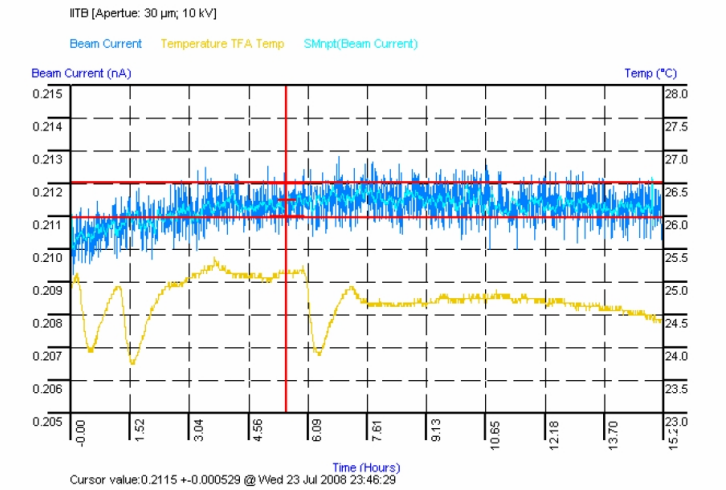

Figure 1.13: Beam current drift done with resting stage and reading the current value in Faraday cup, at 10 kV

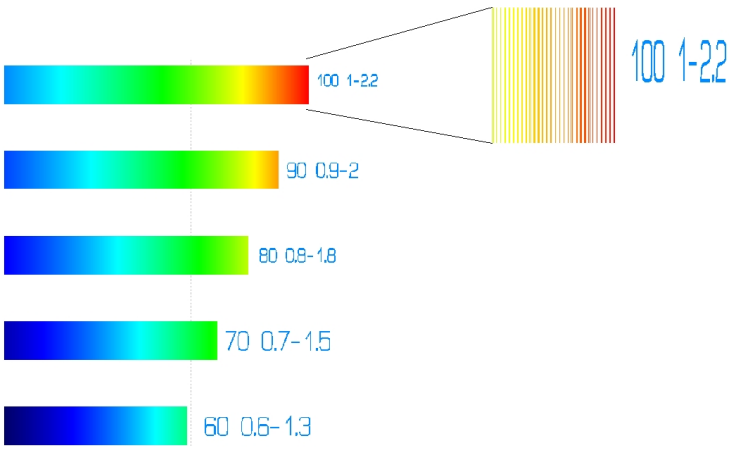

Figure 1.14: Gratings pattern for high resolution exposure test

High Resolution Exposure Test - Gratings

Fig. 1.14 shows the gratings pattern used for high resolution exposure test. These patterns were exposed at 20 kV using 100 um write-field. Details of exposure would be clear in the subsequent chapters. Fig. 1.15 shows the post develop image.

- 70 nm period with 30 nm line width was achieved

Minimum Feature Size Test

Fig. 1.16 shows the pattern used for minimum feature size test. These patterns were exposed at 100 $\mu C/cm^2$ at 10 kV. Fig. 1.17 shows the post develop image. Details of exposure would be clear in subsequent chapters

- Minimum feature size of 15.63 nm is attained

Stitching Test

Fig. 1.18 shows the pattern and post develop image for stitching test. Exposure was carried out at 10 kV with dwell time > 1 us. Details and procedure for stitching would be clear in subsequent chapters.

- Stitching error is 32.2 nm

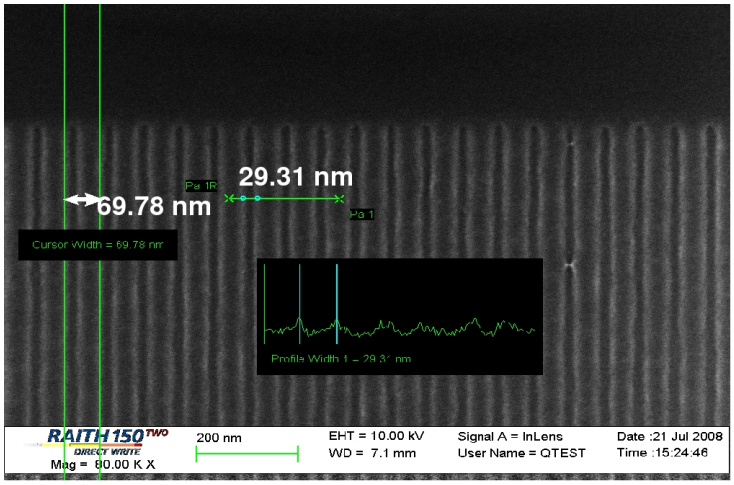

Figure 1.15: Post develop image of high resolution gratings exposed at 20 kV with dose of 100 $\mu C/cm^2$

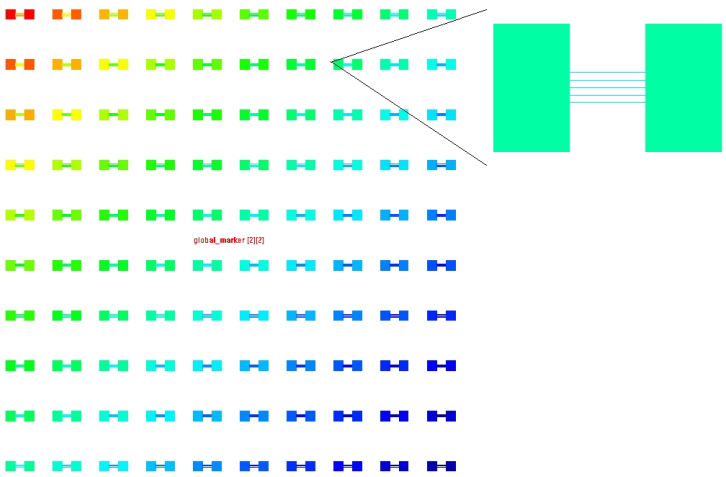

Figure 1.16: Pattern for minimum feature size test

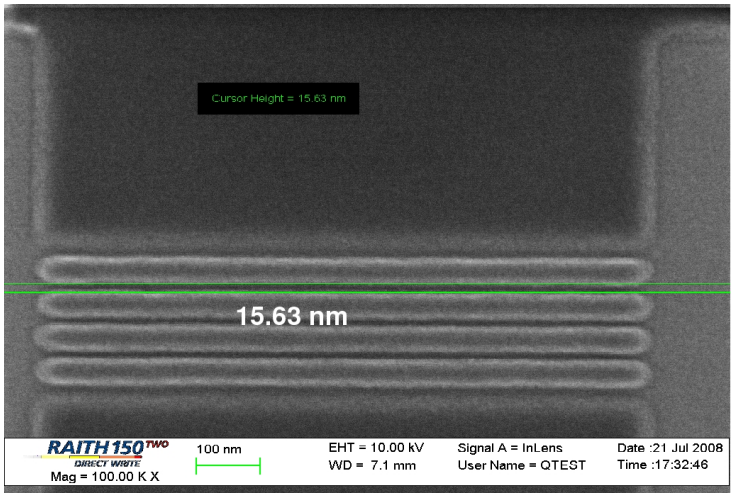

Figure 1.17: Post develop image of patterns shown in Fig. 1.16 exposed at 10 kV with dose of 100 $\mu C/cm^2$

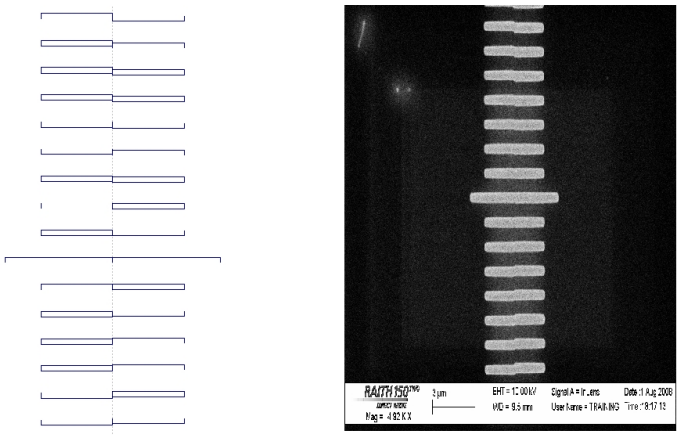

Figure 1.18: Pattern and post develop image for stitching test

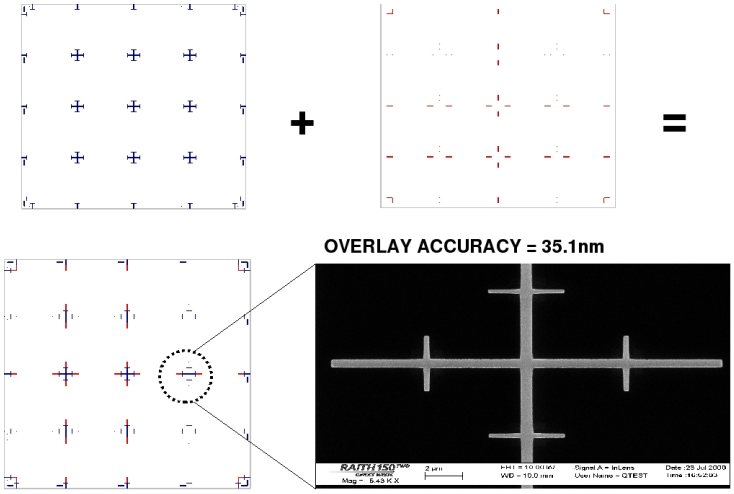

Figure 1.19: Pattern and post develop image for overlay test

Overlay Test

Fig. 1.19 shows the pattern and post develop image for overlay test. Exposure was carried out at 10 kV with dwell time $>$ 1 us. Details and procedure for overlay would be clear in subsequent chapters.

- Stitching error is 35.1 nm

1.4.2 Results of tests performed

- Beam Size Test
  - 1 kV using the 30 um aperture : 3.4 nm
  - 20 kV using the 30 um aperture : 1.7 nm
- Beam Stability Test
  - Beam Position Drift : maximum 80 nm in 14 hours
  - Beam Current Drift : below 0.5% in 11 hours
- Lithography Specifications
  - Minimum Grating Periodicity : 70 nm period with 30 nm line width
  - Minimum Feature Size : 15.93 nm

  - Stitching Error in 100 um write-field : 32.2 nm
  - Overlay Error in 100 um write-field : 35.1 nm

1.5 Typical Electron Beam Lithography process using PMMA

A typical E-Beam Lithography process flow is shown in Fig. 1.20. Below is a brief description of individual process step. Detailed description about the process would be clear from subsequent chapters.

- Mask Design
  - Mask Layout, which has to be printed on to the resist, is designed in software viz. Auto cad, Clewin, Cadence Virtuoso
  - All masks for this project has been designed in Cadence Virtuoso tool, which had to further imported to GDSII format
  - As required by device process flow, appropriate alignment marks are included in the mask layers
  - GDSII is a standard format which is used by most E-beam lithography tool software
- Substrate Preparation
  - Clean the substrate using standard RCA cleaning process
  - Perform dehydration bake on hot plate at 130C for 30 mins
  - Place the substrate on the spinner chuck and drop a few ml of resist using a dropper
  - Select ramping, spin speed and timing based on spin speed curve from data sheet
  - Pre Bake at 180C on hot plate for 90 sec
- Writing Preparation
  - Load the sample on to a stage that has Faraday cup on it
  - Load stage in to the chamber
  - Pump down the chamber
- Electron Beam Alignment and Exposure

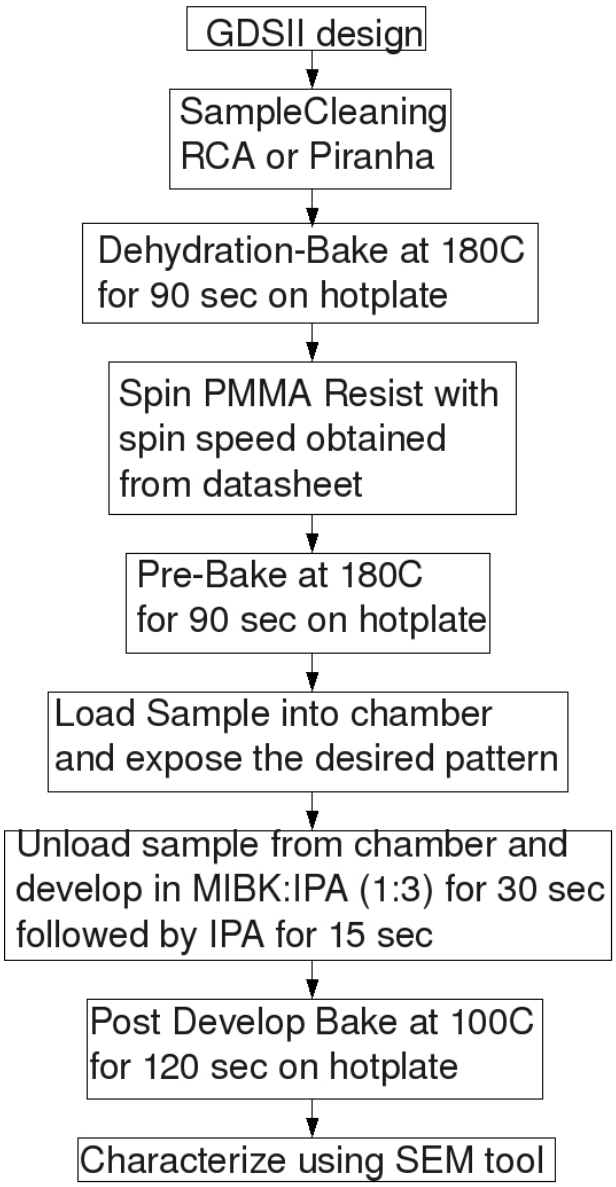

Figure 1.20: Typical Electron Beam Lithography step-by-step process using PMMA

  - Select accelerating voltage and the appropriate working distance from hardware
  - Adjust the focus, astigmatism and aperture alignment
  - Perform stage adjustment and define origin with reference to the sample
  - Move the stage such that Faraday cup is exactly below the e-beam and measure the current
  - Go to the desired location, calculate the dose, select design in position list and expose

- PMMA Developing Process
  - Prepare 30 ml of developer MIBK:IPA (1:3) and stopper IPA in separate labeled beakers
  - Unload the sample from the chamber
  - Immerse the sample in the developer for 30 sec
  - Rinse the sample with IPA for 15 sec
  - Dry the sample with nitrogen gun
  - Post bake at 100C for 120 sec

1.6 Organization of Report

The first two chapters of this report focuses on the fundamental concepts behind the working of the Raith 150 Two EBL tool. The second chapter delves deeper into the EBL process, describing in detail the process of pattern writing and overlay of successive patterns (/layers) using the tool. The third chapter discusses the optimization experiments done with two principal positive and negative e-beam resists - PMMA and HSQ respectively. It details the contrast experiments done using these resists with the Raith 150 Two EBL tool. Chapters 4 and 5 move on to focus on the work done on the mask plates for 500 nm MOSFET fabrication - outlining the mask design process and describing in chronological detail the hurdles faced and solutions obtained during the mask write optimization experiments. Once the mask plates were successfully written, efforts were directed towards successful pattern transfer onto silicon using the DSA optical lithography tool. Chapter 6 describes the experiments done in this regard. The last chapter of this report is devoted to additional process optimization experiments done for specific applications.

Chapter 2

Overlay And Alignment Procedures

Integrated circuits are constructed by successively depositing and patterning layers of different materials on a silicon wafer.[5] Hence the patterning process becomes quite complex as it consists a combination of exposure and development of photo-resist which is followed by etching and doping of the underlying layers and deposition of another layer. In addition to that, the exposure process consists of spinning the photo-resist on to the wafer, projecting the image of the next level pattern onto the resist and finally developing it. Each successive projected image must be accurately matched to the patterns already on the wafer for proper functioning of the IC. This involves the process of determining the position and orientation of the patterns already on the wafer and then placing the projected image in correct relation to these patterns. This process is referred to as *alignment* and the actual outcome or the accuracy with which the successive patterned layer is matched to the previous layer, is termed as *overlay*.
This chapter details the step-by-step procedure to be followed for alignment, exposure and overlay using the Raith 150 TWO e-beam lithography tool. It gives an overview of the concepts involved and then teams it with specific details regarding the tool usage for the same. To begin with, an overview of the main steps of the alignment and overlay procedures on RAITH150 TWO is given as follows[6]

- Stage Adjustment
  - Angle Correction
  - Origin Correction
  - Digital Addressing

- Write Field Alignment
  - Locating a mark or particle
  - Defining the alignment procedure
  - Executing the alignment procedure
- Exposure
  - Measuring the beam current
  - Exposure
  - Developing the sample
  - Multiple exposure
- Overlay Exposure
  - Defining UV positions of marks
  - Locating the first mark
  - 3-point adjustment
  - Semi-automated write field alignment
  - Automated write field alignment
  - Exposure

The following sections describe each of the above steps in detail.

2.1 Stage Adjustment

Stage adjustment allows navigation with blanked beam on the sample in order to find a new exposure area without pre-exposing. It also helps to find an already exposed and processed area for inspection or multilayer exposure.[6] The two coordinate systems viz. XY for the stage and UV for the sample permits the determination of the correct UV sample coordinates independent of how the samples has been mounted on the stage.[6]
The aim of stage adjustment is to perform a permanent coordinate transformation between both XY and UV coordinate systems by finding the relationship between them with respect to shift, scaling and rotation.[6]

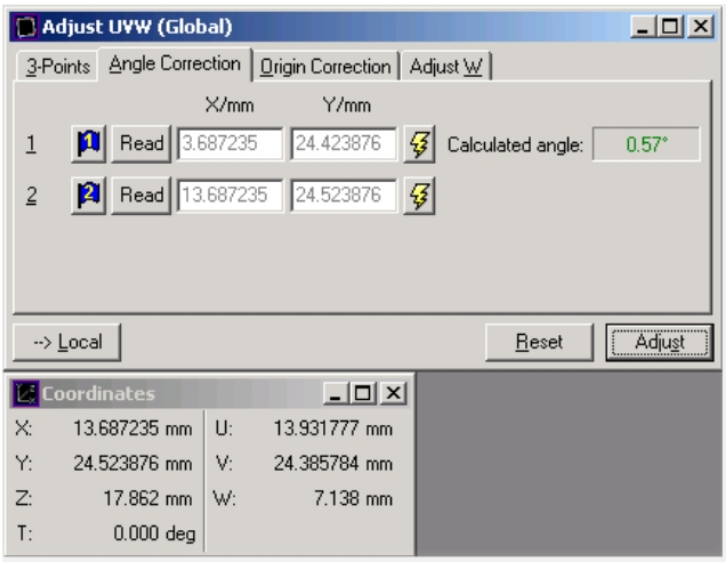

Figure 2.1: Adjust UVW window on Raith150 lithography software[6]

2.1.1 Angle Correction

The axes of the sample surface will not be parallel to the axes of the stage. This difference is compensated by angle correction[6]

- Image the sample at medium magnification, approximately 100x. Ensure that the cross hair is switched ON in the column desktop. Identify the lower edge of the sample and follow this edge to the lower left corner. Adjust the sample such that the cross hair is situated above the lower left corner.

- Open AdjustUVW window on the lithography desktop. Ensure that it is in mode Global; if it is mode Local, click on the button once to change it. Click on Angle Correction Tab (refer Fig. 2.1)

- The actual XY coordinates are displayed in the coordinate window (refer Fig. 2.1). Click on Read at the first position of Flag1 in Adjust UVW and the coordinates will be displayed in the window

- Now switch back to low magnification and move the stage a few millimeters along the sample edge to the lower right corner or any location along the edge itself. Adjust the stage such that the cross hair is situated above the lower right corner or on a location at the edge. Click on

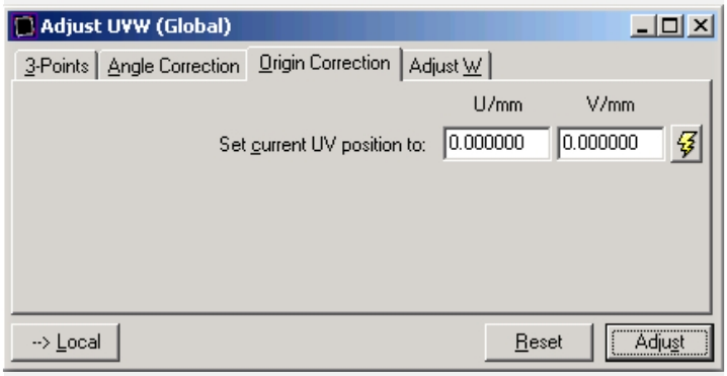

Figure 2.2: Origin Correction tab of Adjust UVW window on Raith150 lithography software[6]

Read at the second position of Flag2 and the second set of coordinates will be displayed in the window

- Click on Adjust to calculate the angle

This angle will now compensate the difference between the sample surface and the stage axes.

2.1.2 Origin Correction

Sample can be placed at any location on the sample holder. Origin correction is applied to compensate for the different origins of XY and UV.[6]

- Make sure that the beam is blanked
- Click on the lightning button of the first coordinates pair to move back to the lower left corner (refer Fig. 2.1).
- Under the tab Origin Correction in Adjust UVW window (ref Fig. 2.2), enter 0 for both U and V values and click on Adjust. The lower left corner is now defined as the origin of this UV coordinate. It is now possible to move the stage to any point on the sample using UV coordinates.

2.1.3 Digital Addressing

Digital addressing allows an user to enter a digital location as coordinates and the stage will drive to this location. This aids navigation on the sample. This task is not vital for the exposure sequence.[6]

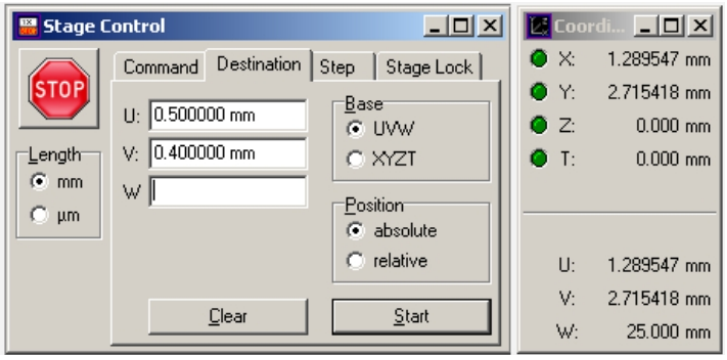

Figure 2.3: Destination tab on Stage Control window on Raith150 lithography software[6]

- Under the destination tab of Stage Control window (refer Fig. 2.3), click on Base UVW and Position absolute. This allows the user to address the stage to any position in UV. W, which is the working distance, is directly related to stage height. That line could be left blank if user does not wants to change the stage height.

- After clicking Start, the stage will move to the sample position entered. In the coordinates window you will see the addressed sample position and the corresponding position in XYZ.

2.2 Write-Field Alignment

Write-field alignment is the adjustment of the electromagnetic/electrostatic deflections system inside the column to the high precision laser interferometer XYZ stage. It is a very central adjustment in the process of getting the best possible e-beam lithographic result. After the alignment, the stage is considered to be "correct" and the electron beam deflection system is aligned to it.[6]
The Align Write Field is a very important task, as it aligns the write field to the sample coordinates UV. For pattern stitching it is essential that the write field is exactly parallel to UV and this can be achieved with the Align Write procedures.
The principle of Write-Field alignment is simple and is as follows[7]

- Some unique and recognizable feature viz. contamination spot, is selected as a mark in the sample

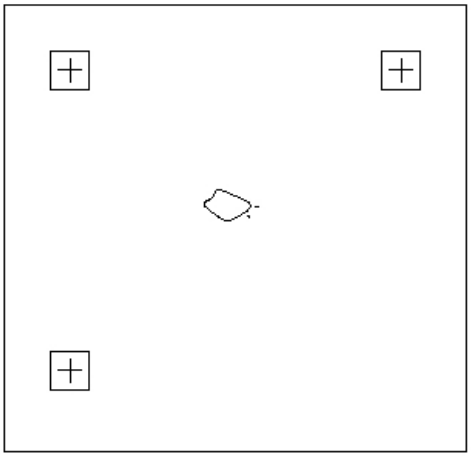

Figure 2.4: Contamination spot at center and three scan fields at the corners of 100 um X 100 um write field[7]

- Magnification corresponding to the write-field size is selected on the lithography software and this setting is transferred to the column software
- The stage moves the centered feature to the three indicated positions shown in Fig. 2.4
- The e-beam is deflected at each position as much as to be able to scan that area
- A scanned image is presented to the operator which indicates the position of the cursor
- This position is taken as a "corrective" position
- This procedure is repeated for all the marks
- The new correction parameters are computed and presented to the operator to acknowledge
- The above steps are repeated with smaller scan fields until there is no decrease in correction factors

The laser interferometric stage is considered to a perfect reference coordinate system with X and Y axes exactly perpendicular to each other and of

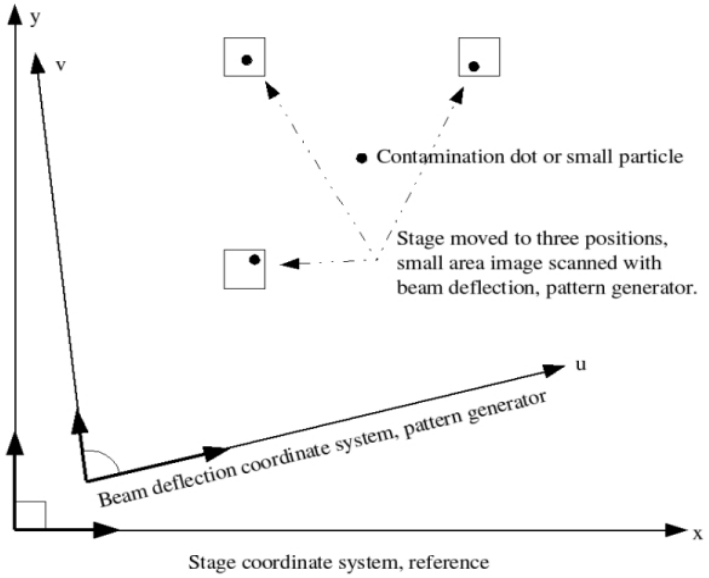

Figure 2.5: Stage and Beam deflection coordinate system showing that the U and V axes are not parallel to either of the stages X or Y axes, neither the U and V axes are perpendicular to each other[7]

exactly the same scale. But, the coordinate system for the e-beam deflection inside the column has long term drift in its components due to the several stages (D/A converters, drive amplifiers, etc.) that the signal, that deflects the beam, passes through. Hence, the U and V axes are not parallel to either of the stages X or Y axes, neither the U and V axes are perpendicular to each other (refer Fig. 2.5).

The following sections shows how a write-field alignment procedure is carried out using Raith150 TWO Lithography software[6]

2.2.1 Locating a mark or particle

- Move stage back to the lower left corner of the sample by pressing the lightning icon in the AdjustUV window (refer Fig. 2.2) on the origin correction
- Locate a small dust particle or contamination spot that can be used as a mark for the following tasks
- Choose the window Microscope Control which can be found in the Microscope Control part at the right side of the lithography software

(refer Fig. 2.6)

- The appropriate write field is selected and activated at the top part
- All WF-alignment procedures are available in the Scan manager window.

2.2.2 Defining the alignment procedure

- Choose scan manger on Microscope Control window (refer Fig. 2.6)
- Choose Align Write Field procedure and Manual from the sub-procedure menu
- Start with 100 um WF with 25 um mark scans
- Drag and drop 100 um WF - Manual ALWF 25 um marks in to the position list and press "Scan" (refer Fig. 2.7)

2.2.3 Executing the alignment procedure

We will now execute the alignment procedure, which will scan the three mark areas to determine the difference between the real and ideal positions.

- Ensure that the position list, where the procedure has been stored, is active.Choose from the menu Scan > Selection
- Each mark will be scanned and the image will be presented to the operator, who in turn will indicate the position of the selected feature with mouse as shown in Fig. 2.8
- Fig. 2.9 shows one of the positions scanned and the feature selected with the cursor
- The order of pressing keys is important so as to the position of the feature[7]
  - Press and hold down the <ctrl>-key
  - Press and hold down the left mouse button, pointer can be anywhere inside the scanned picture
  - Drag the mouse so the cursor indicates the desired feature, a rubber-band should appear
  - Release the left mouse button

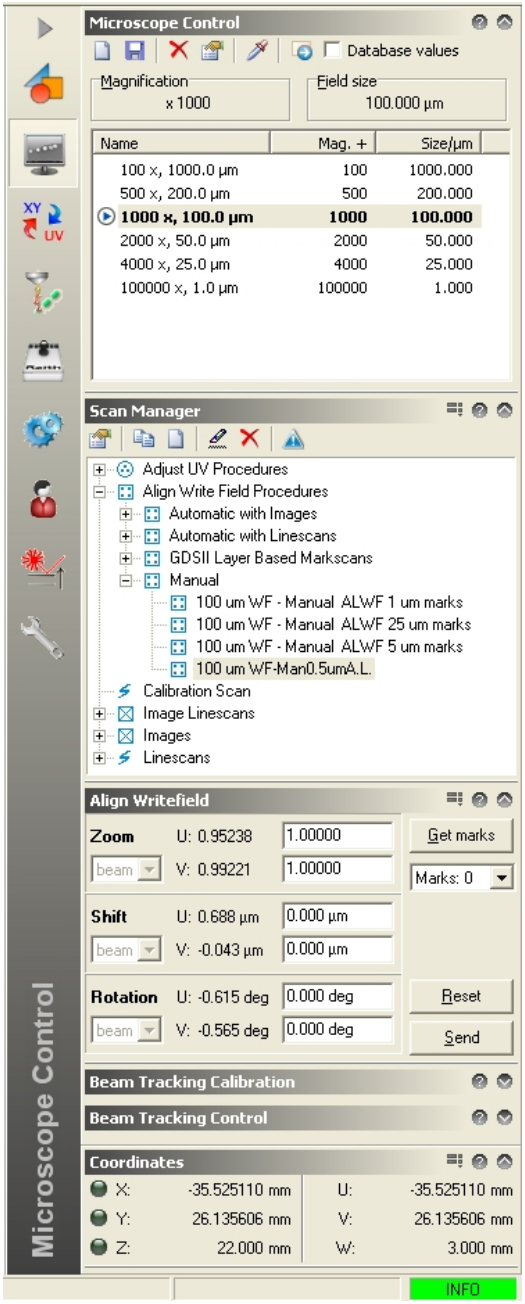

Figure 2.6: Microscope Control Window

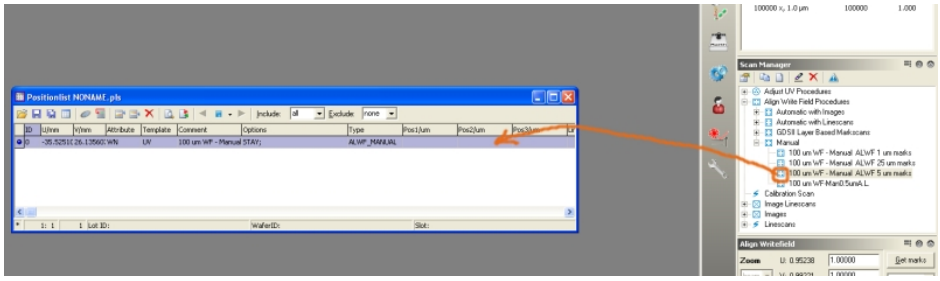

Figure 2.7: Positionlist with manual write field alignment procedure selected. This procedure is carried out with 100 um write field and 5 um mark scans

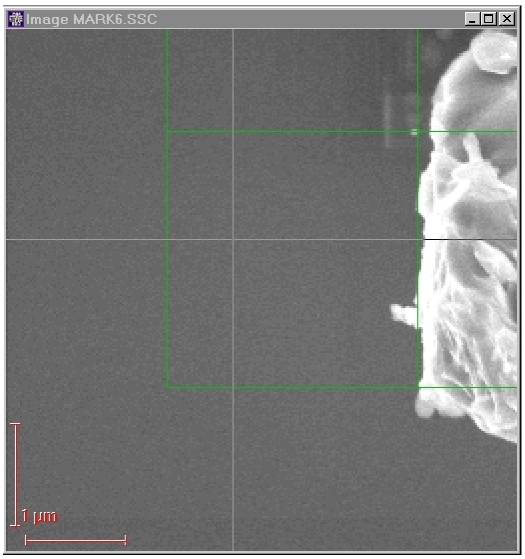

Figure 2.8: Image Scan presented before the operator who in turn will indicate the position of the selected feature[7]

Figure 2.9: Image Scan presented before the operator at the new position showing one of the positions scanned and the feature selected with the cursor[7]

  - Release the <ctrl>-key
  - A blue cross should appear centered over the selected feature as shown in Fig. 2.9

- These steps must be repeated for each mark
- At the end of the position list a dialog window opens and write field correction has to be confirmed as shown in Fig. 2.10. Note the values of the Align Write field for Zoom, Shift and Rotation in UV and confirm if the values are acceptable
- Left column of numbers shows the alignment parameters before alignment whereas the new alignment parameters have been calculated as shown in the center column. These values would be then sent to the pattern generator and displayed on the left side

2.3 Exposure

The aim of this section is to guide through the steps needed to carry out an exposure.[6]

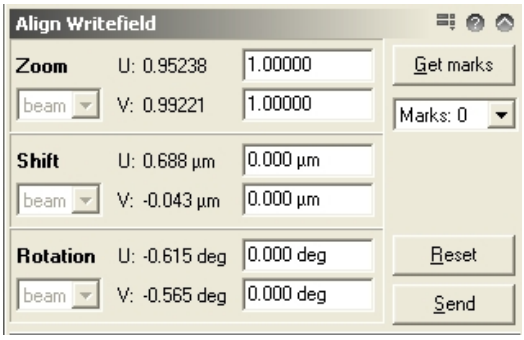

Figure 2.10: Window showing WF parameters Zoom, Shift and Rotation in UV[7]

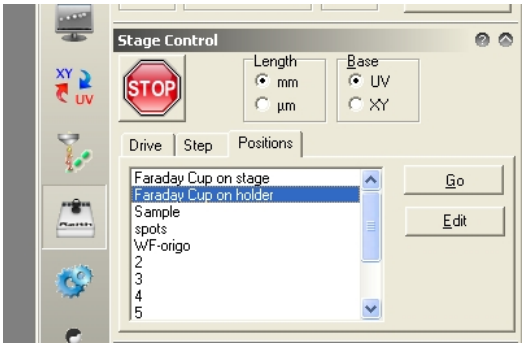

Figure 2.11: Stage Control Window showing positions which may already be stored as one of the user positions[7]

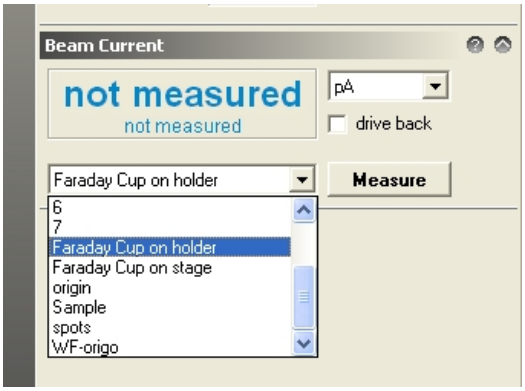

Figure 2.12: Beam Current Window where you click "measure" to take the current value which will change the blue text from "not measured" to the current value[7]

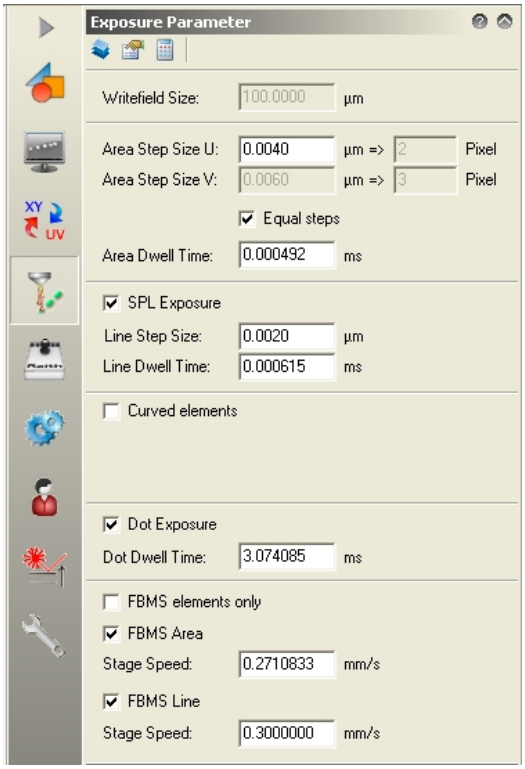

Figure 2.13: Exposure Parameter window showing the small calculator icon at the top to open the exposure parameter calculation window shown in Fig. 2.14[7]

2.3.1 Measuring the beam current

- Open the Stage Control window and drive to one of the Faraday cups. Its position may already be stored as one of the User positions as shown in Fig. 2.11
- All the electrons from the beam are captured at the Faraday cup, and a true value of the probe current can be measured
- Open the beam current window as shown in Fig. 2.12 and click "measure" to take the current value. The blue text will change from "not measured" to the current value

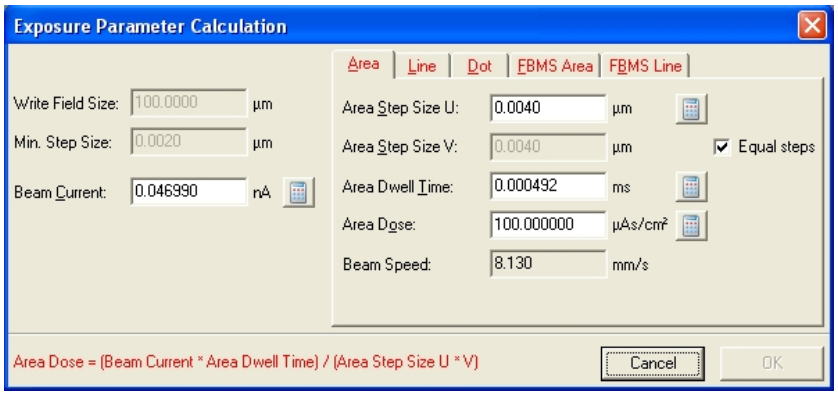

Figure 2.14: Exposure Parameter Calculation window where you select the area, line, dot, FBMS Area and FBMS Line tabs to enter the dose value, which depends on your resist[7]

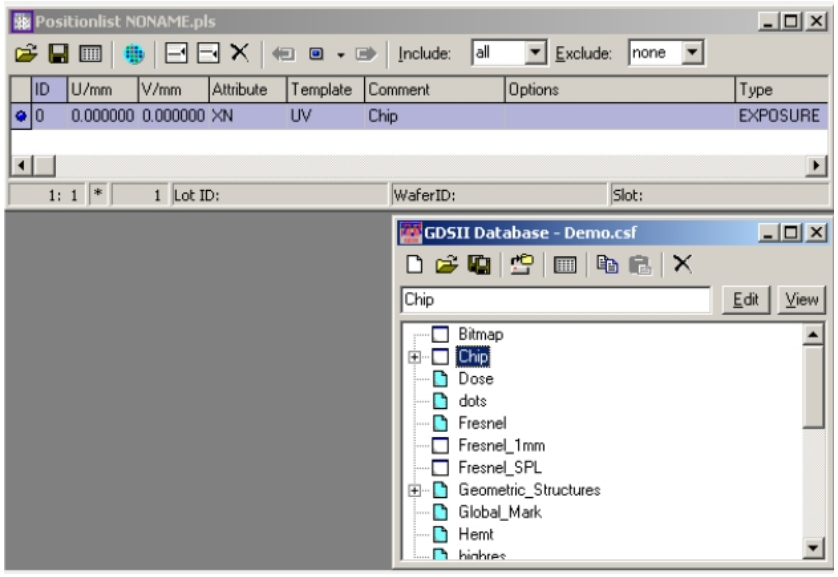

Figure 2.15: Positionlist window showing the design selected and location of design, for exposure[6]

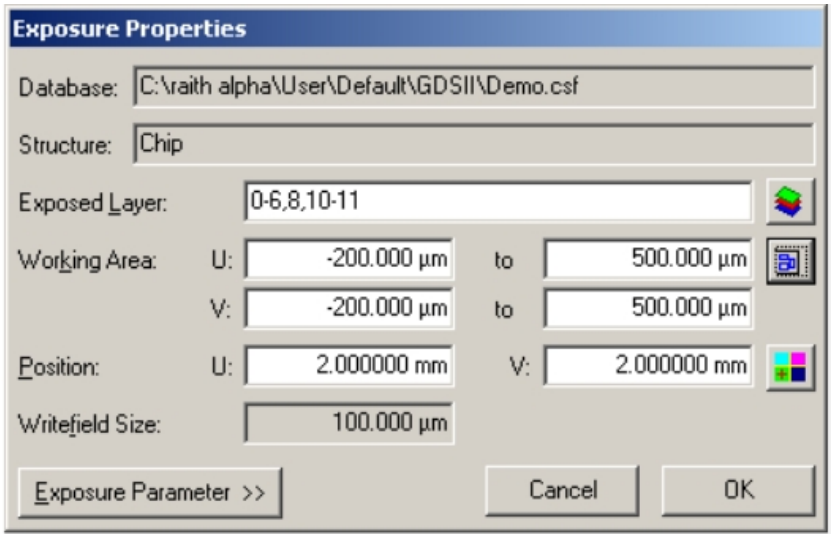

Figure 2.16: Exposure Properties window showing the current sample position where the exposure is scheduled[6]

2.3.2 Exposure

- Open a New Position list as shown in Fig. 2.15. Drag and drop Design Chip into the position list
- The exposure is scheduled for the current sample position by default. Hence, the next step is to change the exposure position to the required location. The new location is entered in the "Position" field of the exposure properties window shown in Fig. 2.16
- In the exposure properties window (refer Fig. 2.16), enter the appropriate layer
- Open the exposure parameter calculation window shown in Fig. 2.14, by clicking the small calculator icon at the top of the Exposure Parameter window shown in Fig. 2.13, select the area tab, and enter the dose value, which depends on your resist. For e.g., if you use PMMA 950K molecular weight with 100 nm thickness and a beam voltage of 10kV, the area dose is 100 $\mu C/cm^2$.

$$AreaDose = \frac{DwellTime * BeamCurrent}{StepSize^2} \tag{2.1}$$

- Enter the step size of 0.020 um and click on the calculator button next to Dwell time shown in Fig. 2.14

  - **Dwell time** is the time the beam is still at each location
  - The length the beam is moved between each dwell time is referred to as **step size**

- Activate the position list. Go to the Menu Bar > Scan > All. The stage will now drive to the position to expose the pattern

2.3.3 Developing the sample

- Unload the sample
- Prepare 30 ml of developer MIBK:IPA (1:3) and stopper IPA in labeled beakers
- Immerse the sample in the developer for 30 sec
- Rinse the sample with IPA for 15 sec
- Dry the sample with nitrogen gun
- Load the sample back to the chamber for inspection. Perform the stage alignment and address the corresponding sample positions

2.3.4 Multiple Exposure

This step is needed for obtaining the optimized dose for a given pattern. If the correct dose is not known, a method is explained demonstrating exposure of the same pattern with different doses to reduce the dose parameter range values.

- The same structure is exposed several times with different doses, as it has no dose variation.Highlight the line in the position list, select Filter > Matrix Copy, the window shown in Fig. 2.17 will pop-up
- Enter values or Matrix size, step size and dose scaling
- For the example window shown in Fig. 2.17, the structure will be exposed 4 times with a different dose, always increasing by 50 %

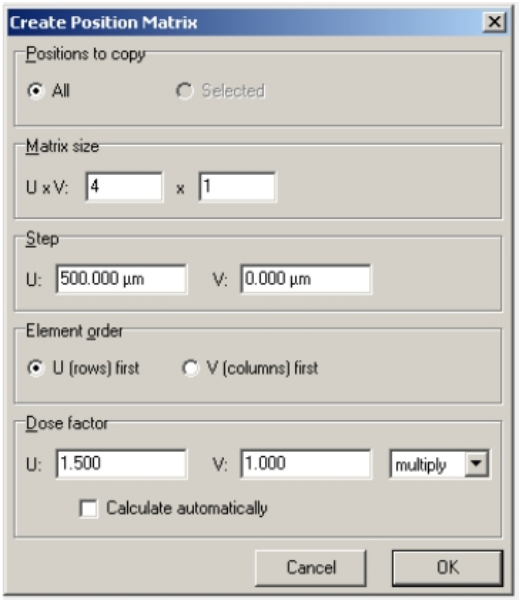

Figure 2.17: Create Position Matrix window which shows that the structure will be exposed 4 times with a different dose, always increasing by 50 %[6]

2.4 Overlay Exposure

Overlay exposure is necessary when a device flow necessitates multiple lithography steps. Overlay is the successive lithography step, involving the placement of a new pattern(/layer) on to an existing pattern. For achieving maximum accuracy in this procedure, global and local alignment marks are included in the pattern design. Global alignment marks are needed to locate the design and local alignment marks are used for semi-automated and automated write field alignment. It is necessary that these alignment marks are included in the first pattern (/layer) and are exposed during the first pattern(/layer) e-beam write procedure. These alignment marks are then imaged, scanned and used for aligning the successive patterns (/layers) as described in the following sections. An example of the position and location of global as well as local alignment marks to be used for overlay exposure is shown in Fig. 2.18

2.4.1 Defining UV positions of marks

- Open the pattern shown in Fig. 2.18 in GDSII viewer along with the tool bar. Drag and drop green flag 1 onto first alignment mark (refer

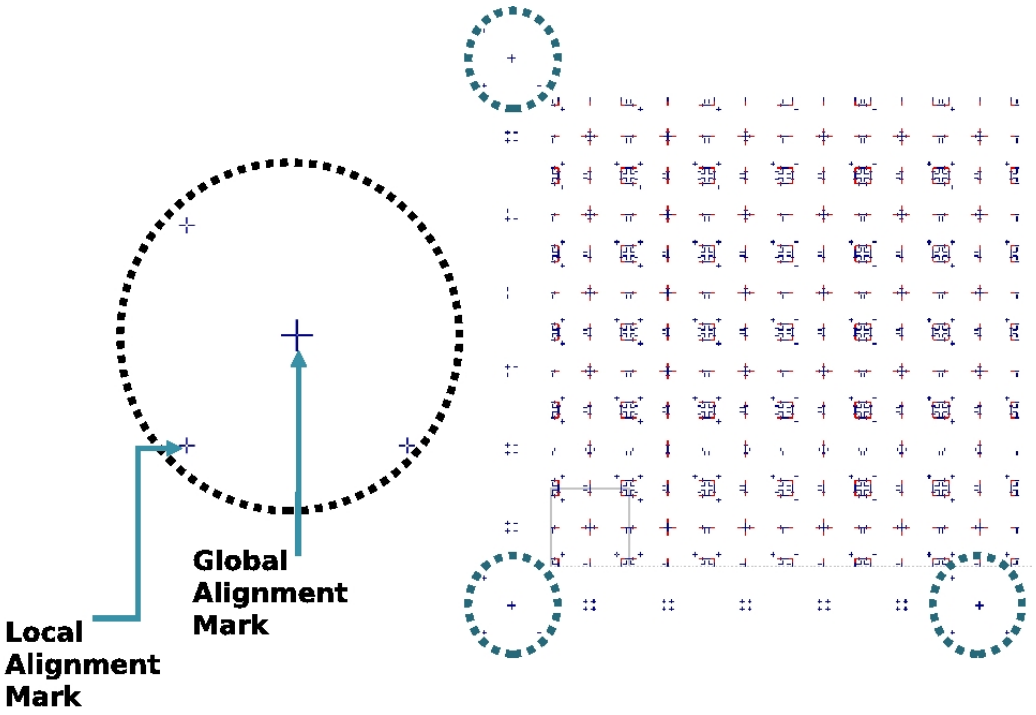

Figure 2.18: Placement of Global Alignment marks and Local Alignment marks

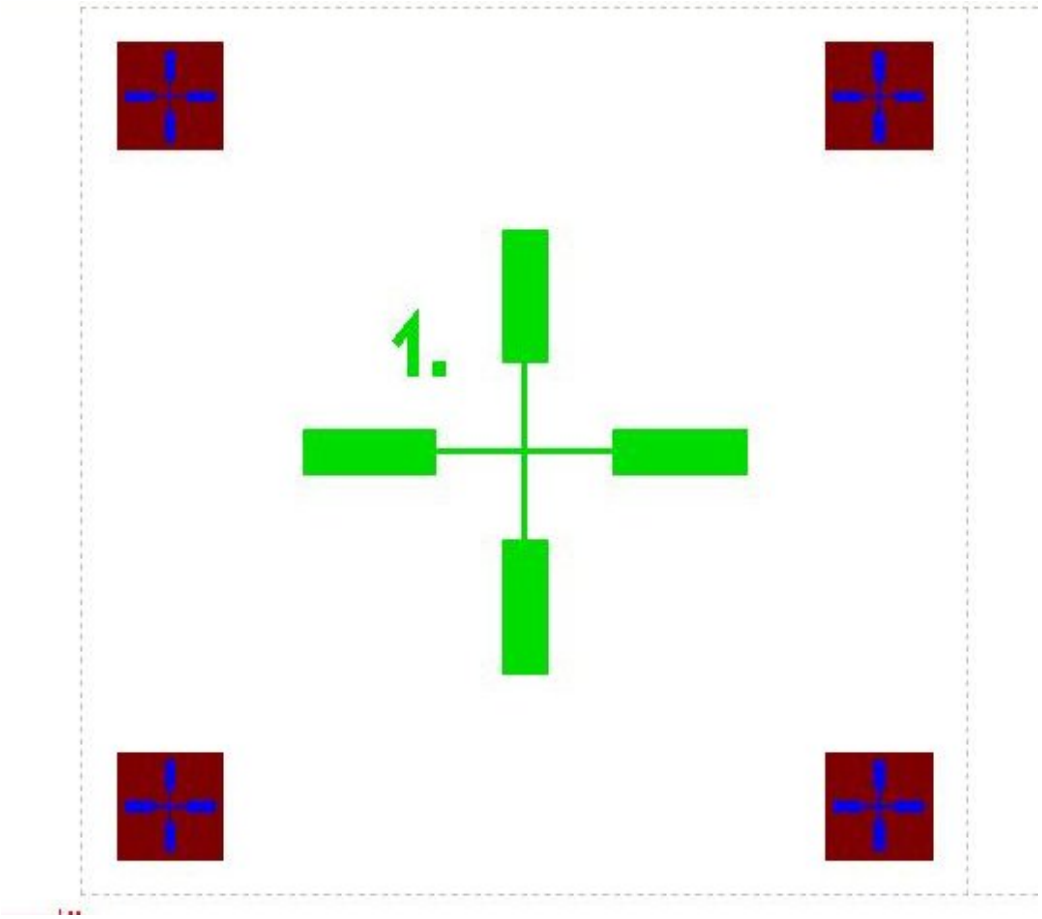

Figure 2.19: Global Alignment mark at the center which is used only to locate the design and local alignment marks at the corners with manual marks scans used for semi-automated write field alignment

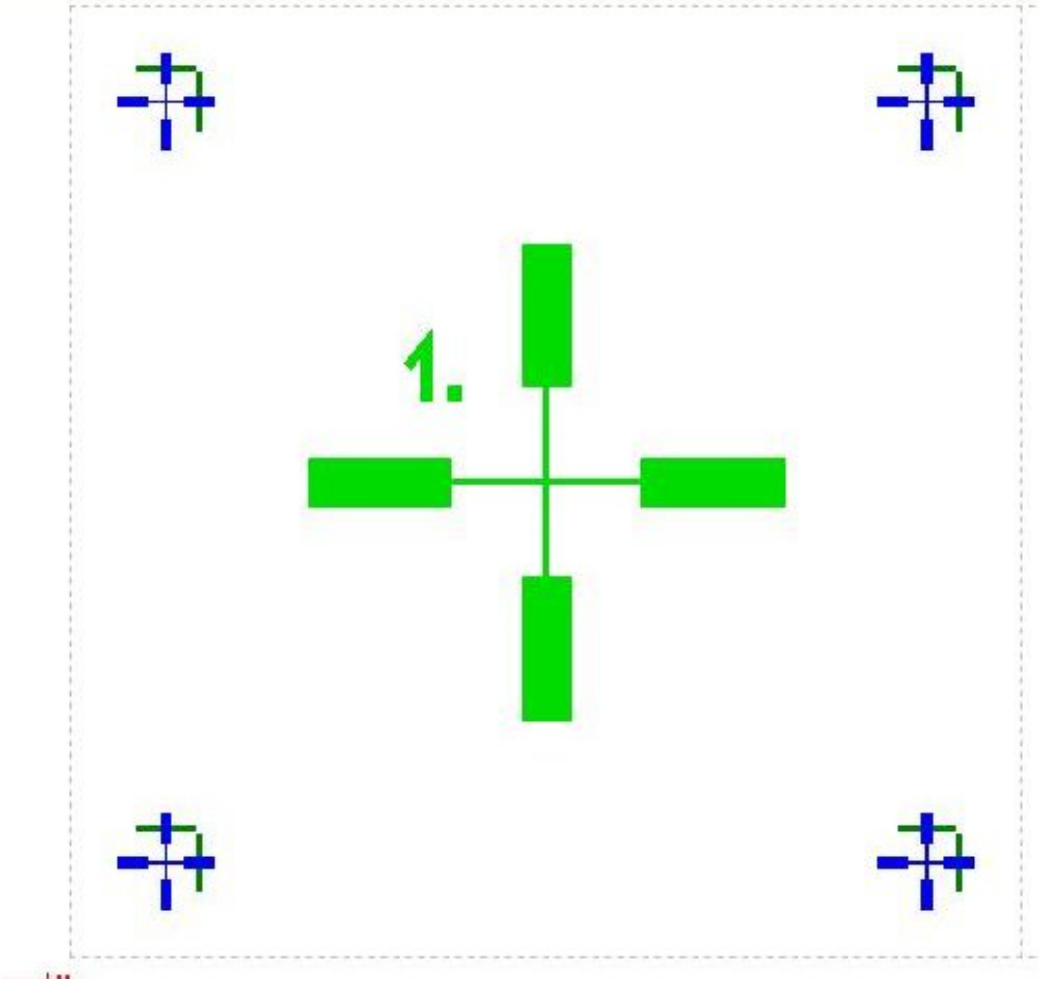

Figure 2.20: Global Alignment mark at the center which is used only to locate the design and local alignment marks at the corners with line scans used for automated write field alignment

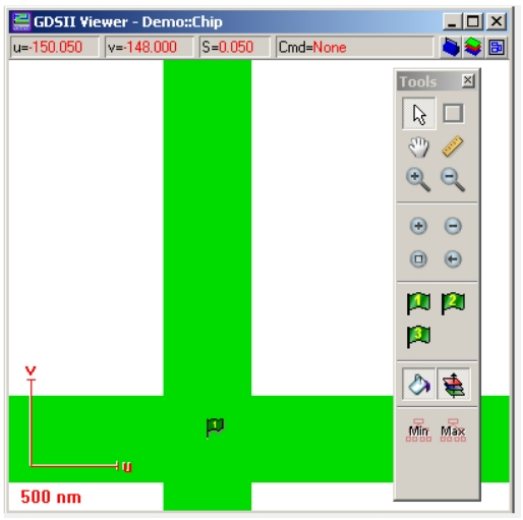

Figure 2.21: GDSII viewer alongwith the toolbar where we need to drag and drop green flag 1 onto first alignment mark[6]

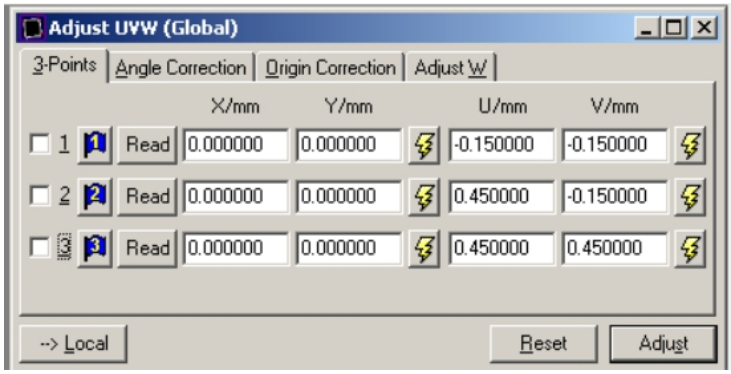

Figure 2.22: 3-points tab of Adjust UVW(Global) window which displays the UV coordinates for mark 1[6]

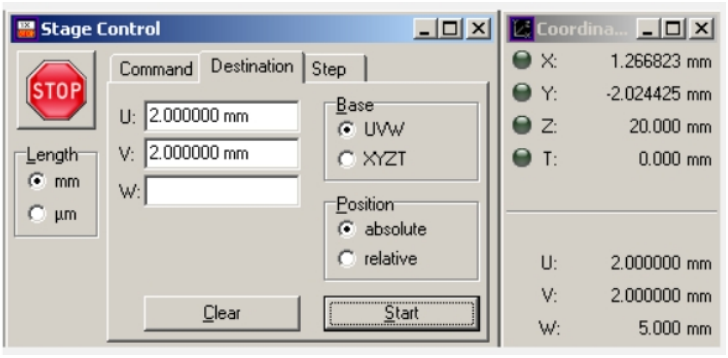

Figure 2.23: Stage Control window where you need to enter the UV values for your design[6]

Fig. 2.21). The UV coordinates for mark 1 will now be displayed in the Adjust UVW window (refer Fig. 2.22)

- Repeat the same procedure for marks 2 and 3
- According to our example (as observed from Fig. 2.22), mark 1 is located at U=V=-150 um, mark 2 is located at U=450 um and V=-150 um and mark 3 is located at U=V=450 um
- Uncheck all three positions as shown in Fig. 2.22

2.4.2 Locating the first mark

These steps are performed after the exposure and development procedure which are mentioned in previous sections. After developing the sample, load the sample into the system again, and perform steps described in the section 'Stage Adjustment'[6]

- To locate the first mark, open the stage control window shown in Fig. 2.23 and enter the UV values for your design. Click on Start
- Select a magnification of 3000x on the column software, switch ON the cross hair and unblank the beam. The first mark should now be visible as shown in Fig. 2.24. Move the cross hair over the mark using joystick and switch OFF the beam
- The next task is to perform 3-point adjustment

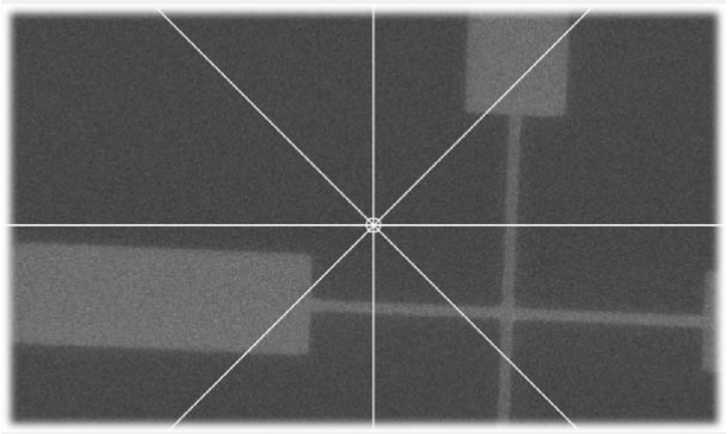

Figure 2.24: Location of first Global alignment mark. The cross hair should be moved over the mark using joystick[6]

2.4.3 3-point adjustment

- Select the tab 3-points in the Adjust UVW window and switch to Local coordinator transformation as shown in Fig. 2.25. Do not confuse this with local alignment marks. Both are separate issues
- Choose Read to update the current XY coordinates of the first mark position. Activate check box 1 of the same position (refer Fig. 2.25)
- In principle, we have performed an origin correction i.e. the origin of the coordinate system has been redefined
- Click on the lightning icon of mark 2 related to the UV coordinates. This will move the stage to the second mark
- Select a magnification of 3000x on the column software, switch ON the cross hair and unblank the beam. Move the cross hair over the second mark using joystick and switch OFF the beam
- Click on Read of mark 2. The XY coordinates in the Adjust UVW window will be updated
- Click the check box of mark 2 and click Adjust
- Click on the lightning icon of mark 3 related to the UV coordinates. This will move the stage to the third mark

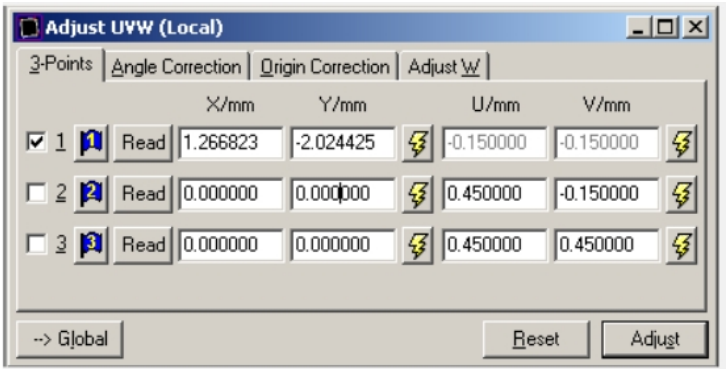

Figure 2.25: 3-points tab of Adjust UVW window where we need to switch to Local coordinator transformation[6]

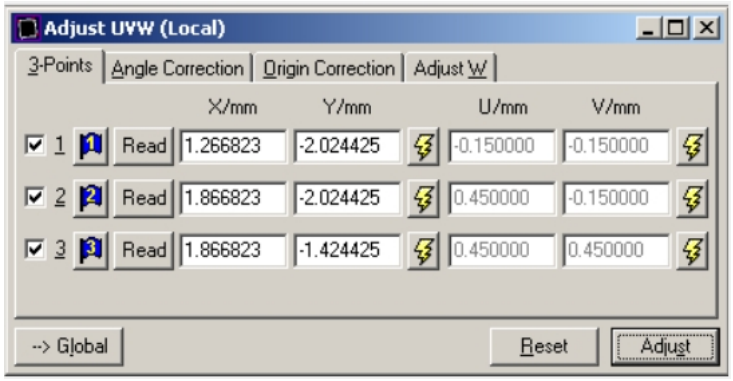

Figure 2.26: 3-points tab of Adjust UVW(Local) window which shows updated XY coordiantes of the first mark position[6]

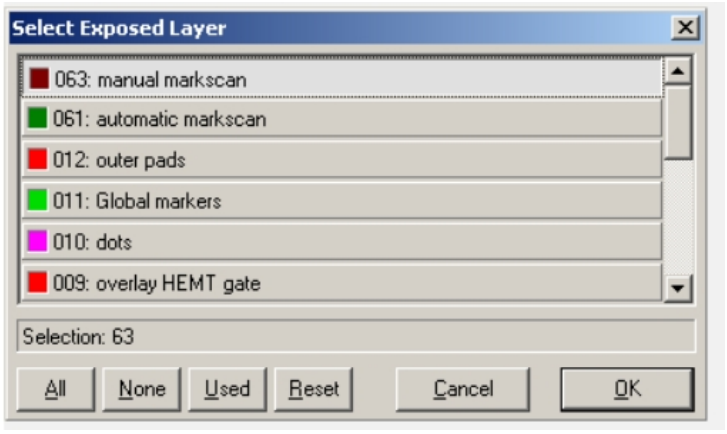

Figure 2.27: Layer Selection Window with "manual markscan" layer selected[6]

- Select a magnification of 3000x on the column software, switch ON the cross hair and unblank the beam. Move the cross hair over the second mark using joystick and switch OFF the beam
- Click on Read of mark 3. The XY coordinates in the Adjust UVW window will be updated
- Click the check box of mark 3 and click Adjust. Please note that the UV coordinates have been updated after the adjustment has been performed refer(Fig. 2.26)

2.4.4 Semi-automated write field alignment

In applications, where only a small number of alignments are necessary, or difficult mark detection conditions exist, a semi automated procedure is more appropriate. This procedure interacts with the operator and hence, more reliable results can be achieved. Refer Fig. 2.19 for alignment mark pattern and manual mark scan[6]

- Move the stage back to the first mark by pressing the corresponding lightning icon shown in Fig. 2.26
- Open the microscope control window and select 100 um write field with magnification 1000x (refer Fig. 2.6)
- Open a new position-list and drag and drop the GDSII design in the position list

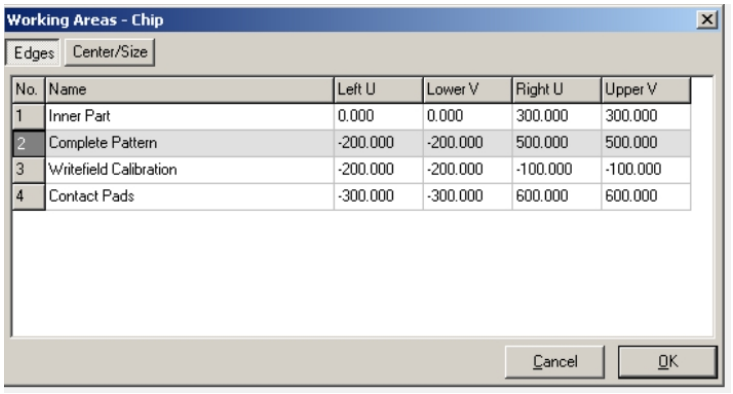

Figure 2.28: Working Area Window[6]

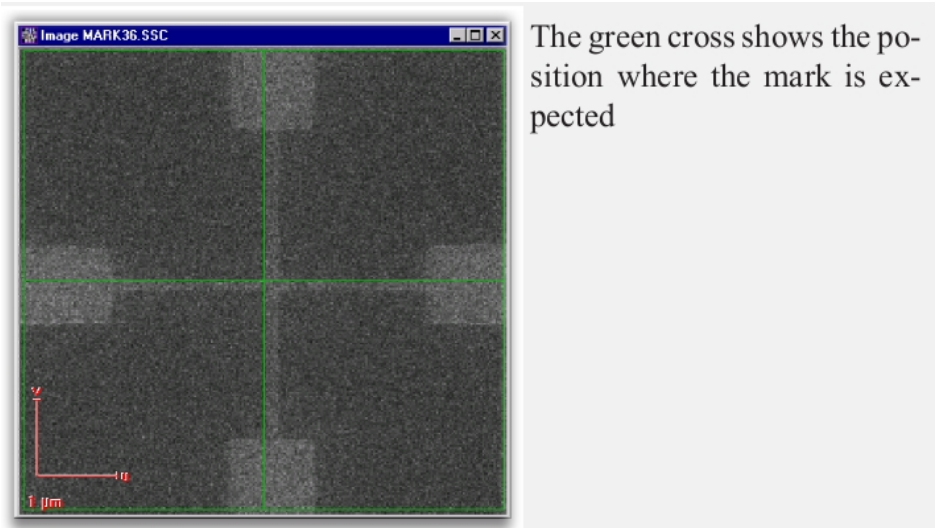

Figure 2.29: Image Scan Window with green cross showing the position where the mark is expected[6]

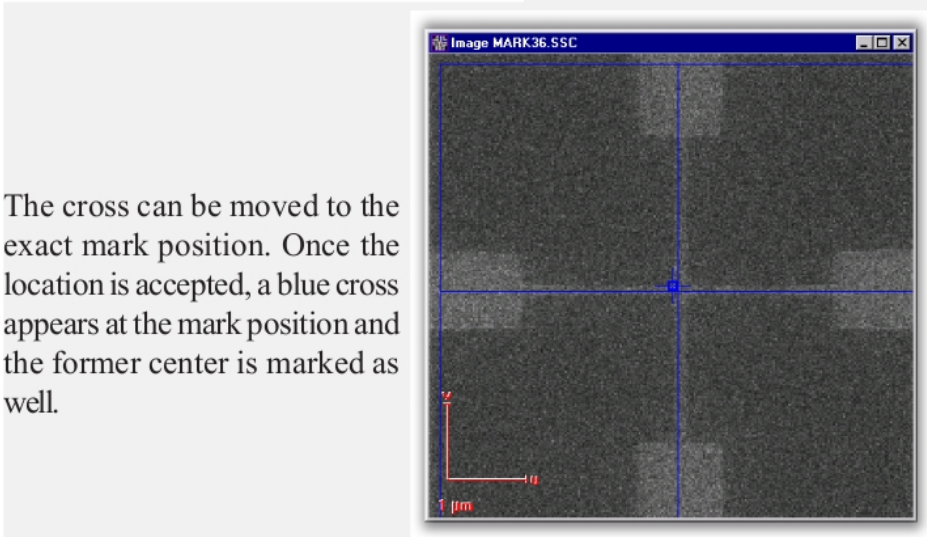

Figure 2.30: Image Scan Window with blue cross showing that the location is accepted[6]

- Select the line in the position list using the right mouse button. Select Properties. Click on the layer icon and select layer 63 which is "manual markscan" (refer Fig. 2.27). Manual markscan is nothing but a box placed around the local alignment marks shown in Fig. 2.19. This markscan procedure scans the whole box, and hence the local alignment marks are scanned. This would be more clear in subsequent steps

- Click on the Working area icon and select the Working area Write field Calibration and confirm with OK (refer Fig. 2.28). Adjust the UV position by pressing the corresponding button (refer Fig. 2.16) This command will use the pre-defined working area and the write field size to calculate the correct sample UV position. It is very important to set-up the write field and working area beforehand

- Activate the position list and select Scan > All from menu bar. This would drive the stage to the corresponding position and exposure on layer 63 will be initiated. After the first scan, the software will pause to await interaction with the user (refer Fig. 2.29)

- Green cross displayed at the center of the image (refer Fig. 2.29) defines where the mark is expected. The mark will probably not be at the center, but it can be now defined manually. To define the position of the mark, follow the instructions below

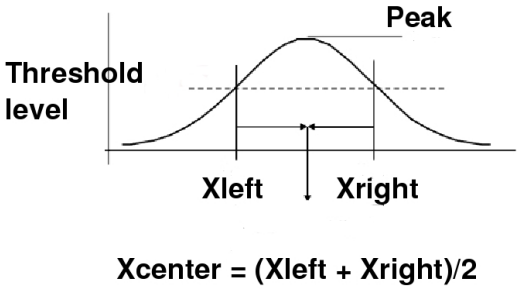

Figure 2.31: The threshold algorithm estimates the center mark *Xcenter* by finding the midpoint between the threshold crossover positions *Xleft* and *Xright*[5]

  - Keep <ctrl> key and left mouse button depressed
  - Move the mouse cursor to the required position
  - On reaching the new position, release the <ctrl> key and a blue cross will be displayed at the selected position as shown in Fig. 2.30

- Click on Continue to proceed with the position list and the following mark scans

2.4.5 Automated write field alignment

Automated write field alignment is based on "Threshold algorithm". Consider an isolated single bump in the signal data i.e changes in intensity over the length of scan as shown in Fig. 2.31. The threshold algorithm attempts to find the bump centroid by finding the midpoint between the two values of x at which the bump has given a value called, the threshold.

- Move the stage back to the first mark by pressing the corresponding lightning icon shown in Fig. 2.26
- Open the microscope control window and select 100 um write field with magnification 1000x (refer Fig. 2.6)
- Open a new position-list and drag and drop the GDSII design in the position list
- Select the line in the position list using the right mouse button. Select Properties. Click on the layer icon and select layer 61 which is "Automatic markscan" (refer Fig. 2.32). Automatic mark scans are

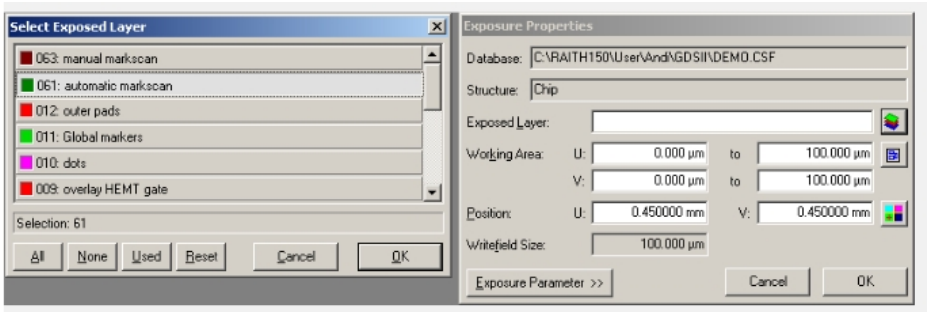

Figure 2.32: Exposure Layer window with layer 61 (i.e. automatic markscan) selected[6]

lines drawn across each cross of the local alignment marks shown in Fig. 2.20. This would be more clear in subsequent steps

- Click on the Working area icon and select the Working area Write field Calibration and confirm with OK (refer Fig. 2.28). Adjust the UV position by pressing the corresponding button (refer Fig. 2.16) This command will use the pre-defined working area and the write field size to calculate the correct sample UV position. It is very important to set-up the write field and working area beforehand

- Activate the position list and select Scan > All from menu bar. This would drive the stage to the corresponding position and exposure on layer 61 will be initiated. A new position list called *align.pls* will be created which stores a set of mark detections and is executed automatically. During the execution, several line scans will be displayed. It is unlikely that there will be a valid parameter set for mark detection within line scanning, and hence many errors will be shown. Once the execution of the position list is complete, the software closes the position list, which will closes all the line scans

- Now we have to find a parameter set such that during the automated align write field procedure, the software will be able to detect all the marks. For this, open the position list *align.pls* which is usually stored in user directory "Data"

- The position list looks something like shown in Fig. 2.33. The red light indicates that the line scans could not be completed successfully. The corresponding attributes show LE for Line scan error and LS for Line scan Successful

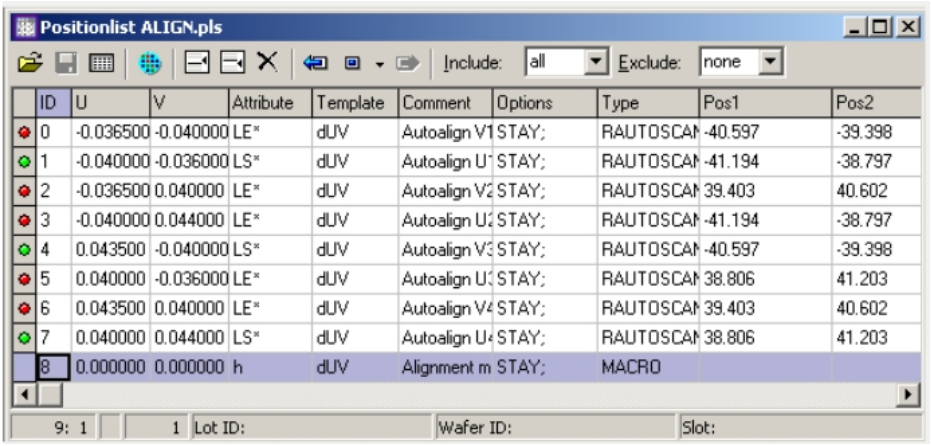

Figure 2.33: Position List *align.pls* which stores a set of mark detections and is executed automatically[6]

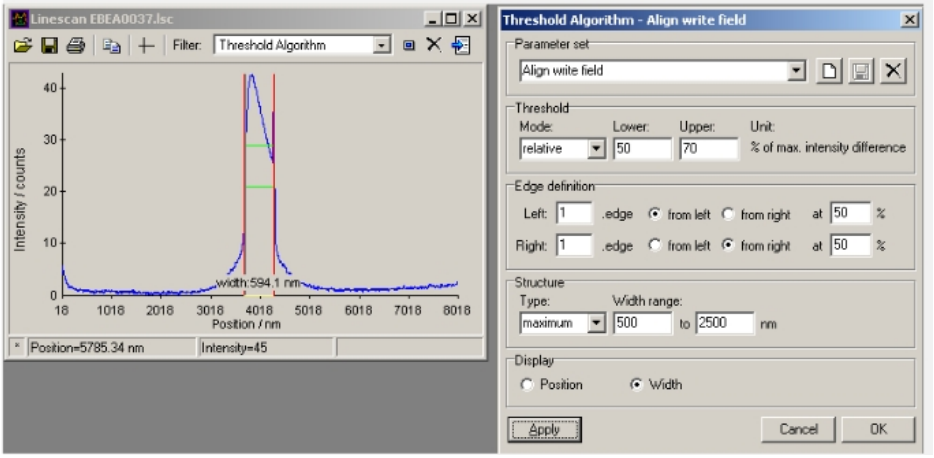

Figure 2.34: Line scan window with Threshold algorithm selected[6]

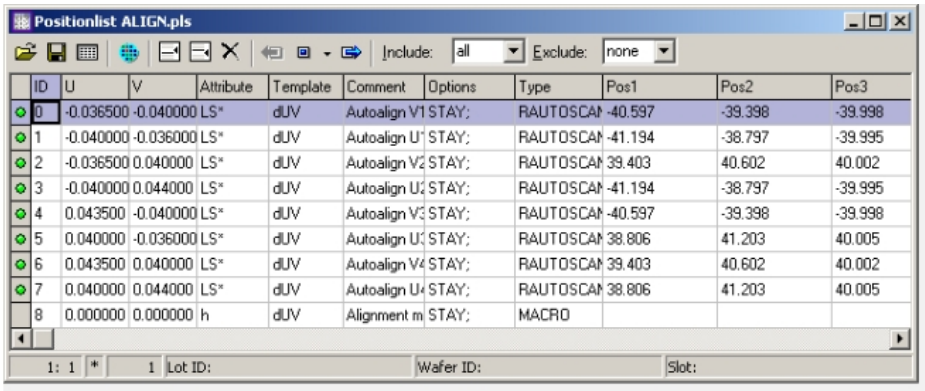

Figure 2.35: Positionlist *align.pls* with all successful line scans[6]

- Double click on one of the lines with an error and the corresponding Line scan will be opened (refer Fig. 2.34). Select the Threshold Algorithm from the drop down list and choose the Apply button
- Now select the parameter called "Align Write-field" from the drop down list and select "Relative". Select 50% of max. intensity difference for Lower and select 70% of max. intensity difference for Upper
- For edge definition, select 1^{st} edge from left and 1^{st} from right. Select 50% for both edges
- For structure, select type Maximum and a width range from 500 nm to 2500 nm
- On pressing Apply, the software applies the threshold algorithm with the parameter set chosen to the corresponding Line scan. If it were able to detect a mark, then the corresponding result will be displayed in the line scan by plotting red bars and a particular line width bar
- Save the parameters and close the window
- Now to verify the parameter set, activate the window "Positionlist align.pls and in menu bar, press Scan > All
- It is very likely that the software will now be able to apply the Threshold algorithm to all the Line scans. Therefore, there will no longer be an error message in the position list (refer Fig. 2.35)
- Open a new position list. Drag and drop the GDSII design and select second layer from layer window

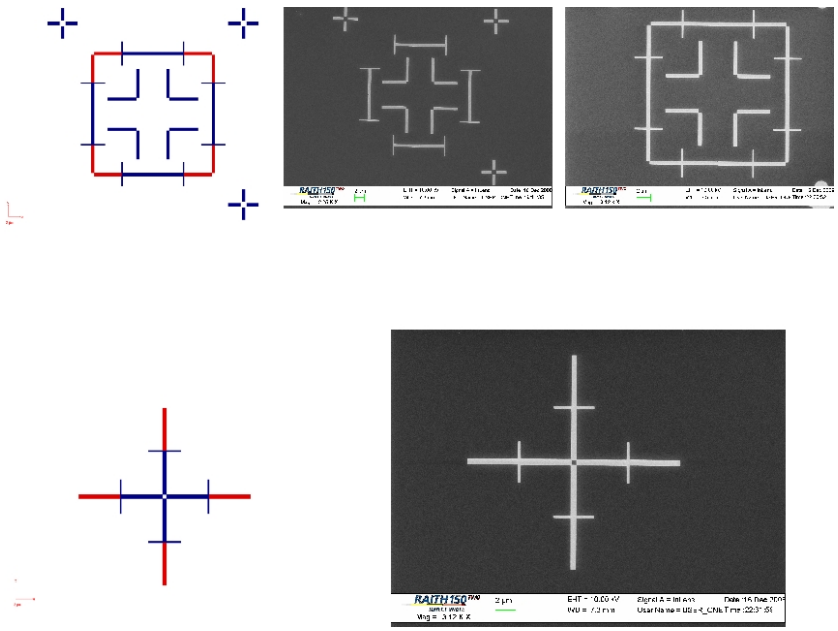

Figure 2.36: Overlay Exposure Results. Blue layer is layer 1 and Red layer is layer 2

- Select working area as "Complete Pattern", and adjust UV position by pressing the corresponding button. The remaining steps remain same as discussed above in the Exposure section of this chapter
- Fig. 2.36 shows the results of overlay exposure. Blue layer was exposed in first level, followed by the red layer which is exposed in the second level using manual and automatic write field alignment procedures discussed

Chapter 3

Pr cess Optimization for High Resolution Nanolithography

This chapter details the experiments done to extract the contrast values of e-beam resists used in the Raith 150 TWO tool. Two e-beam resists - namely, PMMA and HSQ, were evaluated in this context. Furthermore, different developing conditions were tested for their effect on the resist contrast values. Based on the clearing dose window obtained from the contrast curve experiment, direct transfer of high-resolution (100 nm) pattern lines onto silicon was attempted. The results of the same are presented at the end of the chapter.

3.1 Contrast and Critical Modulation Transfer Function

The recording and transfer media for e-beam lithography are electron beam resists, which are usually polymers that dissolve in a liquid solvent. PMMA is an example of positive tone e-beam resist that undergoes main chain scission, when exposed to e-beam as shown in Fig. 3.1.[3]
Contrast and Critical Modulation Transfer Function are the two basic parameters often used to describe the properties of photo-resists. Contrast is actually a measure of the resist's ability to distinguish light from dark areas in the aerial image produced by the exposure system.
Contrast can be expressed by the following equation:

$$\lambda = \frac{1}{log_{10}\frac{D_{CL}}{D_0}} \tag{3.1}$$

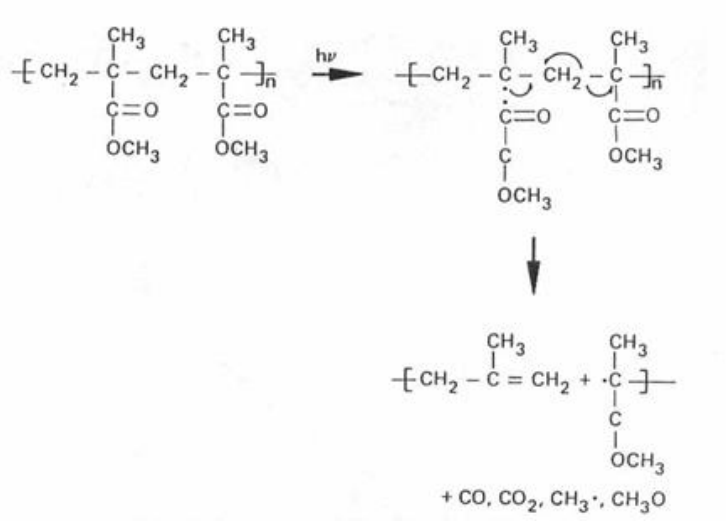

Figure 3.1: Radiation induced chain scission in PMMA[3]

where
D_{CL} = Clearing Dose in $\mu C/cm^2$
D_0 = Dose in $\mu C/cm^2$ at which the exposure first begins to have an effect
The modulation transfer function(MTF) is, as the name suggests, a measure of the transfer of modulation (or contrast) from the subject to the image. Fig. 3.2 explains the concept of MTF. It shows the use of a reducing lens system to image a mask pattern in resist. The optical intensity pattern as the light exits the mask will be almost an ideal representation of the mask as diffraction effects are only important after light passes through the mask.[8] However, the aerial image produced at the resist plane will not be perfectly black and white because of diffraction effects and other non-idealities in the optical system.[8]

A useful measure of the quality of the aerial image is the MTF that can be defined as[8]

$$MTF = \frac{I_{MAX} - I_{MIN}}{I_{MAX} + I_{MIN}} \tag{3.2}$$

In other words, it measures how faithfully the lens reproduces (or transfers) detail from the object to the image produced by the lens. It is often useful to define a similar quantity for the resist, in this case, it is called the Critical MTF
It is given by :

$$CMTF_{resist} = \frac{D_{CL} - D_0}{D_{CL} + D_0} = \frac{10^{\frac{1}{\lambda}} - 1}{10^{\frac{1}{\lambda}} + 1} \tag{3.3}$$

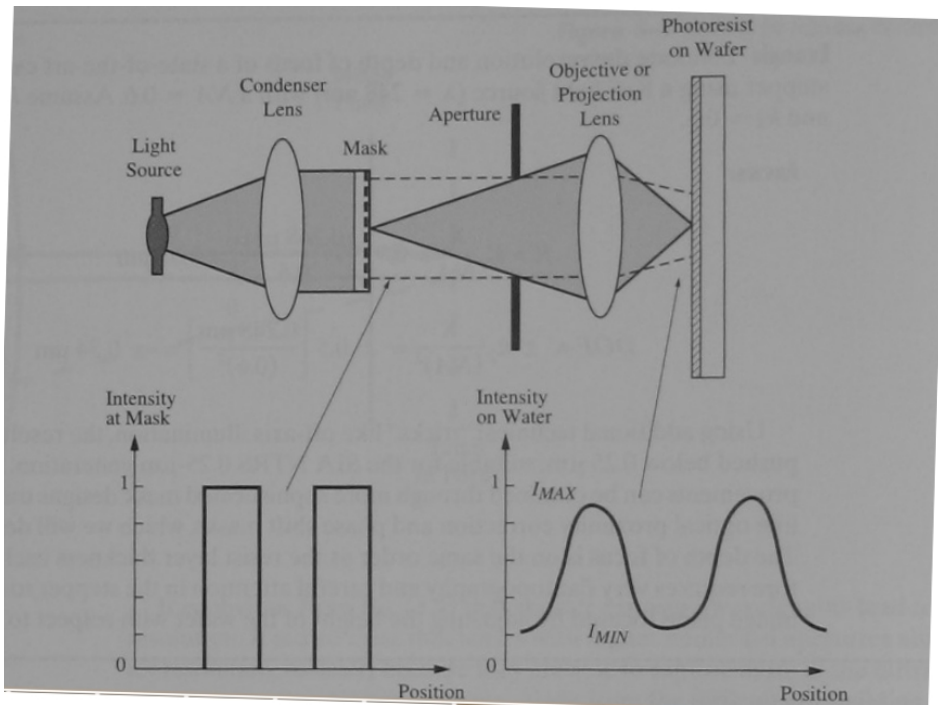

Figure 3.2: A generic lithography system with a mask being imaged on photo resist on a wafer. Mask almost has an ideal MTF (MTF = 1) whereas the aerial image MTF is much lower (MTF approx. equal to 0.6) because of diffraction effects in the optical system[8]

Following sections explains the design of experiments and the process recipe for those experiments in order to obtain values of clearing dose, contrast and CMTF for positive tone resist PMMA 950K 2% Anisole and a negative tone resist HSQ XR1541.

3.2 Contrast Curve Experiments for PMMA

For positive resists like PMMA, samples receiving small exposure doses will not be attacked by the developer to any appreciable extent; those receiving large doses will completely dissolve in the developer. Intermediate doses will result in partial dissolution of the resist.
For negative resists, the opposite behavior occurs.

3.2.1 Process Steps

- PMMA 950k 2% Anisole was spin coated on silicon substrate with spin speed of 4000rpm to obtain 80-nm nominal thickness and pre-bake at 180C for 90 sec on hot plate
- Samples were exposed to electron beam with a field area of 100μm X 100μm for contrast curve measurements with Raith150^{TWO} operating at 10kV and doses varying from 10 - 250 $\mu C/cm^2$. The test pattern is shown in Fig. 3.3
- Samples were developed in MIBK:IPA (1:3) which is the standard developer and a single IPA
- Development in MIBK:IPA was done at 25C for 30 sec
- The development time for IPA developer was varied from 30 sec to 5 sec
- After development, all samples were baked at 100C for 2 min
- For contrast curve analysis, the removed resist thickness of each sample at varying doses were measured by profilometry
- Subtract removed resist thickness from actual resist thickness to obtain remaining resist thickness
- Contrast values and sensitivity were determined by linear fitting of the data in between the remaining thickness

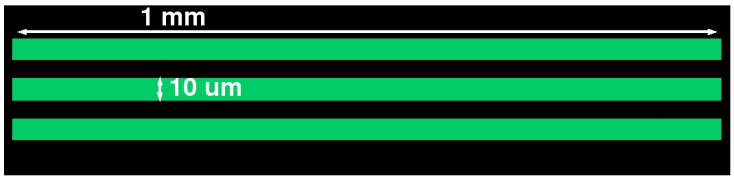

Figure 3.3: Single test patterns for contrast curve experiments. Such multiple test patterns were exposed on PMMA with varying doses in the range of 10 - 250μC/cm^2 with steps of 10μC/cm^2. Since PMMA is a positive tone resist, cross linking happens in the green area of the pattern and gets washed away in developer. The black area is retained after development

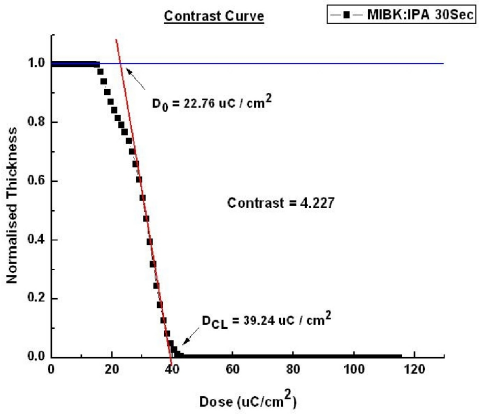

Figure 3.4: Contrast Curve for 80-nm thick PMMA developed in MIBK:IPA 1:3 for 30 sec

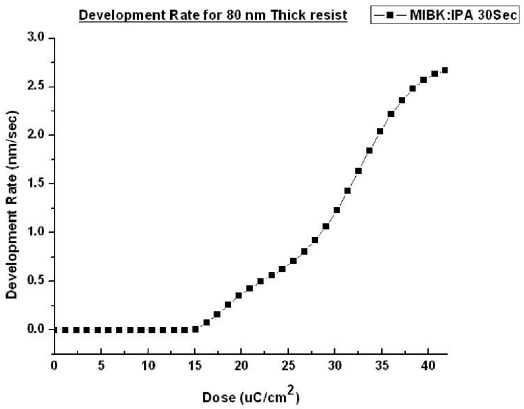

Figure 3.5: Development Rate for 80-nm thick PMMA developed in MIBK:IPA 1:3 for 30 sec

3.2.2 Results and Discussions

Fig. 3.4 through Fig. 3.11 shows the contrast curves and development rates while using MIBK:IPA (1:3) mixture and IPA as developers at different developing times. The data in Fig. 3.4 and Fig. 3.10 clearly shows that the clearing dose has increased from 39.24 μC/cm^2 for MIBK:IPA (1:3) to 124.75 μC/cm^2 for IPA with 30 sec development time. This shows that IPA has a small solvating power for PMMA as compared to MIBK:IPA mixture. Hence, a large exposure dose is required. But enhancement in contrast value when using IPA as a developer is an advantage in terms of resolution of PMMA. Also, by reducing the development time of IPA from 30 sec to 5 sec, the critical dose gradually increased as expected, but the contrast values has increased from 7.54 to 13.77. This is comparatively better than contrast value of 7.6

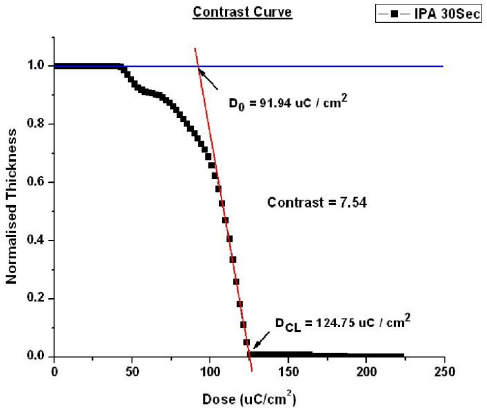

Figure 3.6: Contrast Curve for 80-nm thick PMMA developed in IPA for 30 sec

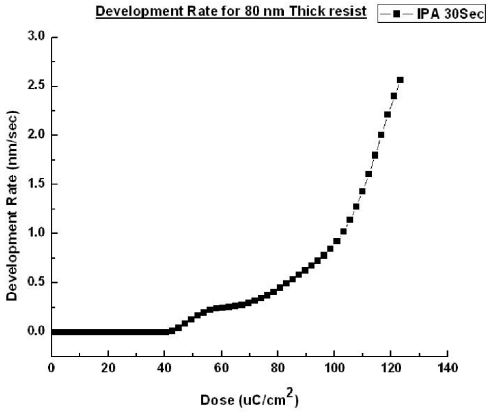

Figure 3.7: Development Rate for 80-nm thick PMMA developed in IPA for 30 sec

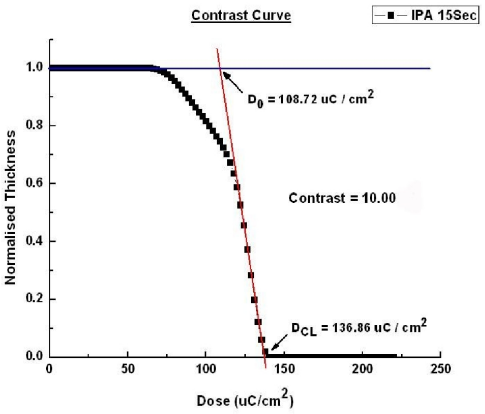

Figure 3.8: Contrast Curve for 80-nm thick PMMA developed in IPA for 15 sec

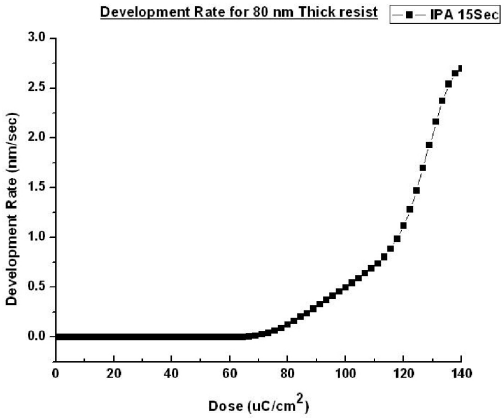

Figure 3.9: Development Rate for 80-nm thick PMMA developed in IPA for 15 sec

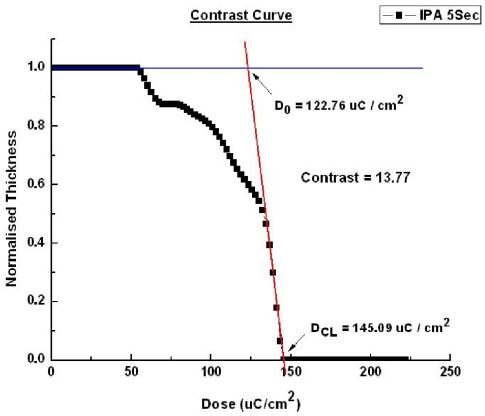

Figure 3.10: Contrast Curve for 80-nm thick PMMA developed in IPA for 5 sec

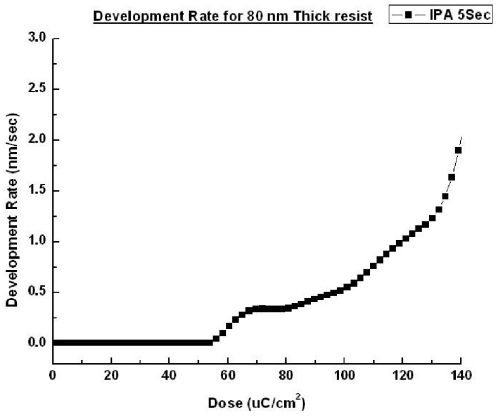

Figure 3.11: Development Rate for 80-nm thick PMMA developed in IPA for 5 sec

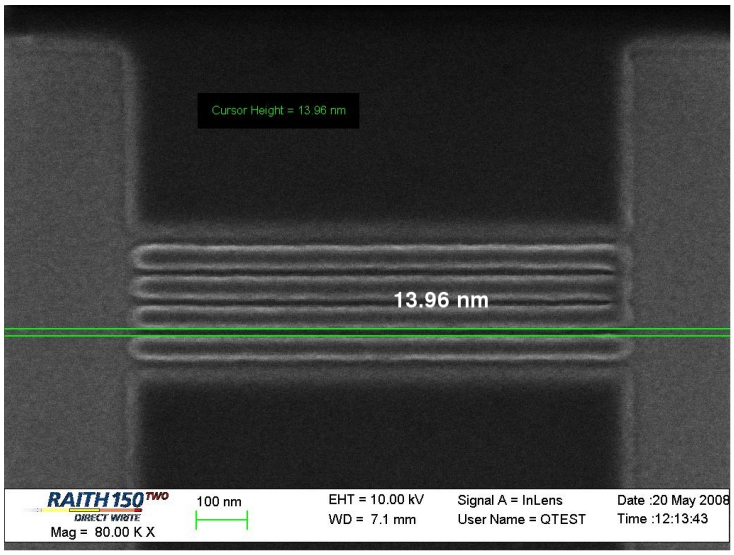

Figure 3.12: Post Develop Image on 80 nm thick PMMA resist with an exposure dose of 100 $\mu C/cm^2$

in IPA for 5 sec, as reported in literature.[12]
An improvement in contrast by reducing the development time is explained by the development rate of PMMA in.[12] Fig. 3.7, Fig. 3.9 and Fig. 3.11 shows the development rate curves from IPA development process. It can be clearly deduced from the graphs that the development rate is not a function of development time, but instead a function of exposure dose. The development rate increases abruptly as exposure dose increases i.e. for the same difference in dose in upper range, there is a large difference in development rate.[12] Greeneich describes development rate, R, with a fragmented molecular weight, M_f.[13] PMMA which is exposed to electron beam is fragmented into small polymer with a molecular weight of M_f.

$$R = \frac{\beta}{{M_f}^{\alpha}} \tag{3.4}$$

$$M_f = ({M_0}^{-1} + \frac{g\varepsilon}{A_0\rho})^{-1} \tag{3.5}$$

where
α and β = empirical constants
M_0 = initial molecular weight
g = chain scission efficiency
ε = absorbed energy density
A_0 = Avogadro's number
The absorbed energy density, ε, is given by[14]

$$\varepsilon = \frac{D}{q.f(E_0, z, \delta)} \tag{3.6}$$

where
q = Electronic charge
E_0 = Incident electron energy
z = Resist Depth
δ = Resist density
The relationship between development rate(R) and exposure dose(D) can be derived from eqs.(3.2), (3.3) and (3.4), as

$$R = C + C'D^{\alpha} \tag{3.7}$$

where C and C' are constants.
The sensitivity values, contrast and CMTF are summarized in table Tab. 3.1:

Developer	Clearing Dose ($\mu C/cm^2$)	Contrast(λ)	CMTF
MIBK:IPA 1:3 for 30 sec	39.24	4.23	0.27
IPA for 30 sec	124.75	7.54	0.15
IPA for 15 sec	136.86	10.00	0.12
IPA for 5 sec	145.09	13.77	0.08

Table 3.1: Comparison of sensitivity, contrast and CMTF values of PMMA using different developer and development times

3.3 Contrast Curve Experiments for HSQ

3.3.1 Process Steps

- HSQ was spin coated on silicon substrate with 35-nm nominal thickness and pre-bake at 180C for 6 min in baking oven with N_2 ambient
- Samples were exposed to electron beam with a field area of 100um X 100um for contrast curve measurements with Raith 150 TWO operating at 10kV and doses varying from 20 - 2000 $\mu C/cm^2$. The test pattern is shown in Fig. 3.13.
- Samples were developed in TMAH 25% which is the standard developer
- Development was done at 25C for 7 sec
- After development, all samples were baked at 100C for 2 min
- For contrast curve analysis, the remaining resist thickness of each sample at varying doses were measured by profilometry
- Contrast values and sensitivity were determined by linear fitting of the data in between the remaining thickness

3.3.2 Results and Discussions

The clearing dose (as observed in Fig. 3.14)achieved is 200 $\mu C/cm^2$ with a contrast of 6.3. The contrast is 1.9X times better than[15] which reported value of 3.25 for HSQ developed in TMAH 2.38%.
Fig. 3.15 shows the post develop image of pattern exposed on HSQ XR1541 and developed in TMAH for 7sec (refer to Process recipe for HSQ in previous sections). The contrast value can be enhanced even more by the addition of

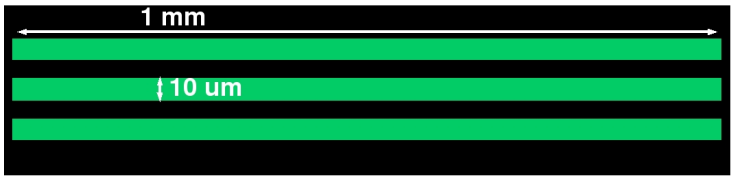

Figure 3.13: Single test patterns for contrast curve experiments. Such multiple test patterns were exposed on HSQ with varying doses in the range of 20 - 2000$\mu C/cm^2$ with steps of 20$\mu C/cm^2$. Since the resist is negative tone, the green area in the pattern gets hardened on e-beam exposure and are retained after development. The black area is washed away in developer

NaOH as shown from Fig. 3.16, but NaOH is not recommended in standard MOSFET process since sodium itself acts as a positive mobile ion (Na^+) in gate oxide resulting in several volts of threshold shift.

3.4 Towards Optimization of Pattern Transfer onto Silicon

In this experiment, based on the clearing dose window obtained from the contrast curve experiment, 100nm lines with varying spacings were written on 138 nm PMMA layer spun on Si(100). Optimum dose for obtaining the high-resolution lines with minimum resist profile spread was deduced.
Resist Profile spread has a very complicated two-dimensional shape. Comparison of shapes of two different profiles requires convenient description for the shapes of the profiles that some how reflects their salient quantities.[5]

The most common description to model a resist profile is a trapezoid with base width W, its height D and the sidewall angle θ as shown in Fig. 3.17. The motive of this work was to provide inputs for high-resolution pattern onto silicon. Initial experiments done with this information has helped in yielding the etch rate of silicon in the AMAT Etch Centura tool.

3.4.1 Process Steps

- PMMA 950k 4% Anisole was spin coated on silicon substrate with spin speed of 4000rpm to obtain 138-nm nominal thickness and pre-bake at 180C for 90 sec in hot plate

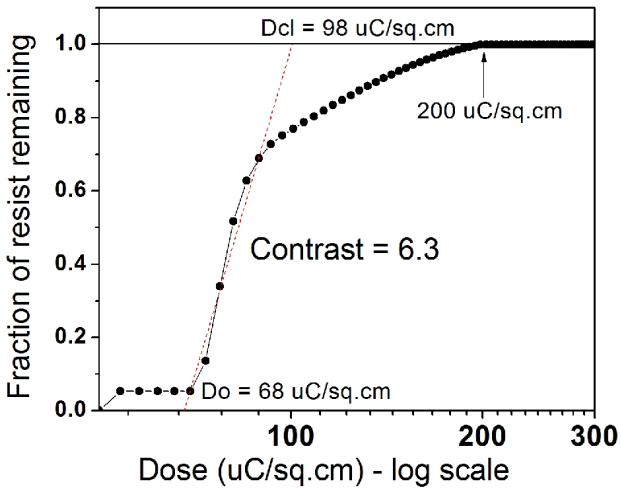

Figure 3.14: Contrast Curve for 35-nm thick HSQ developed in TMAH for 7 sec

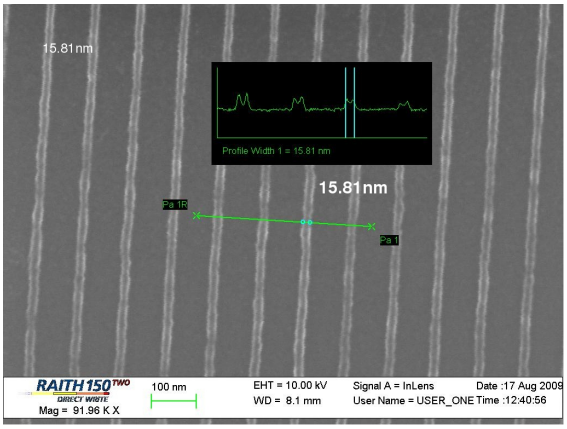

Figure 3.15: Post Develop Image on 35 nm thick HSQ resist exposed at dose of 200 $\mu C/cm^2$ and developed in TMAH for 7 sec

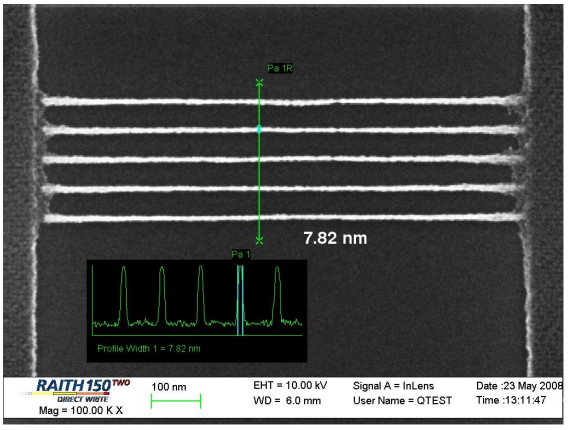

Figure 3.16: Post Develop Image on 35 nm thick HSQ resist exposed at dose of 4000 $\mu C/cm^2$ and developed in NaOH + NaCl + DIW for 4 min

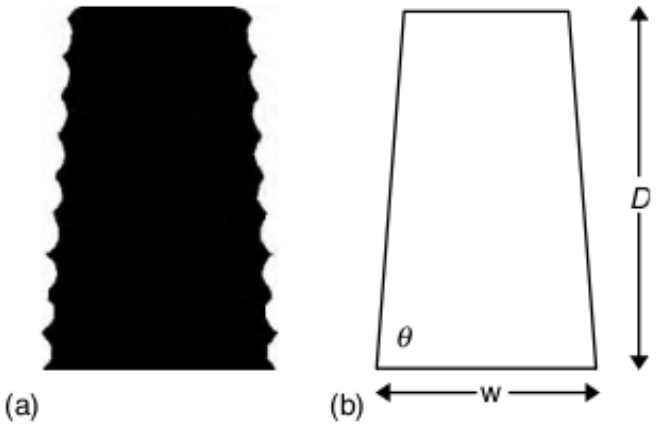

Figure 3.17: Typical resist profile and its corresponding trapezoid with base width W, its height D and the sidewall angle θ[5]

- Samples were exposed to electron beam with a field area of 100μm X 100μm for etch optimization with AMAT etch Centura
- Electron beam energy of 10 kV was used with a working distance of 20 μm and doses varying from 50 - 250 $\mu C/cm^2$ at steps of 50 $\mu C/cm^2$ to find out the optimum clearing dose (refer Fig. 3.18 for pattern used)
- Samples were developed in MIBK:IPA (1:3) at 25C for 30 sec followed by IPA dip for 15 sec
- After development, all samples were baked at 100C for 2 min
- Surface imaging of the samples were done to find out the optimum clearing dose
- Cross section imaging was done to obtain the line edge profile as a function of dose
- Samples were etched using AMAT etch Centura tool with the following recipe:
  - Etch Chemistry : CF4-HBr-Cl2
  - RF source power : 290 Watts
  - RF bias power : 90 Watts

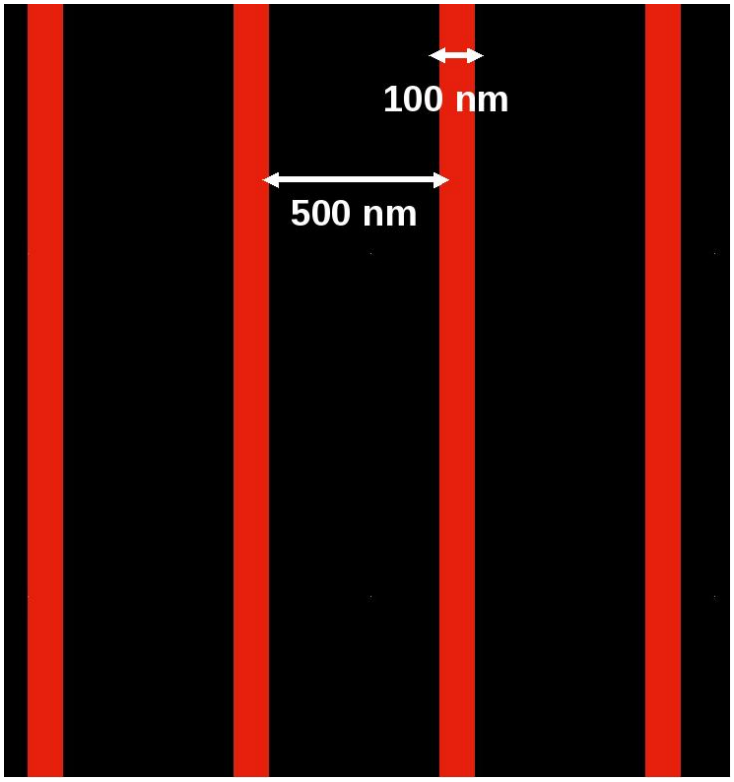

Figure 3.18: Silicon Etching Optimization Pattern

  - Pressure : 15 mTorr
  - Flow rate : CF4 (95 sccm), HBr (66 sccm), Cl2 (33 sccm)
  - Etching Duration : 60 sec

- PMMA was stripped off the sample by acetone dip for 5 minutes followed by IPA dip for another 5 minutes to remove acetone stains
- Cross sectional imaging of the etched samples was done to obtain the etch rate of silicon with the above mentioned etch chemistry at a particular RF power

3.4.2 Results and Discussions

Optimum dose for obtaining the high-resolution lines was found to be 100 $\mu C/cm^2$ as shown in Fig. 3.19. For doses below this value, the pattern was not fully developed, while for doses above this value, the pattern lines were

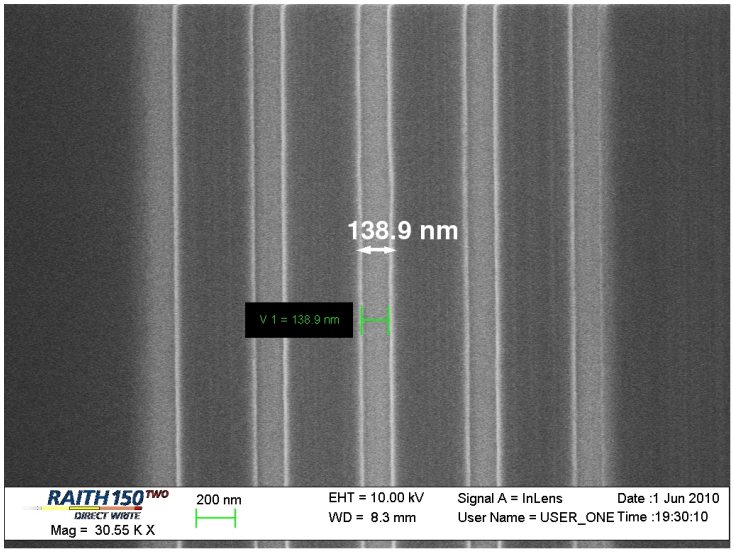

Figure 3.19: Post develop surface image on 138 nm thick PMMA at optimized dose of 100 μC/cm^2

found to increase in width. The resist profile was found to be independent of dose, with a line edge extension of 66.99 nm as noticed in Fig. 3.20. The etching rate was found out to be 35 nm/min by inspecting a series of points on the sample. The line edge extension, as per Fig. 3.21, is 33 nm.

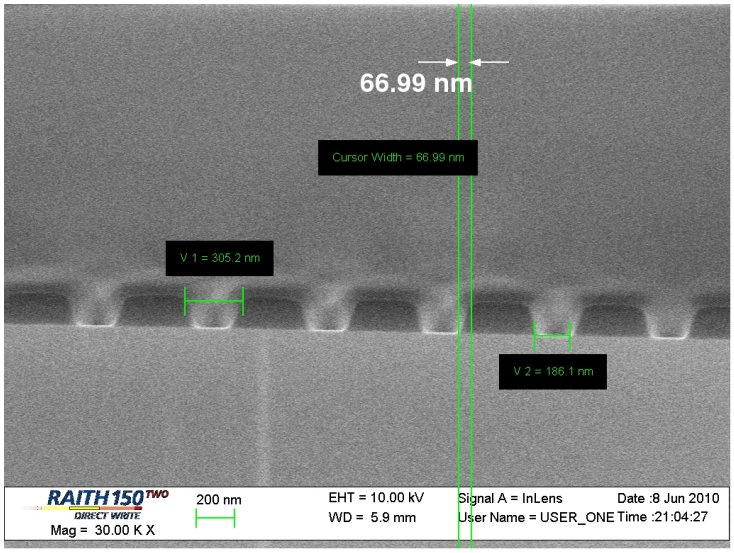

Figure 3.20: Post develop cross section image on 138 nm thick PMMA at optimized dose of 100 $\mu C/cm^2$

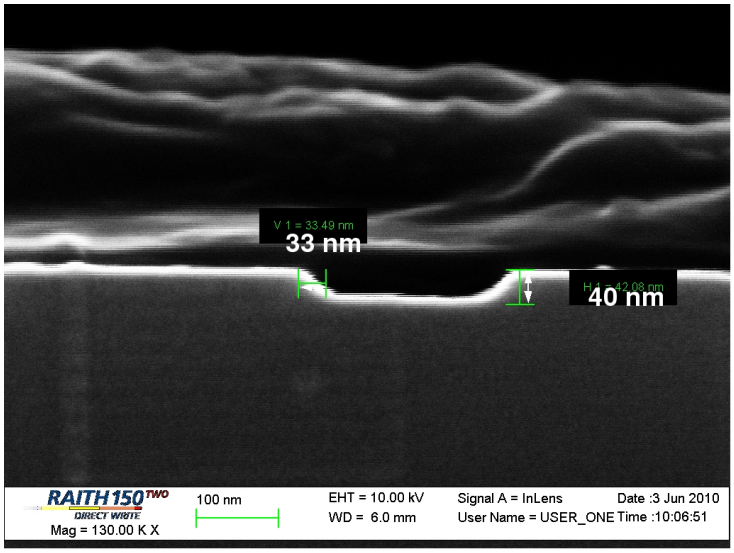

Figure 3.21: Post etch cross section image of silicon at optimized dose of 100 $\mu C/cm^2$. PMMA was stripped off using acetone

Chapter 4

Mask Design

Integrated Circuits (IC) are accurately represented in terms of planar geometric shapes that acts in accordance to constraints i.e. design rules, imposed by manufacturing process. This representation of IC's is referred to as IC layout or mask design. The verification tools performs a series of checks viz. Design Rule Check (DRC) and Layout Versus Schematic (LVS) on the final layout. This chapter outlines the features of the 2-level and 4-level MOSFET masks (soft versions) designed following the DRC rules. Snapshots of a sample die from each mask is provided and the key test structures included in each mask are mentioned.

4.1 Overall Die Design

Fig. 4.1 shows the mask designed using Cadence as one of the most important steps towards sub-100 nm MOSFET fabrication. The die dimension is 1cm X 1cm and it consists of 2-level MOSFET (using salicidation) masks and 4-level MOSFET masks of varying channel lengths from 20 nm to 10 μm. In addition to that, the die also consists masks for MOS capacitors with and without guard-rings, active area sheet resistivity measurement using Van der Pauw's Structure, and poly and metal area sheet resistivity measurement using Kelvin's structure.

4.2 2-level MOSFET mask design

Fig. 4.2 & Fig. 4.3 shows 2-level MOSFET mask design. It consists of active area and gate area of MOSFETs to be fabricated with salicidation technique. Since metal salicides itself acts as contacts and can be used for I-V characterization. Hence, there is no need of additional via and metal area mask.

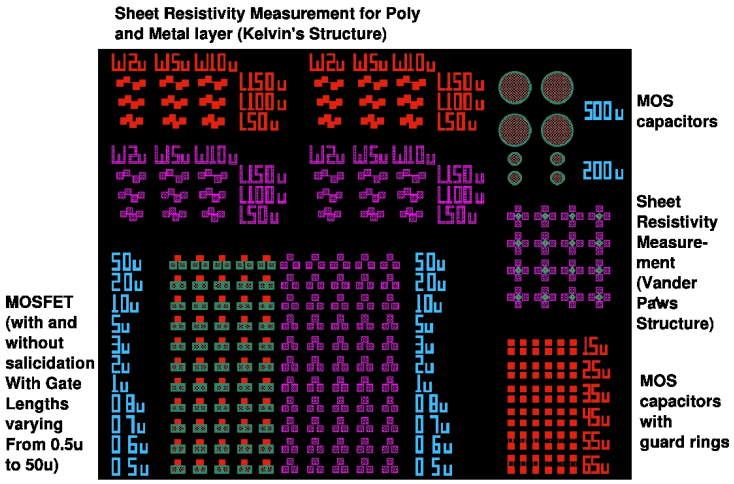

Figure 4.1: 1cm X 1cm Die Design that consists of 2-level MOSFET (using salicidation) masks, 4-level MOSFET masks of varying channel lengths from 20 nm to 10 μm, masks for MOS capacitors with and without guard-rings, active area sheet resistivity measurement using Van der Pauw's Structure, and poly and metal area sheet resistivity measurement using Kelvin's structure

This would be clear in the section "Typical MOSFET fabrication process flow". The gate length(L) was varied from 20 nm to 10 um with a constant width(W) of 10 um. The active area, which itself acts as contact pads, was kept as 100 um X 100 um.

4.3 4-Level MOSFET mask design

Fig. 4.5 & Fig. 4.6 shows 4-level MOSFET mask design. It consists of active area, gate area, via area and metal area. Since these are for MOSFETs without salicidation technique, via mask and metal mask are needed for source-drain metal contacts. The gate length(L) was varied from 20 nm to 10 um with a constant width(W) of 10um. The active area were kept 15 um X 15 um from where via's were taken out for metal contacts. Fig. 4.4 shows the section of die with 2-level and 4-level MOSFETs

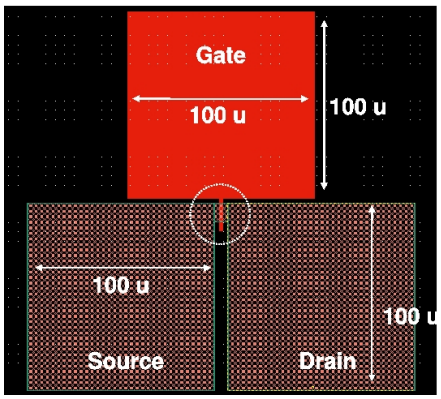

Figure 4.2: 2-Level MOSFET Mask Design which consists of active area and gate area of MOSFETs to be fabricated with salicidation technique

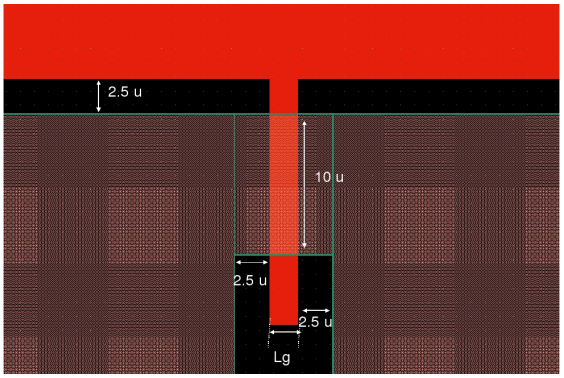

Lg = 10u, 5u, 3u, 2u, 1u, 0.8u, 0.7u, 0.6u, 0.5u, 0.35u, 0.25u, 0.18u, 0.15u, 0.13, 0.1u, 0.08u, 0.06u, 0.04u, 0.02u

Figure 4.3: 2-Level MOSFET Mask Dimensions where gate length(L) was varied from 20 nm to 10 um with a constant width(W) of 10 um and active area, which itself acts as contact pads, was kept as 100 um X 100 um

4.4 Typical MOSFET fabrication process flow

Fig. 4.7 through Fig. 4.13 shows a typical MOSFET fabrication process flow. These images are from process simulations carried out in *sprocess* by Suresh G, PhD student, Electrical Engineering, IITB.

- LOCOS isolation process using Active area mask (refer Fig. 4.7)
  - Grow 10 nm oxide in order to reduce stress due to nitride
  - Pattern nitride using Active mask and grow 200 nm to 250 nm field oxide
  - Strip nitride and etch pad oxide
- GATE stack formation (refer Fig. 4.8)
  - Grow 3 nm gate oxide and deposit 150 nm of N+ poly
  - Pattern N+ poly and gate oxide using Gate area mask
- LDD implant (refer Fig. 4.9)
- Spacer Formation (refer Fig. 4.10)

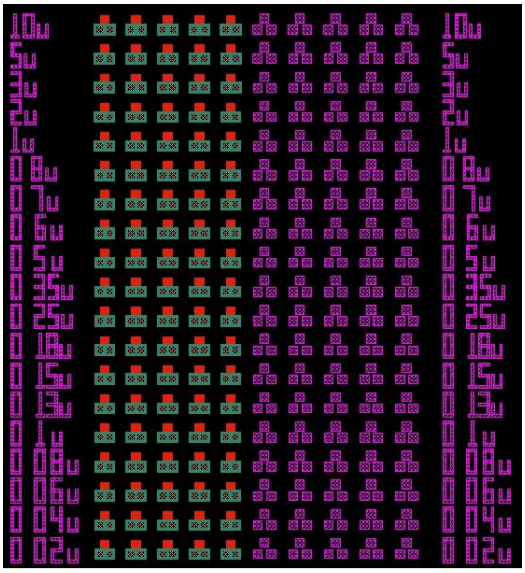

Figure 4.4: Section of die with 2-level and 4-level MOSFET

  - Deposit 10 nm oxide to reduce stress due to nitride
  - Deposit 70 nm of conformal nitride
  - Etch nitride an-isotropically using dry etch
  - Wet Etch 10 nm oxide in 2% HF
- Deep source drain implants (refer Fig. 4.11)
- Salicidation
  - Deposit titanium
  - Annealing step is done to form titanium salicides
  - Strip away unreacted titanium
  - We can stop further processing and probe on the salicides using active area mask with 100 um X 100 um pad areas
- Contact Formation (refer Fig. 4.12 and Fig. 4.13)
  - Deposit 100 nm passivation oxide layer
  - Pattern contact holes using via mask
  - Deposit tungsten and lift off the resist
  - Now deposit aluminum and pattern it using metal area mask

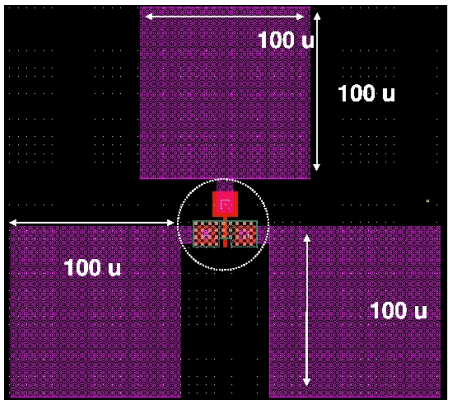

Figure 4.5: 4-Level MOSFET Mask Design that consists of active area, gate area, via area and metal area. These are for MOSFETs without salicidation technique, and hence via mask and metal mask are needed for source-drain metal contacts

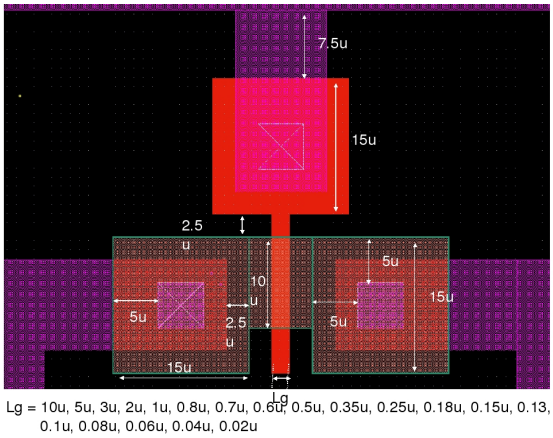

Figure 4.6: 4-Level MOSFET Mask Dimensions where the gate length(L) was varied from 20 nm to 10 um with a constant width(W) of 10um and the active area were kept 15 um X 15 um from where via's were taken out for metal contacts

4.5 Sheet Resistivity

Fig. 4.14 & Fig. 4.15 shows van der Pauw's and Kelvin's structure, respectively, for sheet resistivity measurement. The van der Pauw's Method is a technique to measure the specific resistivity and Hall effect of arbitary shape flat samples.[16] The Kelvin's test patterns is a very popular test structure for measuring the contact resistance of diffusion's and implantation's in semiconductors.[17]

4.6 Alignment Marks

Fig. 4.17 through Fig. 4.20 shows the alignment marks for active area, gate area, via area, and metal area respectively. Fig. 4.16 shows the detailed dimensions of single alignment mark. Active area mask contains 4 sets of alignment marks and other area masks contain only 3 sets of alignment marks. The location & placement of alignment marks in each layer are chosen in such a way that at least one of the 4 alignment marks present in the active area is protected till the end of all processes.

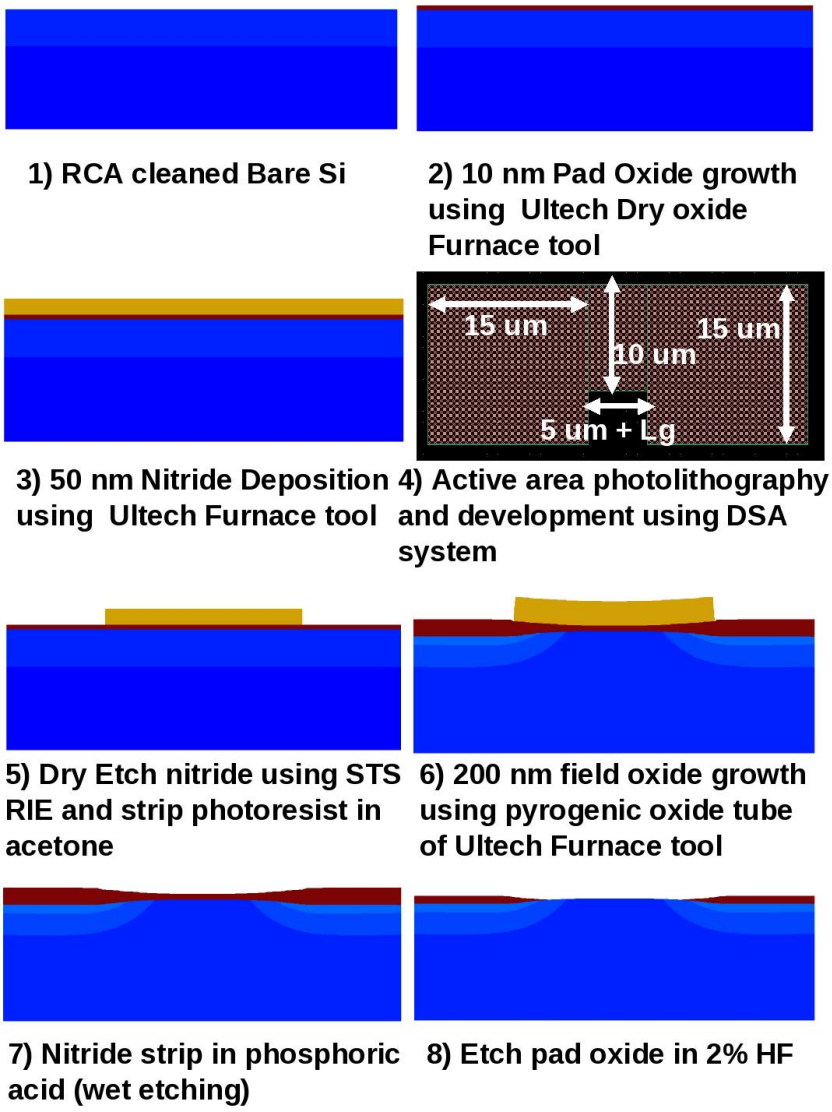

Figure 4.7: Simulation Images which shows nitiride deposition, field oxide growth and nitride strip process with Active area mask

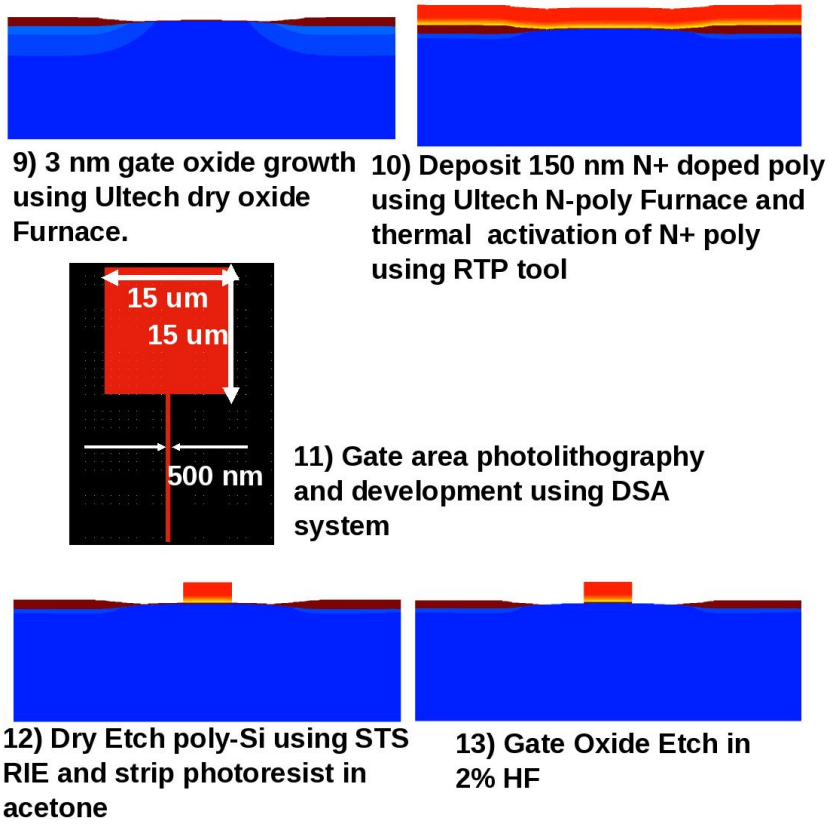

Figure 4.8: GATE stack Formation with N+ doped poly deposition and etching using Gate area mask

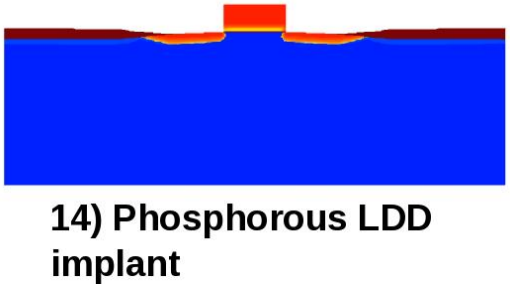

Figure 4.9: Phosphorous LDD (Lightly Doped Drain) implant

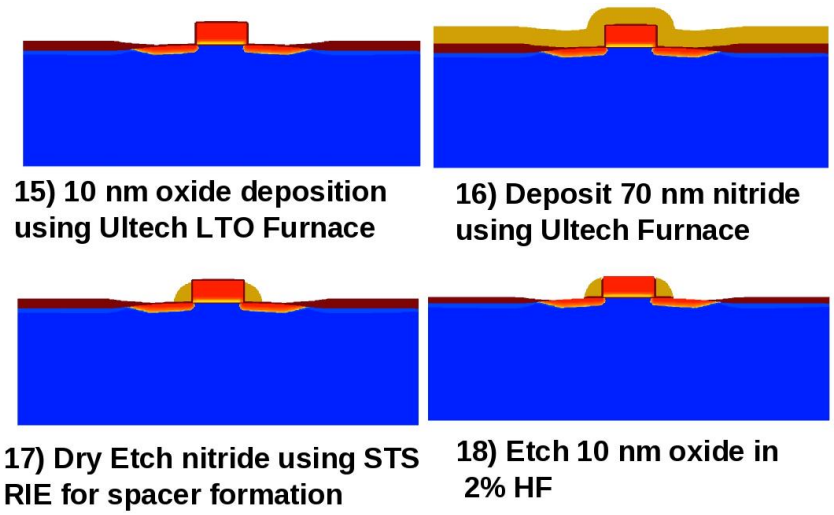

Figure 4.10: Spacer Formation with oxide deposition, nitride deposition and nitride etch process steps

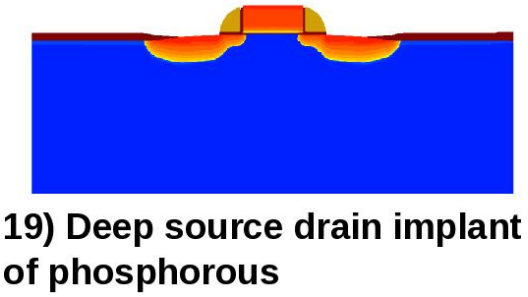

Figure 4.11: Deep source drain implants of phosphorous

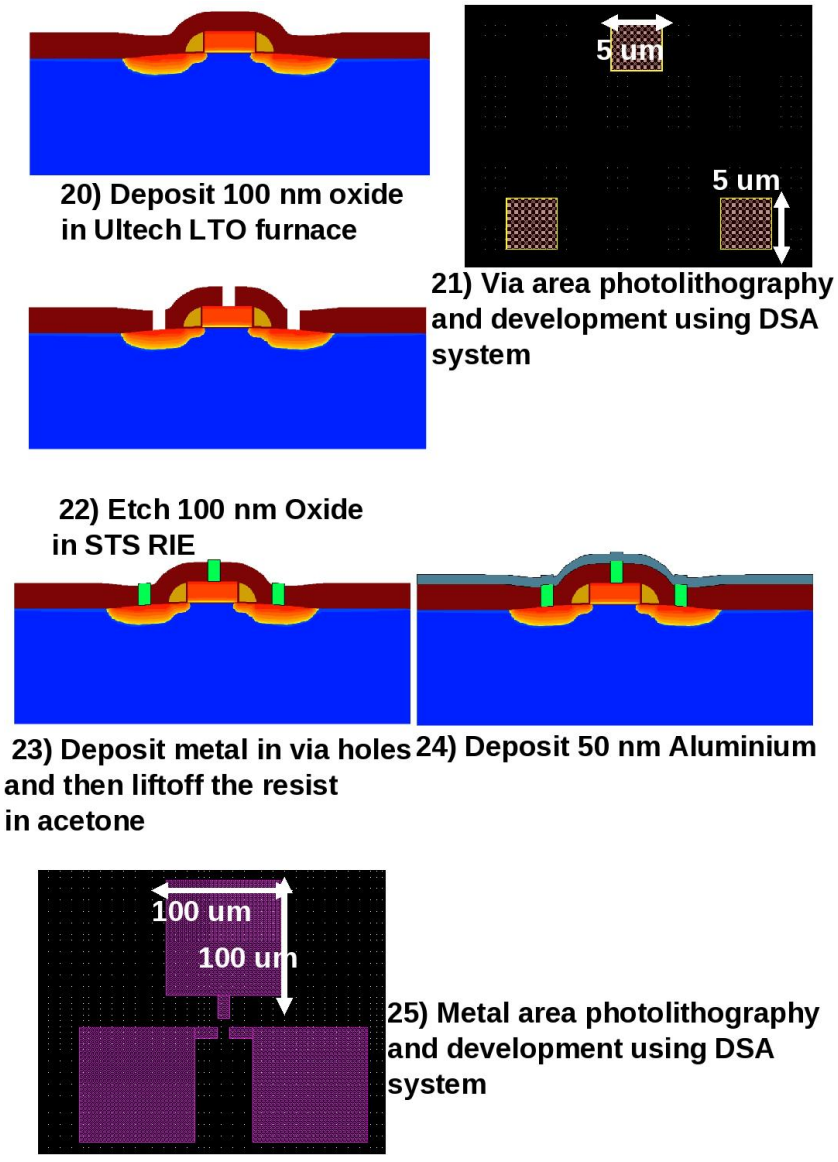

Figure 4.12: Contact Formation with oxide deposition, oxide etch and metal deposition using via mask and metal area mask

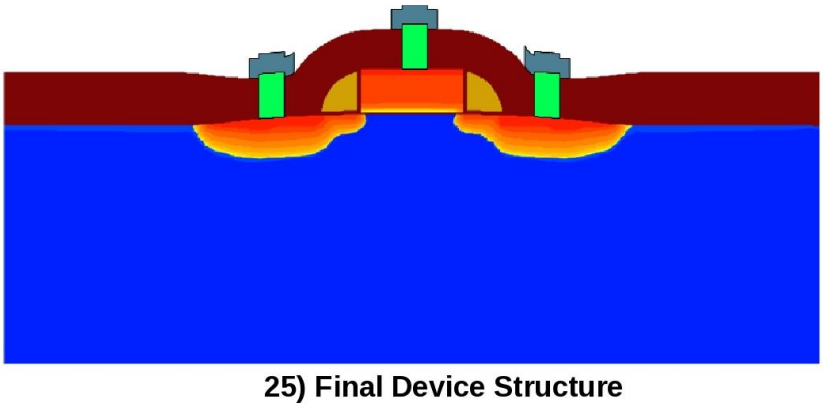

Figure 4.13: Final Device Structure with metal etched

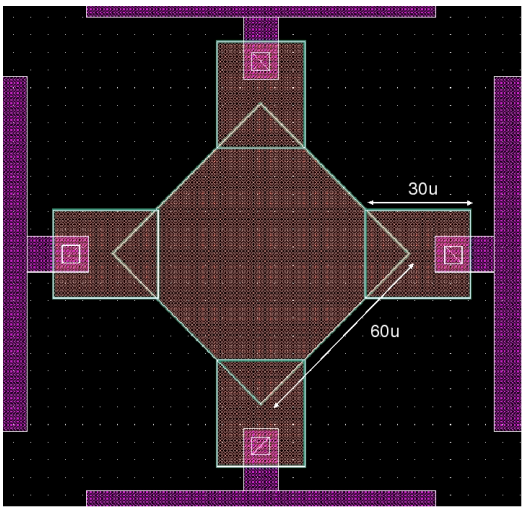

Figure 4.14: Van der Paws structure for sheet resistivity measurement of active area

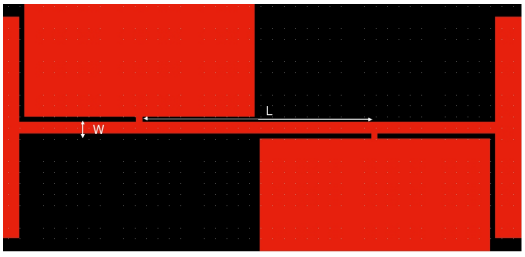

Figure 4.15: Kelvin's structure for sheet resistivity measurement of gate and metal area

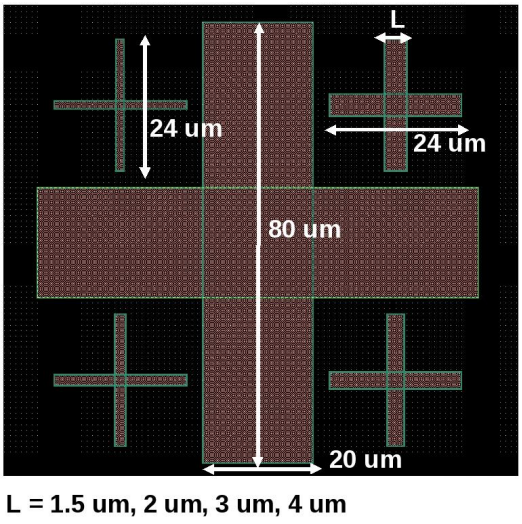

Figure 4.16: Alignment mark Dimensions

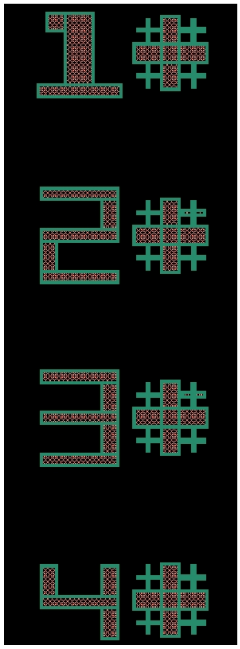

Figure 4.17: Level 1 Active area alignment marks

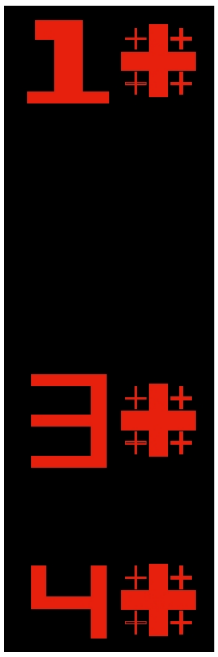

Figure 4.18: Level 2 Gate area alignment marks

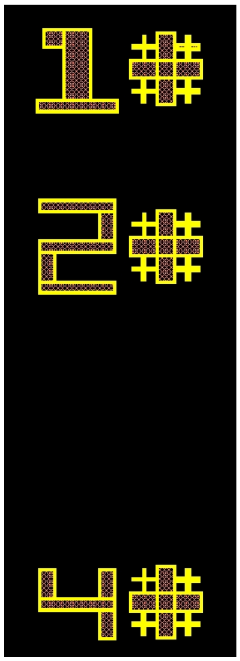

Figure 4.19: Level 3 Via area alignment marks

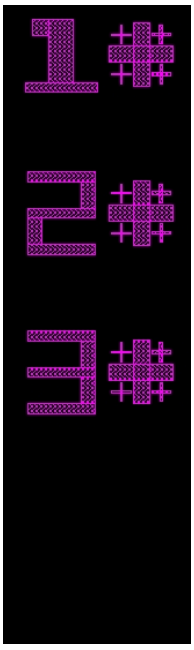

Figure 4.20: Level 4 Metal area alignment marks

Chapter 5

Mask Plate Optimization

A mask plate is an opaque plate with transparent windows/regions that allow light to pass through, in a definite pattern, normally referred to as mask layout. They are commonly used in photo lithography. The motive of the experiments in following sections is to develop a recipe for mask plate using Raith150 Two E-Beam Lithography tool, with a target line width of 500 nm, so that the plate could be used optical lithography for further processes. The target line width of 500 nm is selected, keeping in mind the resolution of the optical lithography tool DSA EVG 620, to be used for further processes.
The types of resist used were PMMA 950K 2% Anisole, which is a positive tone resist, and HSQ-XR1541 which is a positive tone resist. For our initial experiments, ferrous oxide coated soda lime plates obtained from townetech were used for preparing mask plates. HSQ-XR1541 resist was used for patterning these plates.
In the second set of our experiments of mask plate optimization, chrome plates were purchased from Nanofilm Corp. These were soda lime glass plates sputtered with 100 nm of chrome. Negative e-beam resist HSQ-XR1541 and positive e-beam resist PMMA 950K 2% Anisole were patterned with 10 kV Raith 150 TWO E-Beam Direct Write tool to pattern these plates as masks to be used in DSA photo lithography.
Wet etching of chrome was done in-house. The etchant contained 40 ml acetic acid(CH_3COOH), 82.5 gms Cerric Ammonium nitrate($Ce(NH_4)_2(NO_3)_6$), 460 ml DI H_2O.
Further experiment details are given in the following sections.

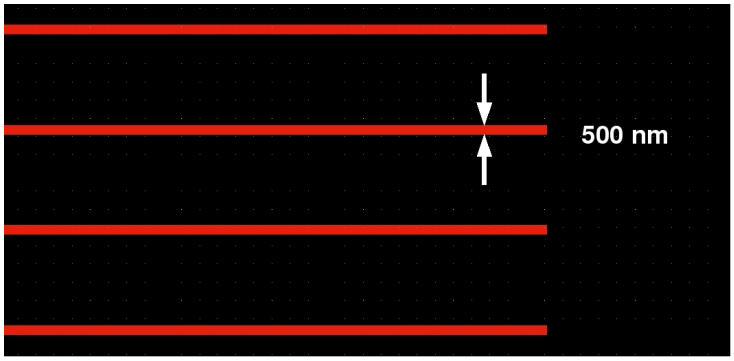

Figure 5.1: Single set of test patterns for mask plate optimization. Such multiple test patterns were exposed on HSQ with dose 200 $\mu C/cm^2$. Since the resist is negative tone, the red area in the pattern gets hardened on e-beam exposure and are retained after development. The black area is washed away in developer

5.1 Ferrous Oxide Mask Plate with HSQ

5.1.1 Process Recipe - Experiment I

- Cleaning of Mask plate : Piranha clean (7:3 H_2SO_4 and H_2O_2)
- Dehydration-Bake : 130C for 30 min on hot plate
- Resist Used : HSQ-XR1541, Spin Speed : 4000rpm, Thickness : 35 nm
- Pre-Bake : 250C for 120 sec on on hot plate
- Energy : 10 kV, Dose : 200 $\mu C/cm^2$. Refer Fig. 5.1 for test patterns used in this experiment
- Post Exposure Bake : 100C for 120 sec on hot plate
- Developer : TMAH 25%, Development Time : 7 sec
- Etchant : 160 gms ferrous chloride crystals, 700 cc conc. HCl, 350 cc water
- Etching Duration : 30 min

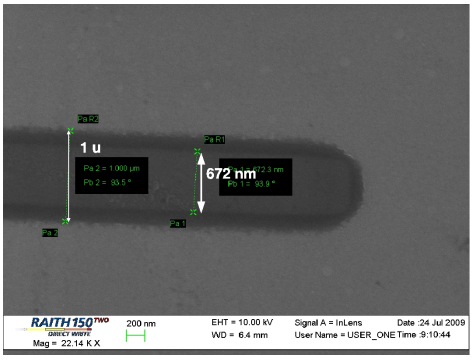

Figure 5.2: Post Develop Image on 35 nm thick HSQ XR1541 at optimized dose of 200 $\mu C/cm^2$

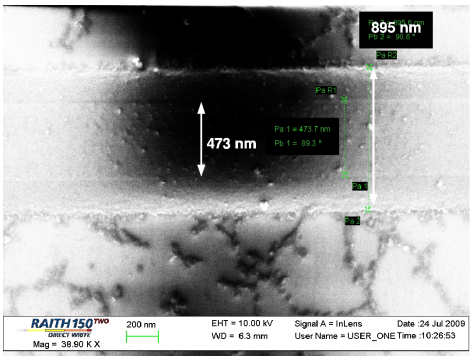

Figure 5.3: Post Etch Image of Ferrous oxide coated mask plates with 35 nm thick HSQ XR1541

5.1.2 Results & Discussions of Experiment I

Fig. 5.2 and Fig. 5.3 shows the post develop and post etch images, respectively. The minimum feature dimension obtained on plate was 672 nm for 500 nm feature on mask layout (refer Fig. 5.1). Also we could observe the side wall getting extended. This is mainly due to the charging effect of iron oxide plates during e-beam exposure. Charging is the condition due to which a material cannot effectively conduct the beam energy passed to it.[4] Non-conducting samples (which in our case is Ferrous oxide mask plate) will obviously accumulate charge.

Hence we needed mask plates coated with conducting layers e.g. chrome. Also, it was observed that chrome plates needed sufficient cooling after dehydration bake else the resist spread is not uniform and also the plate might break while spinning.

5.2 Chrome Coated Mask Plate with HSQ

5.2.1 Process Recipe - Experiment II

- Cleaning of Mask plate : Piranha clean (7:3 H_2SO_4 and H_2O_2)
- Dehydration-Bake : 130C for 30 min on hot plate
- **Wait for 20 min so that the mask plate can come back to room temperature**
- Resist Used : HSQ, Spin Speed : 4000rpm, Thickness : 35 nm

- Pre-Bake : 250C for 120 sec on hot plate
- Energy : 10 kV, Dose : 200 $\mu C/cm^2$
- Post Exposure Bake : 100C for 120 sec on hot plate
- Developer : TMAH 25%, Development Time : 7 sec
- Etchant : 40 ml acetic acid(CH_3COOH), 82.5 gms Cerric Ammonium nitrate($Ce(NH_4)_2(NO_3)_6$), 460 ml DI H_2O
- Etching Duration :120 sec

5.2.2 Results & Discussions of Experiment II

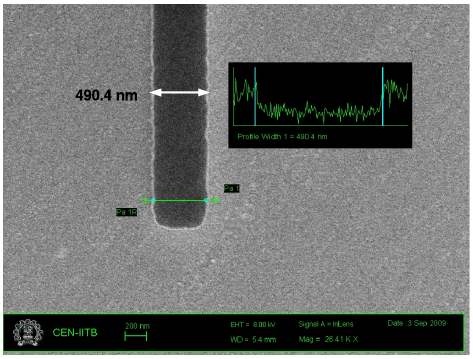

Figure 5.4: Post Develop Image on 35 nm thick HSQ XR1541 at an optimized dose of 200 $\mu C/cm^2$

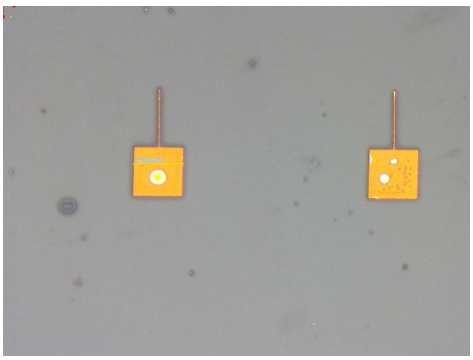

Figure 5.5: Olympus optical microscope post etch image of chrome coated mask plates with 35 nm thick HSQ XR1541

Fig. 5.4 and Fig. 5.5 shows the post develop and post etch images, respectively. The results are promising with respect to achieving the desired pattern size and the recipe could be used to make mask plates which could be further used for optical lithography. However, with time, solidified particles were found in HSQ solvent, leading to pinholes in written patterns (refer to Fig. 5.6 and Fig. 5.7). A series of experiments was done to remove the solidified particles using filters shown in Fig. 5.8. It is conjectured that this may be due to short shelf life of HSQ XR1541, which is roughly 6 months. The possible solutions to overcome this hurdle are (i) to use fresh resist (ii) to use another resist with a higher shelf life. We proceeded with the second option and explored the use of existing PMMA (shelf life of 1 year) by inverting the mask (refer to Fig. 5.9 and Fig. 5.10).

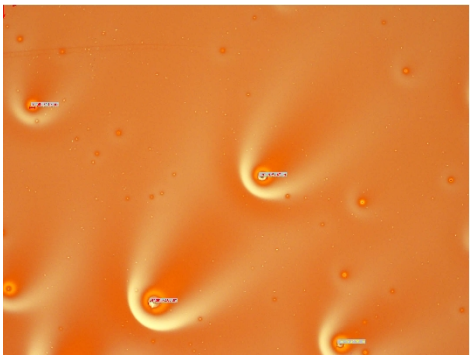

Figure 5.6: Olympus optical microscope image of solidified particle found in HSQ-I

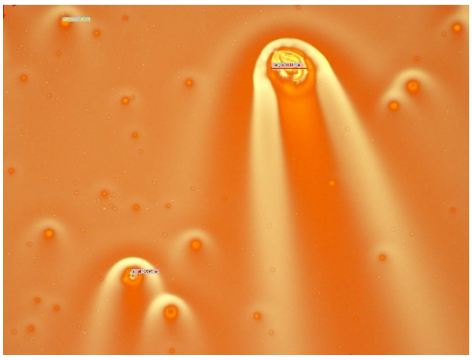

Figure 5.7: Olympus optical microscope image of solidified particle found in HSQ-II

5.3 Chrome coated Mask Plates with PMMA

5.3.1 Process Recipe - Experiment III

- Cleaning of Mask plate : Piranha clean (7:3 H_2SO_4 and H_2O_2)
- Dehydration-Bake : 130C for 30 min on hot plate
- Wait for 20 min so that the mask plate can come back to room temperature
- Resist Used : PMMA 950 K 2% Anisole, Spin Speed : 2000rpm, Thickness : 100 nm
- Pre-Bake : 180C for 90 sec on hot plate
- Energy : 10 kV, Dose : 100 $\mu C/cm^2$
- Developer : MIBK:IPA (1:3), Development Time : 30 sec
- Post Develop Bake : 120C for 90 sec on hot plate
- Etchant : 40 ml acetic acid(CH_3COOH), 82.5 gms Cerric Ammonium nitrate($Ce(NH_4)_2(NO_3)_6$), 460 ml DI H_2O
- Etching Duration : 60 sec

Figure 5.8: 0.45 um pore size filter from Milli pore

5.3.2 Results & Discussions of Experiment III

The post develop and post etch images are shown in Fig. 5.11 and Fig. 5.12 respectively. It was found that large feature lines were reduced in width (e.g.: 2 micron lines reduced to 351 nm in width) and majority of 500 nm features were merged. We deduce the reason for this to be the high overall dose for the inverted patterns due to back scattering of electrons, thereby causing their over-exposure. Also, the exposure time was too high for a single die in the inverted pattern, since the writing area was much higher than that of the original mask. One possible solution to this was to enclose the devices within boxes (to reduce the exposure area and hence,the exposure time), and then perform a dose test to find out the optimum dose for inverted 500 nm lines. This is how we proceeded in the next experiment (refer Fig. 5.13 and Fig. 5.14).

5.3.3 Process Recipe - Experiment IV

- Cleaning of Mask plate : Piranha clean (7:3 H_2SO_4 and H_2O_2)
- Dehydration-Bake : 130C for 30 min on hot plate
- Wait for 20 min so that the mask plate can come back to room temperature
- Resist Used : PMMA 950 K 2% Anisole, Spin Speed : 2000rpm, Thickness : 100 nm

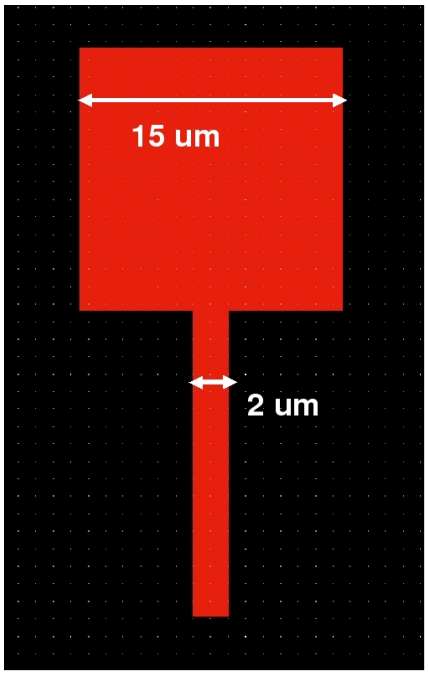

Figure 5.9: Mask design used with HSQ as resist. Since HSQ is negative tone resist, the red region will be exposed to e-beam, and hence retained after development, as required

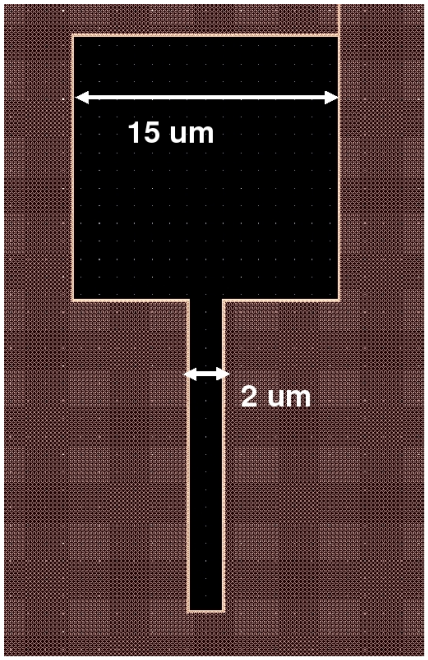

Figure 5.10: Mask design used with PMMA as resist. Since PMMA is a positive tone resist, the black region will be retained after development, as required, and the red region will be exposed to e-beam, and hence, washed away

- Pre-Bake : 180C for 90 sec on hot plate
- **Energy : 10 kV, Dose : varying from 40 $\mu C/cm^2$ to 60 $\mu C/cm^2$. Refer Fig. 5.14 for the test pattern used**
- Developer : MIBK:IPA (1:3), Development Time : 30 sec
- Post Develop Bake : 120C for 90 sec on hot plate
- Etchant : 40 ml acetic acid(CH_3COOH), 82.5 gms Cerric Ammonium nitrate($Ce(NH_4)_2(NO_3)_6$), 460 ml DI H_2O
- Etching Duration : 60 sec

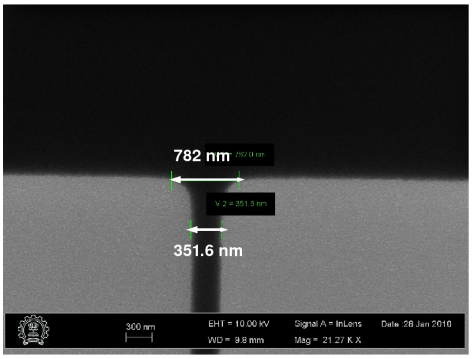

Figure 5.11: Post Develop Image on 100 nm thick PMMA exposed at dose of 100 $\mu C/cm^2$. Gate Length which was supposed to be 2 um got reduced to 351.6 nm

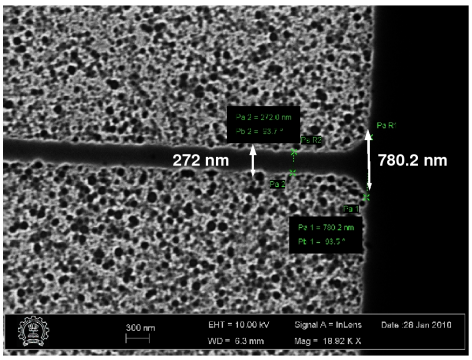

Figure 5.12: Post Etch Image with 60 sec etch duration. Gate Length got further shrinked to 272 nm

5.3.4 Results & Discussions of Experiment IV

The dose test revealed the optimum dose to be 42 $\mu C/cm^2$. The same pattern was thereby written on to the mask plate with 42 $\mu C/cm^2$. Fig. 5.15 and Fig. 5.16 show the post develop and post etch images respectively of the written mask plate. The patterns on this plate were transferred on Si-wafer coated with Shipley resist S1813 using DSA optical lithography. A careful observation of the transferred patterns on the Si-wafer lead to the conclusion of the presence of a thin, remanent layer of chrome even after plate-etching. This may have lead to the incomplete pattern transfer onto Si-wafer during DSA (refer Fig. 5.17). As a result, we needed to increase the chrome etch duration. In our next experiment, we increased the chrome etch duration from 60 sec to 90 sec as well as 120 sec.

5.3.5 Process Recipe - Experiment V

- Cleaning of Mask plate : Piranha clean (7:3 H_2SO_4 and H_2O_2)
- Dehydration-Bake : 130C for 30 min on hot plate
- Wait for 20 min so that the mask plate can come back to room temperature
- Resist Used : PMMA 950 K 2% Anisole, Spin Speed : 2000rpm, Thickness : 100 nm

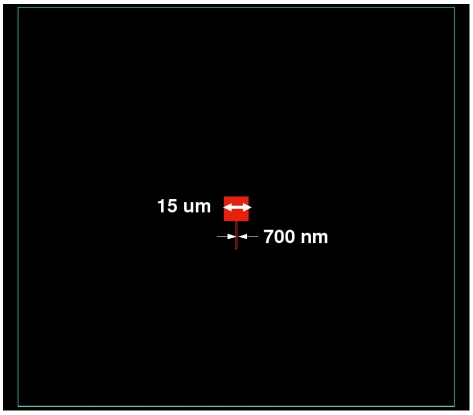

Figure 5.13: Devices enclosed in boxes to reduce the exposure area and hence,the exposure time

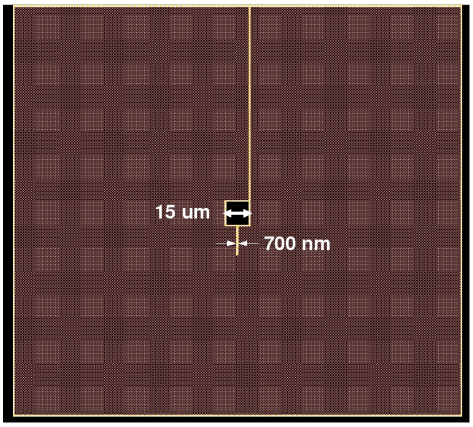

Figure 5.14: Invert of Devices enclosed in boxes to reduce the exposure area and hence,the exposure time

- Pre-Bake : 180C for 90 sec on hot plate
- Energy : 10 kV, Dose : 42 $\mu C/cm^2$(obtained from dose test)
- Developer : MIBK:IPA (1:3), Development Time : 30 sec
- Post Develop Bake : 100C for 120 sec on hot plate
- Etchant : 40 ml acetic acid(CH_3COOH), 82.5 gms Cerric Ammonium nitrate($Ce(NH_4)_2(NO_3)_6$), 460 ml DI H_2O
- **Etching Duration : 90 sec, 120 sec**

5.3.6 Results & Discussions of Experiment V

The above experiment revealed 90sec to be sufficient for complete chrome etching. Fig. 5.18 shows one of the patterns used for this experiment. For patterns written and etched in 90 sec, Fig. 5.19 and Fig. 5.20 show the post develop and post etch images respectively. A grey area boundary was observed in the patterns etched in 90 sec, as shown in the alignment mark image in Fig. 5.20. Further, on transferring these patterns onto Si using DSA, it was found that this grey area possibly lead to overexposure of patterns along their boundary during the transfer, thereby leading to diffused pattern features along their boundary (refer Fig. 5.21). It was hence necessary to modify the chrome etchant concentration and fine tune etching parameters

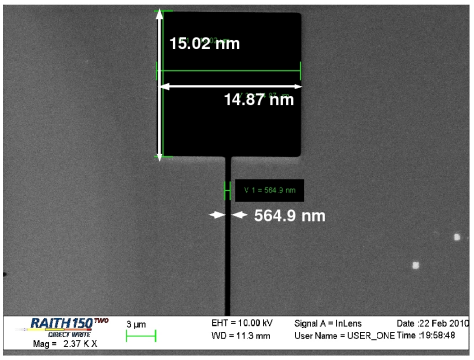

Figure 5.15: Post Develop Image on 100 nm thick PMMA exposed at an optimized dose of 42 $\mu C/cm^2$. Gate Lengths of 700 nm got reduced to 564.9 nm

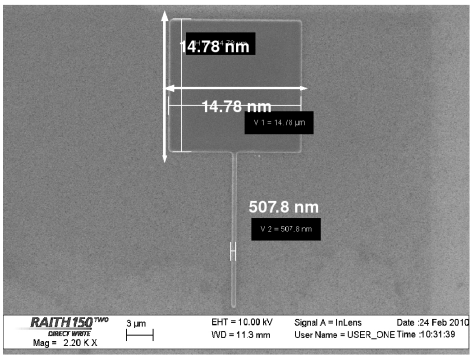

Figure 5.16: Post Etch Image with 60 sec etch duration. Gate Length got further shrinked to 507.8 nm

viz. etching time. In our next experiment, we thereby focused on eliminating the grey area formation using a new test pattern (refer Fig. 5.22).
In Fig. 5.22, the numbers on the left indicate the width of lines viz. 0.5 um, 1 um, 2 um, 3 um, 5 um and 10 um, and the numbers at the bottom indicates spacing between lines viz. 1 um, 2 um, 3 um, 5 um and 10 um.

5.3.7 Process Recipe - Experiment VI

- Cleaning of Mask plate : Piranha clean (7:3 H_2SO_4 and H_2O_2)
- Dehydration-Bake : 130C for 30 min on hot plate
- Wait for 20 min so that the mask plate can come back to room temperature
- Resist Used : PMMA 950 K 2% Anisole, Spin Speed : 2000rpm, Thickness : 100 nm
- Pre-Bake : 180C for 90 sec on hot plate
- Energy : 10 kV, Dose : 42 $\mu C/cm^2$(obtained from dose test), ref Fig. 5.22 for the mask used for optimization purpose
- Developer : MIBK:IPA (1:3), Development Time : 30 sec
- Post Develop Bake : 100C for 120 sec on hot plate

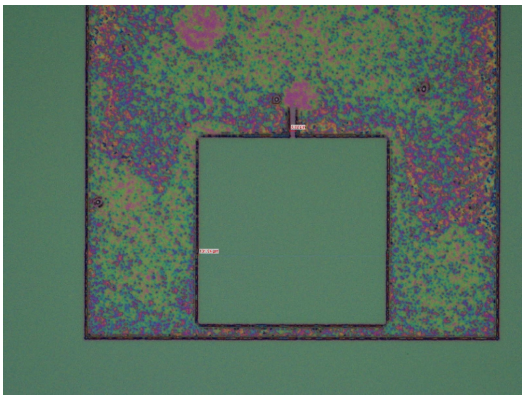

Figure 5.17: Olympus optical microscope post DSA Image. A thin, remanent layer of chrome, present on the plate in the e-beam exposed region, got transferred on Si

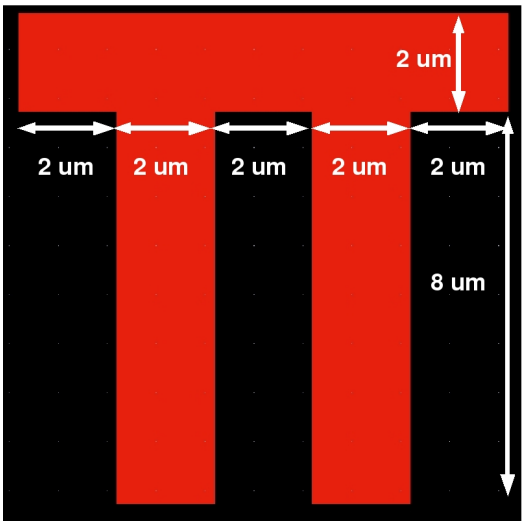

Figure 5.18: Alignment mark patterns used for Experiment V

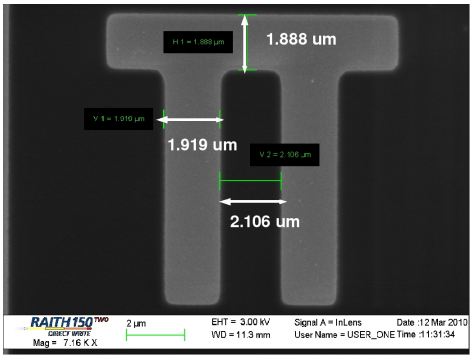

Figure 5.19: Post Develop Image on 100 nm thick PMMA exposed at an optimized dose of 42 $\mu C/cm^2$

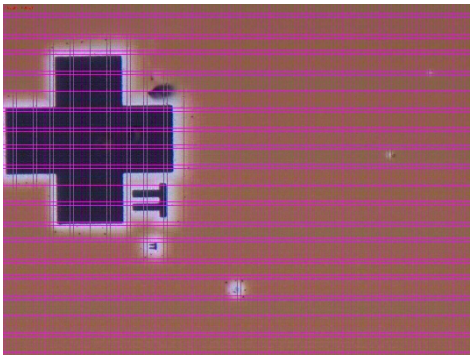

Figure 5.20: Olympus optical microscope post etch image with 90 sec etch duration. Grey area boundary was observed in the patterns

- **Etchant : 40 ml acetic acid(CH_3COOH), 82.5 gms Cerric Ammonium nitrate($Ce(NH_4)_2(NO_3)_6$), 230 ml DI H_2O**
- **Etching Duration : 73 sec, 76 sec, 80 sec**

5.3.8 Results & Discussions of Experiment VI

We wrote the test pattern on the mask plate using the optimized dose of 42 $\mu C/cm^2$. Fig. 5.23 show its post develop images. Further, we doubled the chrome etchant concentration and reduced the etch time to arrive at an optimum recipe for zero grey region formation. However, for all the etch times, the grey area formation persisted as seen from Fig. 5.24 to Fig. 5.29. Hence, it was conjectured that this might be due to interaction of PMMA with chrome. In order to test this hypothesis, in the next experiment, it was decided to introduce an intermediate layer of HMDS (Hexamethyldisilazane) between chrome and PMMA. HMDS is a well-known adhesion promoter for resists. Additionally in the next experiment, a thicker resist layer (approx. 200 nm) was used to maintain a proper aspect ratio. Hence, a dose test was again repeated to deduce the optimum clearing dose for the thicker resist layer.

5.3.9 Process Recipe - Experiment VII

- Cleaning of Mask plate : 2 & 1/2 minutes in acetone and 2 & 1/2 minutes in IPA

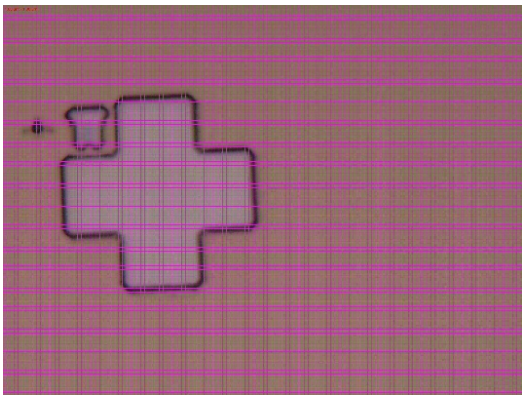

Figure 5.21: Olympus optical microscope post DSA image. Grey area shown in Fig. 5.20 lead to overexposure of patterns along the boundary of alignment marks

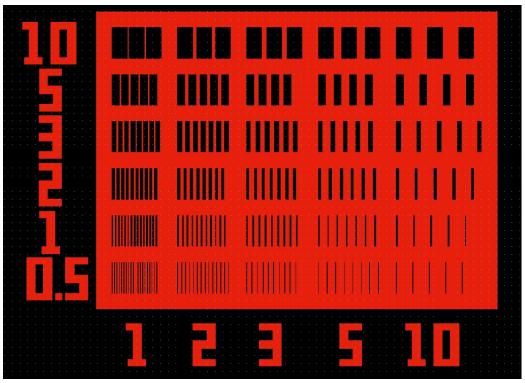

Figure 5.22: Chrome Etching Optimization Mask

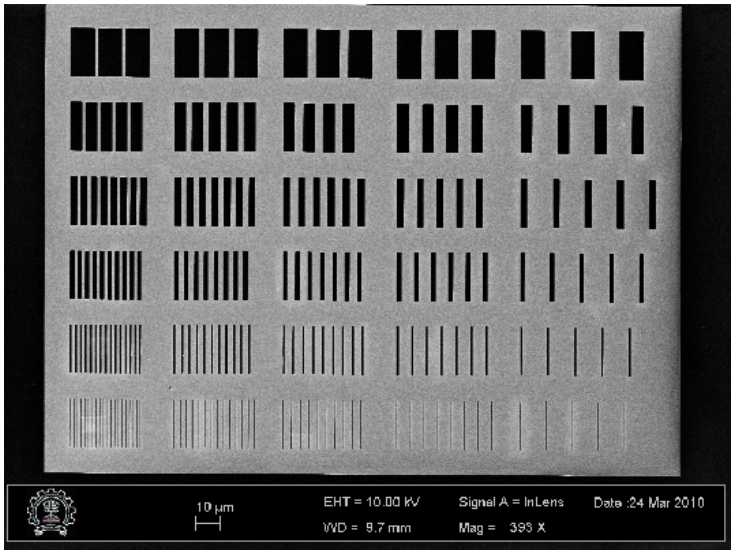

Figure 5.23: Post Develop Image on 100 nm thick PMMA exposed at of 42 $\mu C/cm^2$

- Dehydration-Bake : 130C for 30 min on hot plate
- Wait for 20 min so that the mask plate can come back to room temperature
- **Spin HMDS with spin speed 3500 rpm**
- **Spin Resist PMMA 950 K 4% Anisole, with spin speed 3500rpm to obtain thickness of 200 nm**
- Pre-Bake : 180C for 90 sec on hot plate
- Energy : 10 kV, Dose : varying from 50 $\mu C/cm^2$ to 80 $\mu C/cm^2$(obtained from dose test), ref Fig. 5.30 for the mask used for optimization purpose
- Developer : MIBK:IPA (1:3), Development Time : 30 sec
- Post Develop Bake : 100C for 120 sec on hot plate
- Etchant : 40 ml acetic acid(CH_3COOH), 82.5 gms Cerric Ammonium nitrate($Ce(NH_4)_2(NO_3)_6$), 460 ml DI H_2O
- Etching Duration : 50 sec

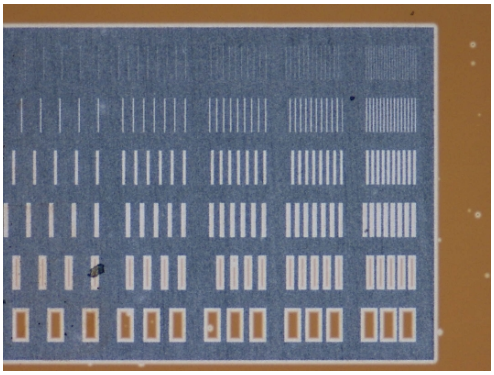

Figure 5.24: Olympus optical microscope bright field post etch image with 73 sec etch duration

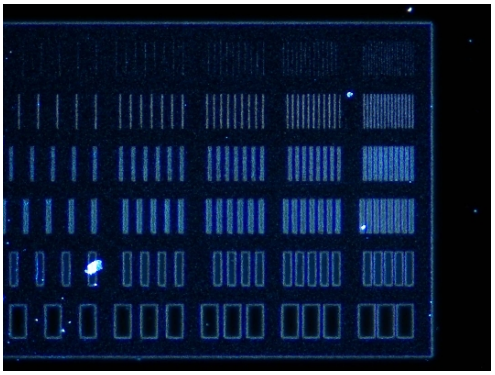

Figure 5.25: Olympus optical microscope dark field post etch image with 73 sec etch duration

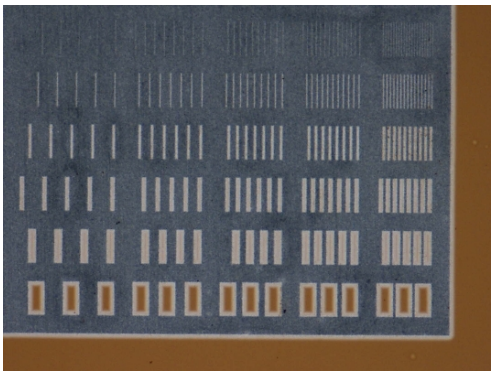

Figure 5.26: Olympus optical microscope bright field post etch image with 76 sec etch duration

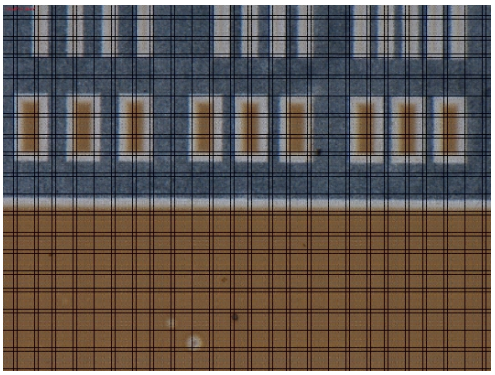

Figure 5.27: Olympus optical microscope dark field post etch image with 76 sec etch duration

5.3.10 Results & Discussions of Experiment VII

The dose test for 200 nm thick PMMA revealed 60 $\mu C/cm^2$ to be the optimum dose for resist clearing. Further, Fig. 5.31 and Fig. 5.32 show the post develop and post etch images respectively of the pattern exposed using HMDS as an intermediate layer between PMMA and chrome. The post etch images revealed that the grey area problem was resolved by introducing HMDS, thereby confirming the interaction of PMMA and chrome to be its cause. Comparison between the obtained feature sizes on plate and actual feature size on design has been tabulated as shown in Tab. 5.1, where W is width in um and S represents spacing in um. Now that the mask plate writing issues have been resolved, we focused next on successfully transferring the

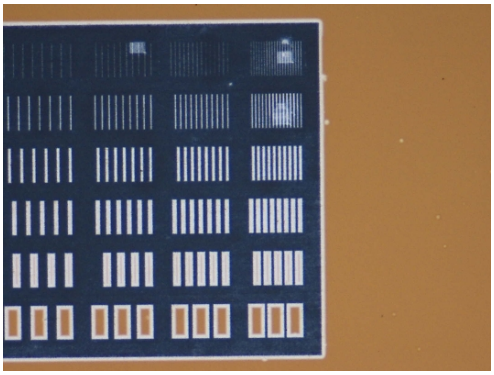

Figure 5.28: Olympus optical microscope bright field post etch image with 80 sec etch duration

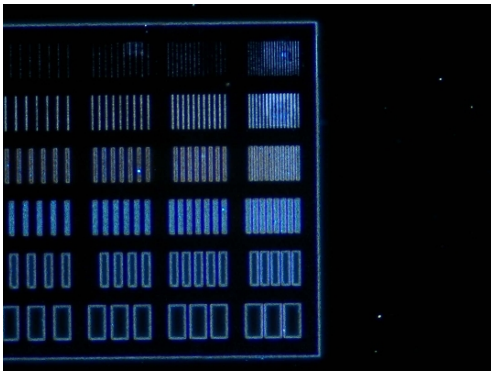

Figure 5.29: Olympus optical microscope dark field post etch image with 80 sec etch duration

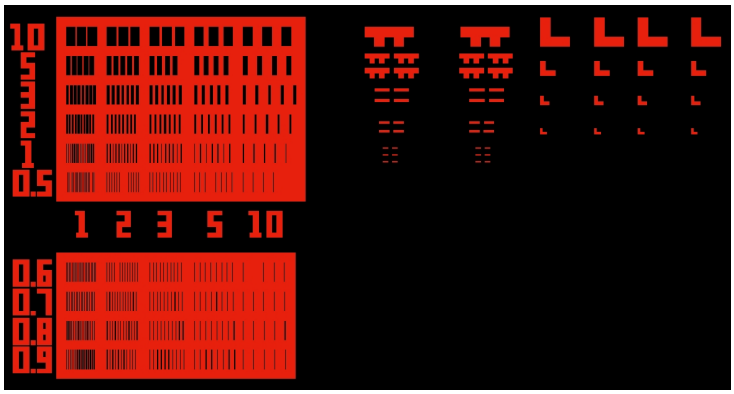

Figure 5.30: Etching Optimization Pattern

mask plate patterns onto a Si-wafer coated with Shipleys positive photo resist S1813 and attain a minimum dimension close to 500 nm using DSA.

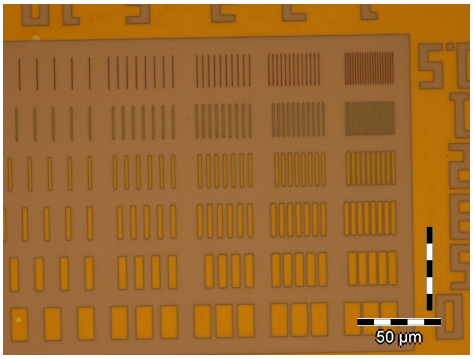

Figure 5.31: Olympus optical microscope post develop image of sample coated with HMDS, followed by 200 nm thick layer of PMMA 950K 4% Anisole. The optimum dose was found out to be 60 $\mu C/cm^2$

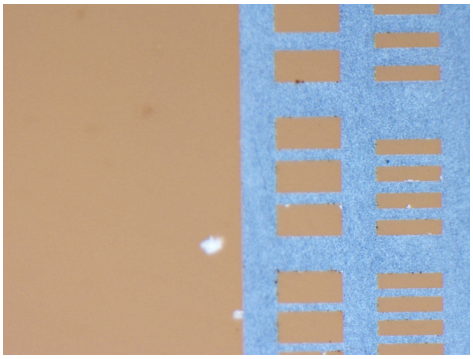

Figure 5.32: Olympus optical microscope post etch image with an etching duration of 50 sec. This image revealed that grey area problem was resolved by introducing HMDS

Cadence Design W um/S um	On Mask Plate W um/S um
2/1	1.265/1.563
2/2	1.210/2.382
2/3	1.210/3.405
2/5	1.265/5.155
2/10	1.191/11.11
3/1	2.159/1.656
3/2	2.196/2.512
3/3	2.233/3.517
3/5	2.177/5.359
3/10	2.233/10.937
5/1	4.224/1.675
5/2	4.094/2.512
5/3	4.205/3.443
5/5	4.150/5.434
5/10	4.410/10.29

Table 5.1: Variation of Feature Sizes on Cadence Design and Mask Plate

Chapter 6

DSA optimization towards 500nm Feature Size

This chapter focuses on the set of experiments done to develop a recipe which would successfully transfer 500 nm patterns on the mask plate to a silicon wafer using Shipleys standard resist S1813. The optical lithography tool used for the same was the DSA EVG 620 system. The DOUBLE SIDED MASK alignment (DSA) EVG 620 system helps in high precision single and double sided alignment.
Specifications of the system are as follows:[18]

- Exposure modes: hard, soft, vacuum contact
- Separation distance between wafer and mask plate: 0-300 microns
- Wafer thickness: 0.1-10 mm
- Lamp: 500W Hg Lamp
- Wavelength range: 350-450 nm
- Alignment accuracy: 0.5 micron for top side and 1 micron for bottom side
- Minimum feature size achievable: 450 nm

The following set of experiments takes off from the mask plate optimization efforts discussed in the previous chapter. It uses the same test pattern used for plate etch experiments (refer Fig. 6.1) and follows the optimized plate writing recipe (using HMDS) for pattern exposure.
In Fig. 6.1, the numbers on the left indicate the width of lines viz. 0.5 um, 1 um, 2 um, 3 um, 5 um and 10 um, and the numbers at the bottom indicates spacing between lines viz. 1 um, 2 um, 3 um, 5 um and 10 um.

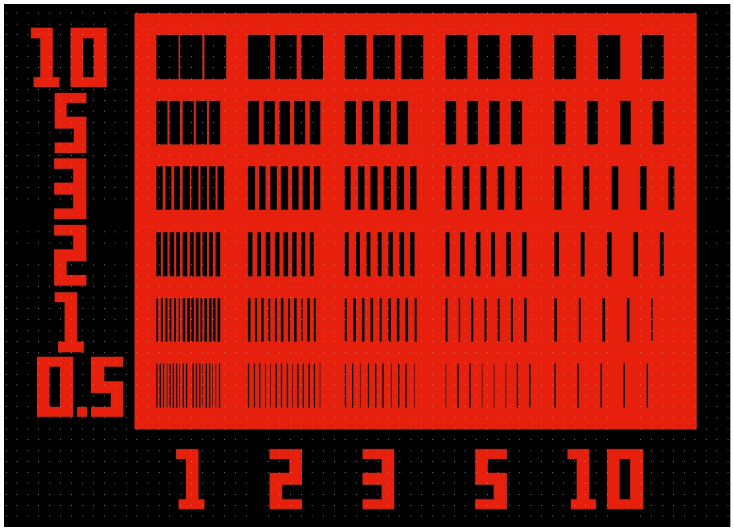

Figure 6.1: Etching Optimization Pattern

6.1 Mask Plate Preparation

- Cleaning of Mask plate : 2 & 1/2 minutes in acetone and 2 & 1/2 minutes in IPA
- Dehydration-Bake : 130C for 5 min on hot plate
- **Wait for 10 min so that the mask plate can come back to room temperature**
- Spin HMDS with spin speed 3500 rpm
- Spin Resist PMMA 950 K 4% Anisole, with spin speed 3500rpm to obtain thickness of 200 nm
- Pre-Bake : 180C for 90 sec on hot plate
- Energy : 10 kV, Dose : 60 $\mu C/cm^2$(obtained from dose test), ref Fig. 6.1 for the mask used for optimization purpose
- Developer : MIBK:IPA (1:3), Development Time : 30 sec
- Etchant : 460 ml DI H_2O, 40 ml acetic acid(CH_3COOH), 82.5 gms Cerric Ammonium nitrate($Ce(NH_4)_2(NO_3)_6$)
- Etching Duration : 50 sec

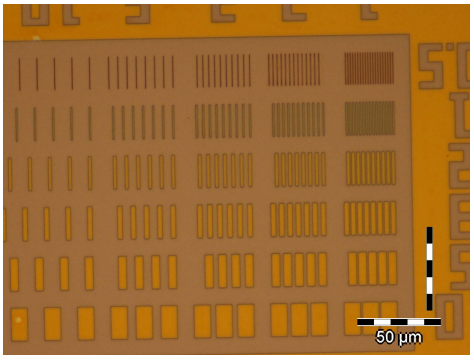

Figure 6.2: Olympus optical microscope post develop image of sample coated with HMDS, followed by 200 nm thick layer of PMMA 950K 4% Anisole exposed at dose of 60 $\mu C/cm^2$

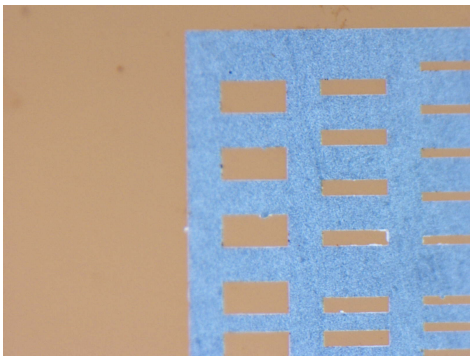

Figure 6.3: Olympus optical microscope post etch image with an etching duration of 50 sec

- Fig. 6.2 and Fig. 6.3 shows the post develop and post etch images, respectively

The post develop and post etch images of the written mask plate, shown in Fig. 6.2 and Fig. 6.3, indicate successful writing of the pattern onto the plate, with absence of any grey region along the pattern boundaries. This pattern was here on transferred onto Si using DSA in the next step. The exposure doses were varied so as to find the optimum dose for realizing approx. 500 nm features on Si.

6.2 DSA exposure with varying doses

6.2.1 Process Recipe

- Cleaning of Samples : 2 & 1/2 minutes in acetone and 2 & 1/2 minutes in IPA
- Dehydration bake : 130C for 120 sec on hot plate
- Resist Used : S1813, Spin Speed : 6000rpm, Expected Thickness : 1.2um, Thickness attained : 1.3 - 1.5 um
- Pre-bake : 90C for 120 sec on hot plate
- Exposure doses tried 170 mJ/cm^2, 160 mJ/cm^2, 140 mJ/cm^2

- Vertical Development for 30 sec in MF319
- Post development bake at 90C for 60 sec on hot plate
- Characterize using cross-sectional SEM imaging

6.2.2 Results & Discussions

The post develop images of exposure performed with varying doses are shown from Fig. 6.4 to Fig. 6.7. It is clearly seen that for doses above 140 mJ/cm^2, there is a side wall extension for all the pattern lines, with their width ranging from 700 nm to 1 um. The presence of this side wall extension hampers efforts to achieve 500 nm pattern lines on Si. However, for a dose of 140 mJ/cm^2, there is almost no side wall extension seen. Fig. 6.6 through Fig. 6.9 show different pattern line widths written using 140 mJ/cm^2 and all of them show no side wall extensions. This is promising for achieving high resolution lines and also for liftoff process recipe optimization.
Hence, to verify repeatability of above results, in the next experiment we repeated the test pattern exposure at the optimized dose of 140 mJ/cm^2. We also noted the variation of feature sizes on mask plate and on the wafer using top-down SEM characterization of the patterns post-development on Si.

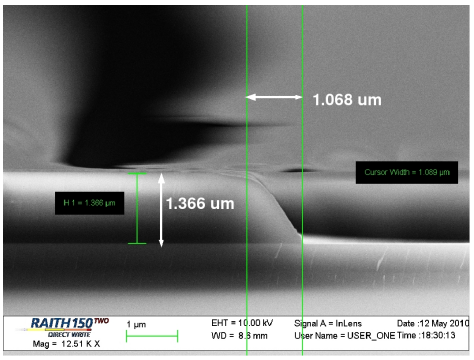

Figure 6.4: Post Develop Cross-sectional Image for 1.366 um resist thickness at dose 170 mJ/cm^2

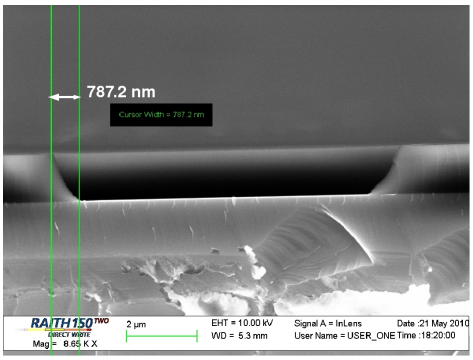

Figure 6.5: Post Develop Cross-sectional Image for 1.366 um resist thickness at dose 160 mJ/cm^2

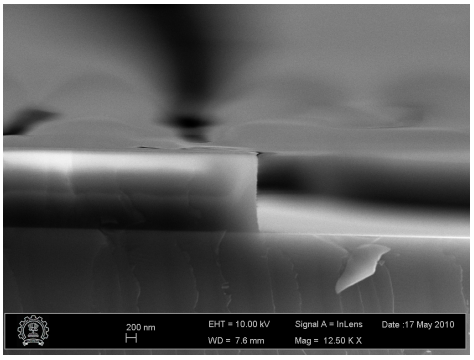

Figure 6.6: Post Develop Cross-sectional Image-1 for 1.545.um resist thickness at dose 140 mJ/cm^2

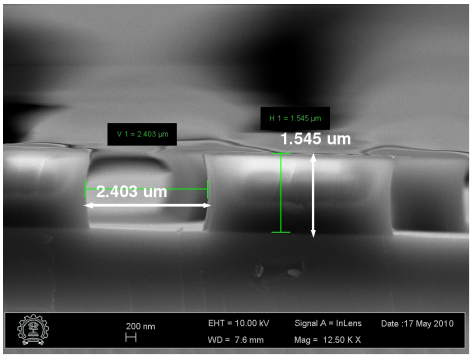

Figure 6.7: Post Develop Cross-sectional Image-2 for 1.545.um resist thickness at dose 140 mJ/cm^2

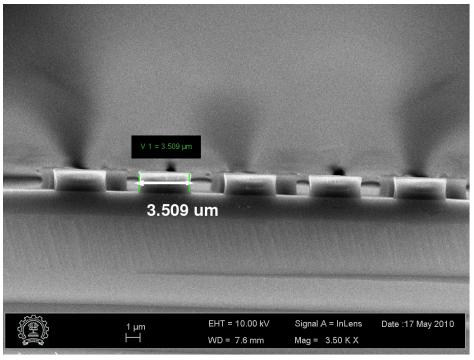

Figure 6.8: Post Develop Cross-sectional Image at magnification 3.5KX for 1.545.um resist thickness at dose 140 mJ/cm^2

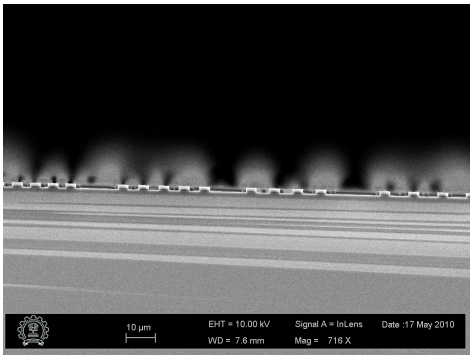

Figure 6.9: Post Develop Cross-sectional Image at magnification 716X for 1.545.um resist thickness at dose 140 mJ/cm^2

6.3 DSA exposure with optimized dose of 140 mJ/cm^2

6.3.1 Process Recipe

- Cleaning of Samples : 2 & 1/2 minutes in acetone and 2 & 1/2 minutes in IPA
- Dehydration bake : 130C for 120 sec on hot plate
- Resist Used : 1813, Spin Speed : 6000rpm, Expected Thickness : 1.2um, Thickness attained : 1.3 - 1.5 um

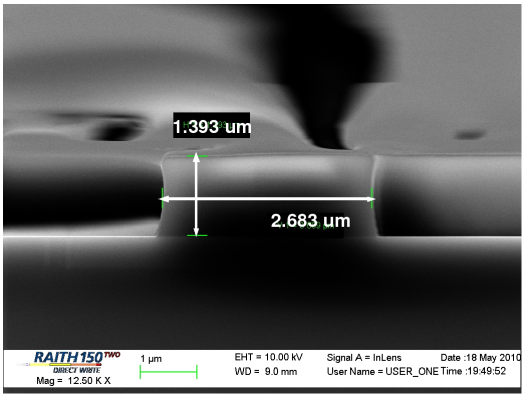

Figure 6.10: Post Develop Cross Section Image for 1.393 um resist thickness at dose 140 mJ/cm^2

- Pre-bake : 90C for 120 sec on hot plate
- Exposure dose : 140 mJ/cm^2
- Vertical Development for 30 sec in MF319
- Post development bake at 90C for 60 sec on hot plate
- Characterize using cross-sectional and top-down SEM imaging

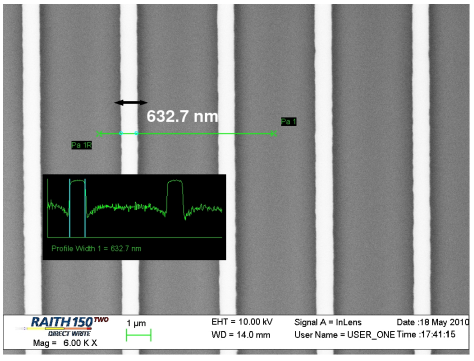

Figure 6.11: Post Develop Image on Si-wafer for 1.210 um width lines with 2.382 um spacing on mask plate at dose 140 mJ/cm^2

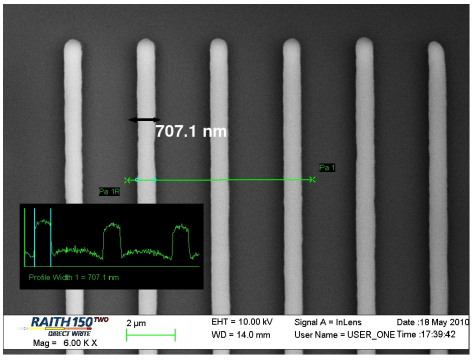

Figure 6.12: Post Develop Image on Si-wafer for 1.265 um linewidth and 1.563 um spacing on mask plate at dose 140 mJ/cm^2

6.3.2 Results & Discussion

From the cross-sectional post develop image shown in Fig. 6.10, it is clear that the above recipe is reproducible with almost zero side wall extensions for patterns exposed at 140 mJ/cm^2. Furthermore, top-down SEM characterization of the samples revealed that the minimum feature size attained was 632 nm (refer Fig. 6.11 and Fig. 6.12). Additionally, optical microscopy was done on selected locations of the mask plate, and top-down SEM imaging was done on the corresponding same locations on the DSA exposed wafer, so as to find out the exact variation of feature sizes after DSA exposure. This helped us obtain a set of values indicating the change in feature size as one writes a pattern onto a mask plate and further exposes it onto Si using DSA optical lithography. This set of tabulated values, comparing the obtained feature sizes at each step, is shown in Tab. 6.1, where W is width in um and S represents spacing in um. It has been observed that there is a reduction of at least 0.5 um in feature size as we transfer a line pattern from mask plate onto Si. This is expected to be an important consideration for future mask designs to be used DSA lithography.

Cadence Design W um/S um	On Mask Plate W um/S um	On Wafer (Post DSA) W um/S um
2/1	1.265/1.563	0.707/2.289
2/2	1.210/2.382	0.632/3.356
2/3	1.210/3.405	0.651/4.280
2/5	1.265/5.155	0.651/6.234
2/10	1.191/11.11	0.669/11.46
3/1	2.159/1.656	1.693/2.252
3/2	2.196/2.512	1.582/3.312
3/3	2.233/3.517	1.638/4.373
3/5	2.177/5.359	1.656/6.327
3/10	2.233/10.937	1.638/11.314
5/1	4.224/1.675	3.610/2.307
5/2	4.094/2.512	3.536/3.349
5/3	4.205/3.443	3.591/4.392
5/5	4.150/5.434	3.536/6.271
5/10	4.410/10.29	3.591/11.28

Table 6.1: Variation of Feature Sizes on Cadence Design, Mask Plate and On Wafer Post DSA

Chapter 7

Additional Process Optimization Experiments

This chapter provides details of two application-specific direct-write process optimization done on the Raith 150 TWO EBL tool. The first example refers to ring resonator structures that were designed and written using a negative e-beam resist (HSQ). The Fixed Beam Moving Stage (FBMS) feature of the Raith tool was successfully used in writing the long features of these structures. The second example refers to photonic crystal structures that were designed and written using a positive e-beam resist (PMMA). Both these application-specific processes were optimized for external users of our facility (viz. IISc Bangalore, and Physics Department, IITB respectively). Experiment design and optimization described in this chapter could be successfully completed due to equal contribution from my colleague Ms. Gayatri Vaidya.

7.1 Ring Resonator[1]

Typically, ring resonator consists of two parallel dielectric straight waveguides with a ring or disk shaped dielectric cavity placed in between them.[1] These two parallel dielectric straight waveguides form four ports for the external connections viz. 2-input ports named 'In-port' and 'Add-port' and 2-output ports named 'Through-port' and 'Drop port'.[1]
The functioning of micro resonators can described by the interaction of harmonic optical waves propagating along the straight waveguide and the cavity, and the interferometric resonances of the waves inside the cavity.[19] A single frequency optical wave, which propagates along the upper straight waveguide, is launched at the In-port of the resonator. This connects the In-port and Through-port, and part of it is loosely coupled to the cavity. While prop-

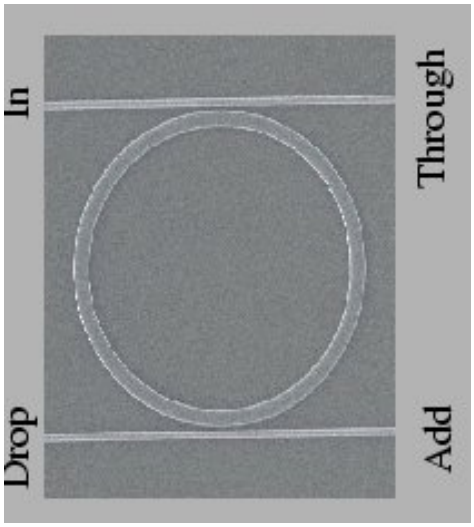

Figure 7.1: Horizontally Coupled Ring Resonator with two parallel dielectric straight waveguides with a ring or disk shaped dielectric cavity placed in between them[1]

agating along the cavity, part of this signal is coupled to the lower straight waveguide and appears at the Drop-port. The remaining part of the signal propagates along the cavity, and interferes with the newly in-coupled signal in the upper interaction region. Depending upon the specific configuration, these two fields undergo constructive or destructive interference.[1]
If the cavity field is out of phase with the newly entering field, then destructive interference takes place inside the cavity and as a result, there is only a small amount of power inside the cavity.[1] Under so-called off resonance conditions, as shown in Fig. 7.2, most of the input power is directly transmitted to the Through-port, and there is comparably low power at the Drop-port.[1]
On the other hand, if the field inside the cavity is in phase with the newly in-coupled signal, then due to constructive interference, energy builds up inside the cavity. This field gets coupled to the Drop-port waveguide. Under so-called resonance conditions, there is a significant power observed at the Drop-port, while less power appears at the Through-port. This situation is shown in Fig. 7.2.[1]

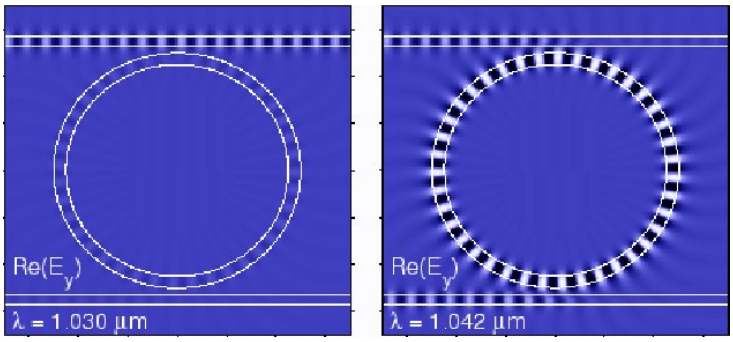

Figure 7.2: Off-resonance state where most of the input power is directly transmitted to the Through-port with comparably low power at the Drop port and resonance state of ring resonator where there is a significant power observed at the Drop-port, while less power appears at the Through-port[1]

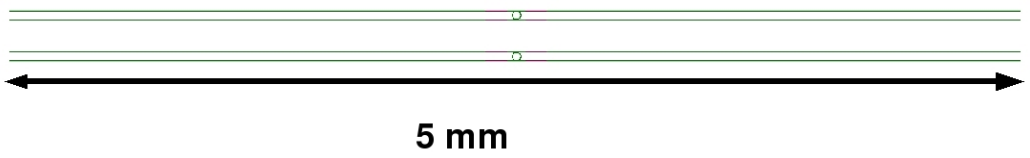

Figure 7.3: Overall Design of ring resonator structure that had a length of 5 mm and circle width of 500 nm

7.1.1 Mask Design Details

As per an external request that we received, a ring resonator structure mask was designed, with its various aspects shown from Fig. 7.3 through Fig.7.7. The overall structure had a length of 5 mm, while the circle width was 500 nm, with an inner diameter of 39 um and outer diameter of 40 um. The waveguide width was kept as 500 nm, following which it was extended using a taper width of 1 um. The main aspect of this experiment was the use and optimization of the FBMS (Fixed Beam Moving Stage) feature of the Raith 150 TWO EBL Tool for writing the long waveguide line. FBMS is a zero stitching error writing strategy.[11] It has the capability of exposing extremely long, smooth, and continuous lines of arbitrary curvature, with zero stitch error and small line width variance, which is major requirement for waveguide fabrication.[11] In keeping with our design requirements, we have therefore used the FBMS mode for writing these resonator structures.

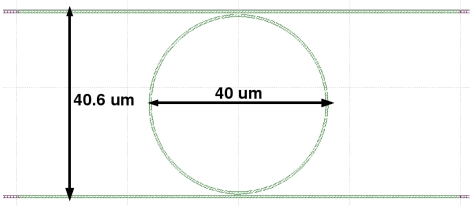

Figure 7.4: Cavity Inner diameter and spacings between waveguides

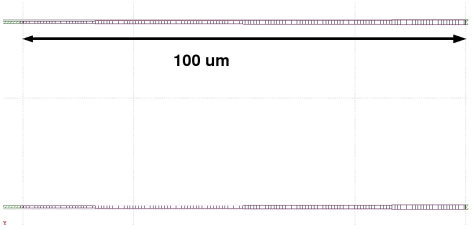

Figure 7.5: Taper Area connecting 500 nm width waveguide to 1 um width FBMS line

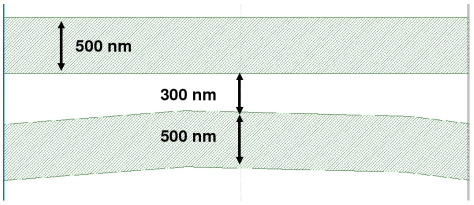

Figure 7.6: Cavity and waveguide width

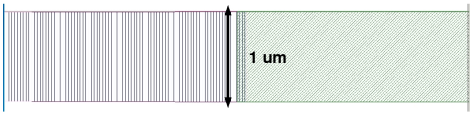

Figure 7.7: Taper and FBMS line Interface

7.1.2 Process Recipe

- Cleaning of SOI substrate samples : Piranha clean (7:3 H_2SO_4 and H_2O_2)
- Dehydration bake at 180C for 5 mins in hot plate
- HSQ XR1541 was spin coated on the substrate at a spin speed of 2000 rpm, to obtain a 45-nm nominal thickness
- Pre-bake at 250C for 90 sec in hot plate
- E-beam pattern exposure with a field area of 100um X 100um, at 8kV and with dose 200 C/cm2
- Post exposure bake (PEB) at 100C for 120 sec on hot plate
- Developed in TMAH 25% solution (standard developer for HSQ XR1541) at 25C for 7 sec
- Surface SEM characterization of the written patterns

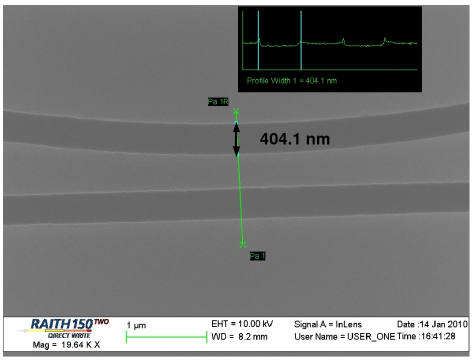

Figure 7.8: Post Develop Image on SOI wafer, for 500 nm circle width, in ring resonator mask design

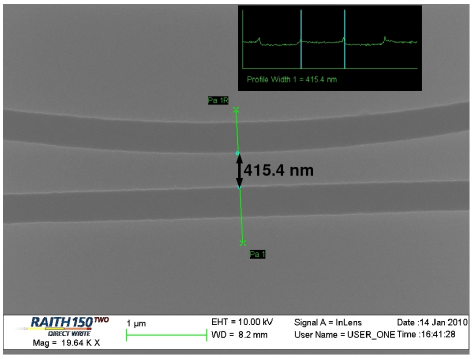

Figure 7.9: Post Develop Image on SOI wafer, for 300 nm seperation between circle and waveguide, in ring resonator mask design

7.1.3 Results & Discussions

Fig. 7.8 through Fig.7.11 show some of the post develop images of the ring resonator pattern exposed on SOI substrate using our recipe. While the structures have been successfully written, their overall dimensions were found to be reduced by 20%. This is attributed to the fact that we are using a negative resist for writing the pattern. Moreover, it has been observed that there were no stitching errors in the waveguide line structures written using the FBMS feature of Raith 150 TWO EBL tool.

7.2 Photonic Crystal[2]

A periodic structure of materials with differing refractive indices is referred to as photonic crystal. Optical multi layer films widely used as anti-reflection films etc. on the surface of television monitors, glasses and other optical components can be considered to be one dimensional photonic crystals. However,generally the term photonic crystal refers to two dimensional and three dimensional structures. The pitch of the structure is usually half the wavelength of the light for which it is designed for. Photonic crystals that are used in the visible optical region are designed and fabricated such that the period is about 300nm.

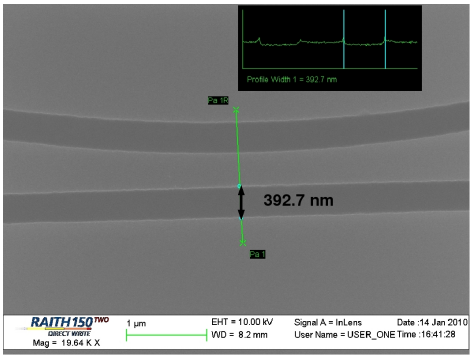

Figure 7.10: Post Develop Image on SOI wafer for 500 nm width waveguide, in ring resonator mask design

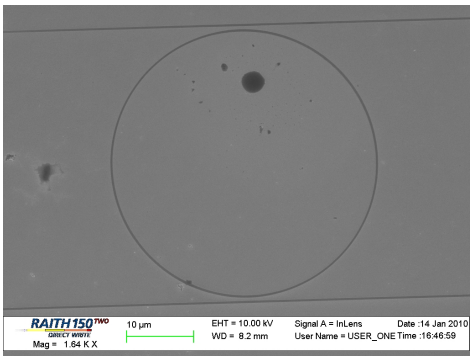

Figure 7.11: Post Develop Image for overall ring resonator structure

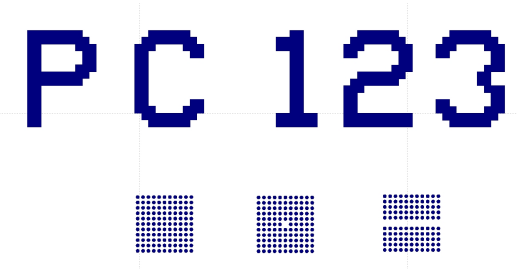

Figure 7.12: Overall Design of photonic crystal structure

7.2.1 Mask Design Details

The photonic crystal size requirements were given to us as 400 nm. It is known (and seen through earlier work) that writing a dark field mask pattern using PMMA leads to a slight increase in the pattern dimensions. Hence, in our mask design,the crystal diameter was reduced on purpose so as to attain a diameter of 400 nm as per specifications. The crystal diameter was kept as 300 nm & the pitch was kept as 500 nm. Fig. 7.12 through Fig.7.16 show the mask design patterns used as photonic crystal structures. While writing these structures, a dose test was done to evaluate the optimum dose value for which the photonic crystals don't merge.

7.2.2 Process Recipe

- Cleaning of SOI samples : Piranha clean (7:3 H_2SO_4 and H_2O_2)

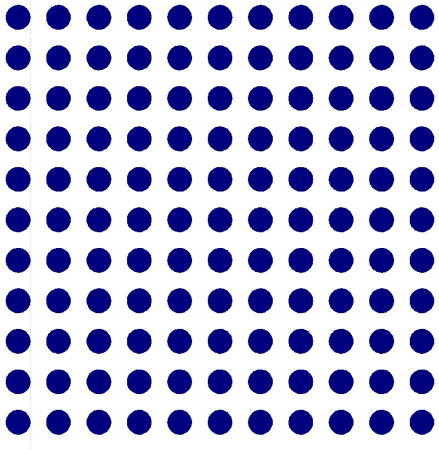

Figure 7.13: Frequently used solid core photonic crystal design

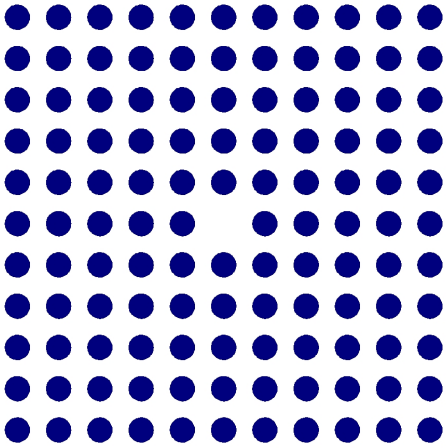

Figure 7.14: Solid core photonic crystal design with central core missing

- Dehydration-Bake : 130C for 5 min on hot plate
- Spin Resist PMMA 950 K 4% Anisole, with spin speed 3500rpm to obtain thickness of 200 nm
- Pre-Bake : 180C for 90 sec on hot plate
- Energy : 10 kV, Dose : varying from 80 $\mu C/cm^2$ to 150 $\mu C/cm^2$
- Developer : MIBK:IPA (1:3), Development Time : 30 sec
- Post Develop Bake : 100C for 120 sec on hot plate
- Surface SEM characterization of the written structures

7.2.3 Results & Discussions

The dose test done during exposure, with doses varying from 80 $\mu C/cm^2$ to 150 $\mu C/cm^2$, revealed 110 $\mu C/cm^2$ to be most suitable for achieving the desired structural specifications. For doses lower than the 110 $\mu C/cm^2$, the features seemed to be under developed, while for doses above 110 $\mu C/cm^2$, the features got merged. Fig. 7.17 through Fig.7.20 show the post development images of photonic crystal structures at an optimized dose of 110 $\mu C/cm^2$. As expected, approx. 400 nm crystals with a pitch of 500 nm were obtained with the mask design kept at 300 nm diameter with 500 nm pitch.

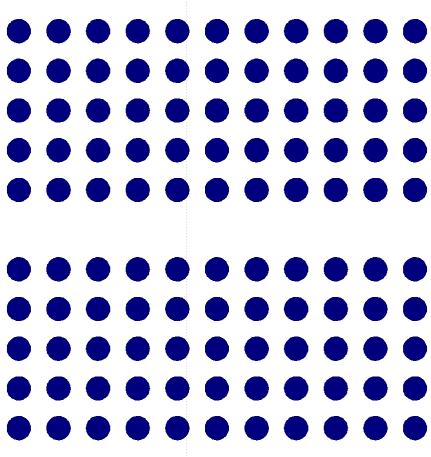

Figure 7.15: Photonic crystal design pattern with central line of cores missing

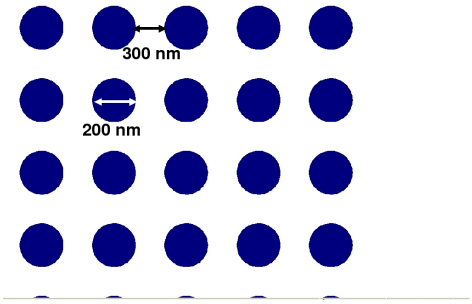

Figure 7.16: Individual core dimension and its pitch i.e. center-to-center distance

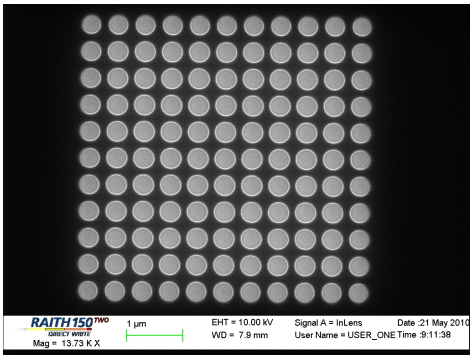

Figure 7.17: Post Develop Image for solid core photonic crystal design

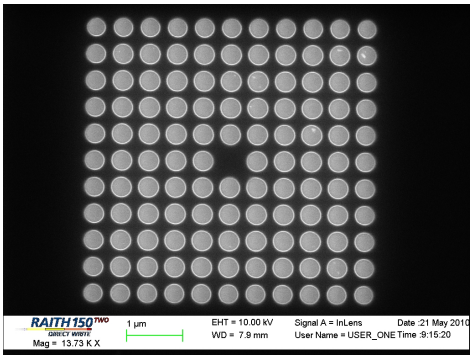

Figure 7.18: Post Develop Image for photonic crystal design with central core missing

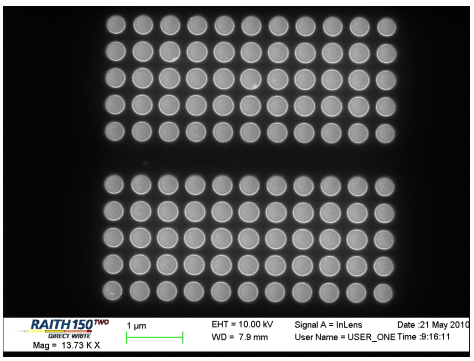

Figure 7.19: Post Develop Image for photonic crystal design with central line of cores missing

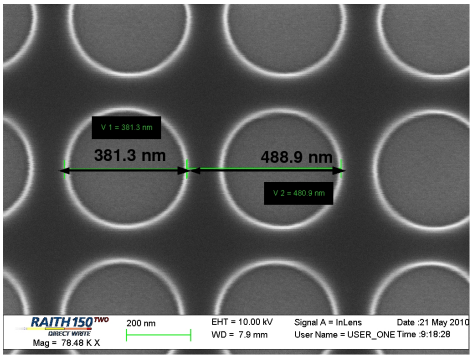

Figure 7.20: Post Develop Image for photonic crystal design with dimensions attained on wafer

Bibliography

[1] K. R. Hiremath, *Coupled mode theory based modelling and analysis of circular optical microresonators*. Enschede, The Netherlands, 2005.

[2] S. G. Johnson and J. D. Joannopoulos, *Photonic Crystals-The Road From Theory to Practice[Thesis]*. Kluwer, 2002. MIT Science Library.

[3] P. Rai-Choudhury, *Handbook of Micro-lithography, and Micro-fabrication*. Spie Optical Engineering Press, 1994.

[4] B. Hafner, "Scanning electron microscopy primer," April 2007.

[5] K. Suzuki and B. W. Smith, *Micro-lithography Science and Technology*. Taylor & Francis Group, 2007.

[6] *RAITH150 Software Operation Manual*, October 2005.

[7] A. Liljeborg, *Raith 150 e-beam lithography software*, February 2010. `http://www.nanophys.kth.se/nanophys/facilities/nfl/manual`.

[8] J. D. Plummer and P. B. Griffin, *Silicon VLSI Technology: Fundamentals, Practice, and Modeling*. Prentice Hall Electronics and VLSI series - Charles Sodini, Series Editor, 2000.

[9] L. de Broglie, "The wave nature of the electron," pp. 244–256, December 1929. Nobel Lecture.

[10] H. Pfeiffer and K. Loeffler, "A high current square spot probe for micropattern generation," in *Proceedings of the 7th International Congress on Electron Microscopy*, pp. 63–64, 1970.

[11] J. E. Sanabia, J. Klingfus, and M. Aktary, "The application of the Fixed Beam Moving Stage (FBMS) lithography mode and the metrology toolset to fabricate and measure waveguide coupling devices," *Nanotech Conference and Expo 2010*, June 2010.

[12] J. S. Wi, H. S. Lee, and K. B. Kim, "Enhanced development properties of IPA (Isopropyl Alcohol) on the PMMA Electron Beam Resist," *Electronic Materials Letters*, vol. 3, pp. 1–5, April 2007.

[13] J. Greeneich, *Electron Beam Technology in Micro-electronic Fabrication*. Academic press, 1980.

[14] J. Greeneich, "Developer characteristics of Poly-(Methyl MethaAcrylate) Electron Resist," *J. Electrochem. Soc*, vol. 122, pp. 970–976, April 1975.

[15] J. Kretz, L. Dreeskornfeld, G. Ilicali, T. Lutz, and W. Weber, "Comparative study of calixarene and HSQ resist systems for the fabrication of sub-20 nm MOSFET device demonstrators," *Microelectronic Engineering*, vol. 78-79, pp. 479–483, January 2005.

[16] L. van der pauw, "A method of measuring specific resistivity and hall effect of discs of arbitary shape," *Philips Research Reports*, vol. 13, pp. 1–9, February 1958.

[17] L. Nanver, E. Goudena, and J. Slabbekoom, "Kelvin test structure for measuring contact resistance of shallow junctions," vol. 9, pp. 241–245, March 1996.

[18] E. Thallner, *EVG620 Users Manual*. EV Group, 2006.

[19] D. J. W. Klunder, E. Krioukov, F. Tan, T. van der Veen, H. Bulthuis, G. Sengo, C. Otto, H. Hoekstra, and A. Driessen, "Vertically and laterally waveguide-coupled cylindrical microresonators in Si_3N_4 on SiO_2 technology," *Applied Physics B: Lasers and Optics*, vol. 73, pp. 603–608, October 2001.